MINERALOGICAL MAGAZINE

JOURNAL OF THE MINERALOGICAL SOCIETY

Vol. 32 December 1959 No. 247

The fibrous zeolite erionite; its occurrence, unit cell, and structure.

By Lloyd W. Staples, B.A., M.S., Ph.D.

Head of Dept. of Geology, University of Oregon, Eugene, Oregon, U.S.A.

and J. A. Gard, B.Sc., Ph.D.

Dept. of Chemistry, University of Aberdeen, Scotland.

[Read 5 June 1958.]

Summary. The type locality for erionite has been identified and specimens compared with Eakle's original material. New determinations of the physical properties and a chemical analysis have been made. Correlation of X-ray powder and fibre rotation data with electron diffraction of single crystals has shown that the unit cell is hexagonal with a 13·26, c 15·12 Å., space-group $P31c$, $P\bar{3}1c$, $P6_3mc$, $P\bar{6}2c$, or $P6_3/mmc$, giving a calculated sp. gr. of 2·07 and atomic cell contents (Ca, Mg, Na_2, $K_2)_{4\cdot5}Al_9Si_{27}O_{72}.27H_2O$. A structure is proposed for the aluminosilicate frame, with space-group $P6_3/mmc$, which gives satisfactory correlation between observed and calculated structure factors for the X-ray fibre rotation pattern.

IN 1898 Arthur S. Eakle, then of Harvard University, and later at the University of California, Berkeley, reported receiving an unusual zeolite from Durkee, Oregon. This proved to be a new mineral for which he proposed the formula $NaK(Ca,Mg)Al_4Si_{12}O_{32}.12H_2O$, and which he named 'erionite' because of its woolly appearance. No description of the exact locality was given in his paper, and it is doubtful if Eakle was ever there. The only other reference to the locality is a statement by Lindgren (1901, p. 764) concerning the new zeolite examined by Eakle from a fire-opal quarry a few hundred feet from the Gold Hill mill. None of the present inhabitants of the Durkee or Baker regions had heard of the mineral, and one of the authors (L. W. S.) in the summer of 1953 set out to rediscover the locality. The reported association with fire-opal was a great help in locating the deposit. Fitzsimmons (1949), in a doctoral dissertation on the area, did not mention erionite but reported that although fire-opals were only a matter of hearsay to him, they were

said to occur on Swayze Creek. When the locality was rediscovered, several hours' search were required before the first seams of erionite were found. Fire-opal is also difficult to find now.

X-ray investigation of Eakle's original material by L. W. Staples showed it to be identical with the newly collected material from Durkee. Information obtained from an electron-optical examination by J. A. Gard was correlated with the X-ray data, and indicated the unit cell and space-group.

Location and geology.

The erionite was found in Baker County, Oregon, at the site of the old Durkee opal mine, which was active in 1897 but which has not been worked in recent years. It is located in Sec. 36, Township 11 S., Range 43 E., which is reached by driving up Swayze Creek 1·6 miles from the junction of the road with U.S. Highway 30. A small quarry site lies on the north side of the road and a dump on the south side. No material was found in place because of the extensive slumping, but erionite was found in the waste rock on both sides of the road.

Fitzsimmons mapped the quarry area as Tertiary rhyolite tuff surrounded by pre-Tertiary foliated rocks, Tertiary lacustrine deposits, and basalt flows. The rhyolite tuff is actually an excellent example of a welded tuff with black glass shards appearing to flow around and through the contrasting lighter coloured matrix. The erionite is in seams, most of which are parallel to the flowage or bedding of the tuff, and the opal also occurs in similar fashion. The opal is later than the erionite and includes the latter in places, but it should not be concluded, as did Eakle, that the opal was formed from the zeolite. Opalitization in tuffs is well known and all stages in the opalitization of the pumice fragments of the tuff are in evidence. It is probable that the pumice fragments, which are now badly decomposed, yielded some of the material for the erionite. One part of the quarry contains a spherulitic phase of the tuff and cavities are lined with small crystals of heulandite. Zeolites other than erionite are rare in the quarry.

Erionite has been reported from other localities but the Durkee occurrence is the only one that has been confirmed by the writers. It was thought from an ambiguous statement by Fernquist (1937) that erionite occurred at the Oregon 'jade' mine on Shirttail Creek near Durkee 'in white, slender, wool-like fibres in cavities in the basalt' but careful search yielded no material and a subsequent communication from Fernquist stated, 'Nothing like erionite was found' (written

communication, 3 December 1953). Reed (1937) reports the occurrence of erionite in layers or bands in amygdules in Columbia River lavas in Idaho. His collected material is no longer available and the writers are unable to confirm this occurrence.

Thugutt (1948, p. 31), in an interesting paper on the chemical relations and origins of the zeolites, mentions orthorhombic crystals of erionite as being found in Silesia near Klodzko, where they form a thin cover upon quartz, and in a rhyolite tuff at Teigarhorn, Iceland. Thugutt (personal communication, 1 June 1955) was unable to provide any further information concerning references or material from these localities, but the writers are continuing to search for them.

Recently, J. Regnier (1958, p. 80) reports finding erionite in altered Pleistocene tuffs of central Nevada, and he concludes it is the product of alteration of the vitric water-laid tuffs, possibly under the influence of mineralized lake waters.

Since this paper was submitted, K. S. Deffeyes (1959) has reported five other localities for erionite, of which three are in central Nevada, one in central Wyoming, and one in South Dakota. In each case it occurs in volcanic-rich Cenozoic sediments. B. Kamb and W. C. Oke (personal communication, 8 May 1959) have identified erionite in basalt dredged from the Columbia River at Rock Island Dam, near Wenatchee, Washington, D.C.; some of the crystals are hexagonal prisms. M. H. Hey (1959) has also identified as erionite two specimens collected in the Faroe Islands before 1824.

In all, there are nine confirmed localities for erionite; in at least eight it occurs in material of volcanic origin.

Physical and chemical properties.

Eakle's (1898) original description of erionite is for the most part accurate and needs additions rather than corrections. His observations concerning the loss of water on heating were checked, and in addition a differential thermal analysis was performed using an Eberbach portable unit. An endothermic peak, although not sharp, is obtained at 235–245° C., and a sharp break occurs at 920° C. Repeated heating and cooling experiments on 0·3 g. of erionite give substantially the same results obtained by Eakle. The erionite remains anisotropic nearly to 810° C., at which temperature the mineral is brittle, isotropic, and the index of refraction is 1·493. X-ray powder photographs for erionite heated to 825° C. show weak cristobalite lines, which become stronger for material calcined at 1000° C. The tendency for cristobalite to form

during devitrification of glass has been noted by Warren and Biscoe (1938).

The first determination of indices of refraction for erionite was made by Larsen (1921) on material from the U.S. Geological Survey. He recorded α 1·438, γ 1·452, and probably on the basis of the mineral being optically positive, he noted β 1·44. These are the indices which are recorded in all reference books. A determination of the indices of refraction on Eakle's original material gives higher values than those recorded by Larsen. Through the kindness of Dr. G. Switzer, two small samples of erionite were obtained from the U.S. National Museum, one of which is probably the material worked on by Larsen. Likewise, new material obtained from the Durkee quarry was examined. All of these specimens, examined in sodium light, gave: ω 1·468, ϵ 1·473, ϵ–ω 0·005, within the usual limits of error. An exception to the above indices was obtained on one specimen which had come from the Roebling collection, although originally supplied by Eakle. This had indices ω 1·472, ϵ 1·476.

The determination of indices of refraction in fibrous materials is difficult and, as indicated by Morse and Donnay (1936), it may result in different values from those for the same substance in non-fibrous form, due in part to form birefringence. Water and opal are often the interstitial media. It is possible that variation in water content has been responsible for some of the variation observed in the indices of refraction. Heating erionite tends to raise its indices, although Hey (1932) in his studies of the zeolites noted in the case of thomsonite and other zeolites that dehydration in the initial stages can cause a drop in refractive index and density. The increase in refractive index of erionite heated to 810° C. has been noted above.

It is interesting that non-rotating fibre bundles of erionite, when placed with their length perpendicular to the X-ray beam, give a pattern similar to that produced by rotating a single fibre, which would seem to indicate that the fibres, often bound together in flat ribbons or bundles, have the slow ray direction in common, parallel to their length, but random orientation otherwise (electron diffraction results tend to confirm this).

The double refraction is not moderately strong as stated by Eakle. First-order yellow is seldom seen even in the thickest bundles of fibres.

The specific gravity of erionite is difficult to estimate because of its fibrous nature. Eakle recorded a value of 1·997 using methylene iodide and Thoulet solution. By the use of the Berman balance, and the Westphal balance with bromoform and alcohol, and various size bundles of

erionite, results were obtained ranging from 1·80 to 1·97, most of which were above 1·90. In a further determination, a small fibre was immersed in a mixture of bromoform and benzene, which was boiled under reduced pressure to remove entrapped air; the specific gravity of the liquid was adjusted until the fibre remained suspended at the same level for several hours. This gave the highest value recorded, 2·02.

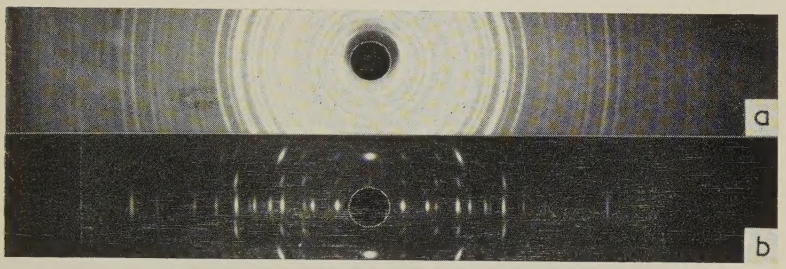

FIG. 1. *a*. Powder X-ray photograph of erionite. Cu-$K\alpha$ radiation in a 11·46-cm. diameter camera. *b*. X-ray photograph of a fibre bundle of erionite, rotated about the elongate axis.

X-ray data.

Although erionite is fibrous, powder photographs were obtainable which yielded fairly sharp lines (fig. 1*a*). A ball of fibres, rolled between the fingers to a spheroid about 1 mm. in diameter and mounted on a glass rod in the powder camera, also produced a pattern with lines almost as sharp as the usual type. Optimum results were obtained with an 8-hour exposure using copper radiation and a nickel filter. The results are listed in table I.

Natural fibre bundles oriented with the elongation direction of the fibres as the rotation axis were used in place of single crystals, identical patterns being produced both with and without rotation (figs. 1*b* and 2). Similar patterns were also obtained regardless of whether the X-ray beam was normal or parallel to the flat direction of the ribbon-like bundles of fibres. The same technique of using fibre bundles was adapted to the powder camera and aided in indexing the patterns. This use of the powder camera for single crystal work has been mentioned in the literature (Lindberg *et al.*, 1953, p. 1131), but it does not seem to be used as frequently as it might be, considering its usefulness and simplicity. One of its principal advantages is that the powder film and single crystal film are of the same size and can be superimposed for ready reference

(fig. 1). The X-ray patterns could all be indexed on an orthorhombic lattice with parameters a 6·625, b 11·53, c 15·12 Å., but electron diffraction of single crystals later showed the unit cell to be a closely related hexagonal one.

Examination in the electron microscope.

Small fibres of the Durkee specimen were rubbed lightly with water on a clean glass slide and drops of the diluted suspension transferred to

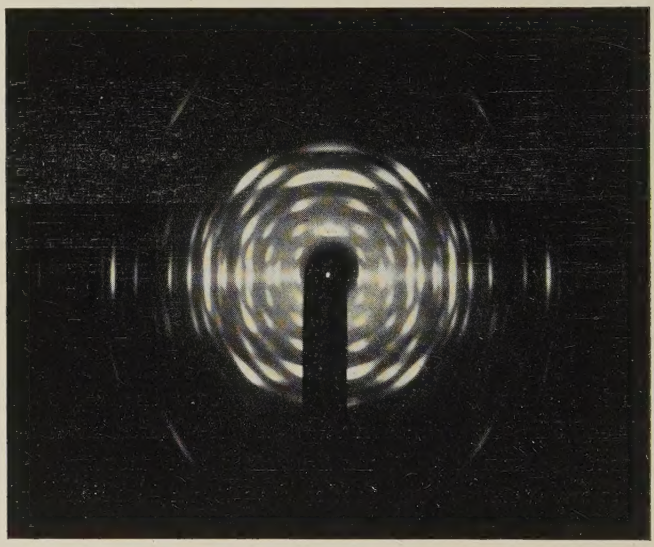

FIG. 2. X-ray photograph of a stationary natural fibre bundle of erionite. Cu-$K\alpha$ radiation in a 6-cm. diameter camera.

formvar-coated specimen grids. After drying in a desiccator, the specimens were shadow-cast with gold-palladium alloy at an angle of $\cot^{-1} 4$, and were examined with a Metropolitan-Vickers EM-3 electron microscope (Haine, Page, and Garfitt, 1950). This instrument can record electron-diffraction patterns from small selected areas of the specimen. The specimen stage may be tilted through a total angle of 10°; a method for calibration of the tilt device has been described elsewhere (Gard, 1956*a*).

Fig. 3 shows a typical electron micrograph of erionite. Most of the specimen was in the form of long fibres, of mean width 550 Å. and mean thickness 300 Å., but some fine powder and larger particles were also

present. Electron-diffraction patterns from individual fibres showed that they were single crystals. The spots in the patterns lie on rhombic networks, from which two unit-cell parameters in the plane of the supporting film can be estimated. Comparison with micrographs shows that in each pattern a row of spots lies parallel to the fibre direction, which will provisionally be called c, showing that c^* coincides with c. A few

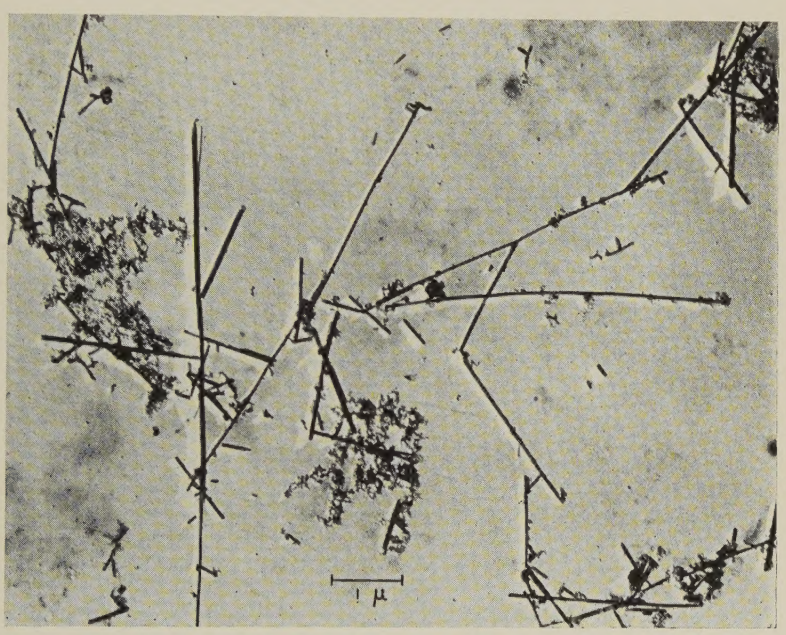

FIG. 3. Typical electron micrograph of erionite, shadowcast with Au-Pd at $\cot^{-1} 4$. The scale represents 1 μ.

patterns have distinct circular Laue zones arising from rows of lattice points nearly parallel to the electron beam, the spacings of which were estimated by tilting the fibres around their axes, using a procedure described elsewhere (Gard, 1956*b*). Figs. 4 and 5 show examples from series of diffraction patterns recorded from two crystals lying at different orientations on the supporting film. In both series, rows of spots parallel to c in the odd-order Laue zones lie halfway between those in the even-order zones, indicating a C-centred lattice. Parameters estimated from the patterns of fig. 4 are 15·1 Å. for c, 22·4 Å. normal to c in the plane of the support, and 13·6 Å. for the row parallel to the beam. Corresponding

parameters for the pattern of fig. 5 are 15·1, 13·3, and 23 Å., respectively. Clearly, the unit cell of the latter crystal is oriented about 90° around c with respect to that of the former. This suggests a unit cell that is, at least approximately, C-centred orthorhombic with a 13·3, b 22·4, c (elongation) 15·1 Å. This was confirmed by correlation with the X-ray powder and fibre data of table I, which gave the refined parameters of

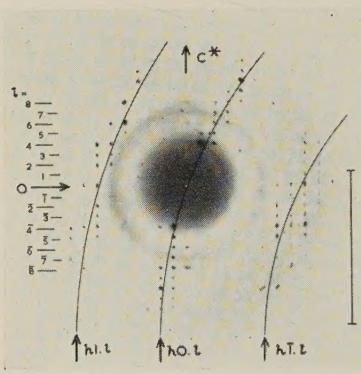

Fig. 4

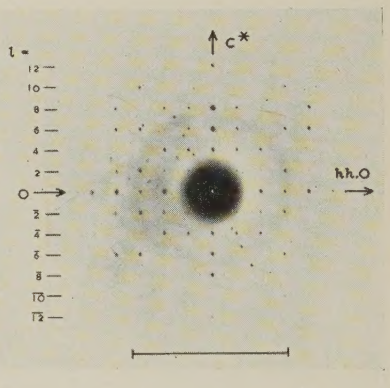

Fig. 5

Fig. 4. Electron-diffraction pattern from an erionite fibre with its $(11\bar{2}0)$ plane approximately normal to the electron beam. Rows of spots parallel to c in the first-order Laue zones, marked $h1.l$ and $h\bar{1}.l$, lie half-way between corresponding rows in the zero-order zone, marked $h0.l$, indicating a C-centred lattice. $000l$ reflections are missing for odd l-indices. The indices are for the hexagonal cell. The scale represents 1 Å.$^{-1}$

Fig. 5. An electron-diffraction pattern from an erionite fibre with its $(10\bar{1}0)$ plane normal to the electron beam. The fibre direction is marked c^*. Reflections with odd l-indices are completely absent. The scale represents 1 Å.$^{-1}$

a 13·26, b 23·08, c 15·12 Å. It is geometrically equivalent to a hexagonal cell with a 13·26, c 15·12 Å. Table I gives the X-ray data indexed on this unit cell; reflections with l-indices not confirmed by the fibre data are shown in parentheses. Indices have been inserted in the electron-diffraction patterns of figs. 4 and 5, and show that the crystals were lying with $(11\bar{2}0)$ and $(10\bar{1}0)$, respectively, normal to the electron beam.

There are no systematic absences of reflections with even l-indices. The only reflections with odd l-indices observed in the early X-ray patterns were $10\bar{1}1$, $10\bar{1}3$, $20\bar{2}1$, and $21\bar{3}1$. These were too few for derivation of the space-group, but indicate pseudo-halving of c. All electron-diffraction patterns (e.g. fig. 4) have $000l$ reflections missing for

TABLE I. X-ray powder data for erionite, indexed on a hexagonal unit cell with a 13·26, c 15·12 Å. All reflections have been confirmed on fibre rotation patterns, except those in parentheses which are not recordable. Indices are too numerous to be included for reflections with d-spacings less than 1·60 Å. Intensities were estimated visually. Cu-$K\alpha$ radiation was used in 6- and 11·54-cm. diameter cameras.

$d_{obs.}$	$I.$	$hkil$	$d_{calc.}$
11·57 Å.	**10**	$10\bar{1}0$	11·48 Å.
9·16	3	$10\bar{1}1$	9·16
7·56	5	0002	7·56
6·63	**8**	$11\bar{2}0$	6·63
6·30	1	$10\bar{1}2$	6·31
5·77	3	$20\bar{2}0$	5·74
5·37	4	$20\bar{2}1$	5·36
4·58	4	$20\bar{2}2$, $10\bar{1}3$	4·57, 4·61
4·34	7	$21\bar{3}0$	4·34
4·16	4	$21\bar{3}1$	4·18
3·80	**9B**	$30\bar{3}0$, $21\bar{3}2$	3·83, 3·76
		$20\bar{2}3$, 0004	3·78
3·58	5	$10\bar{1}4$	3·59
	—	$30\bar{3}2$*	3·42
3·31	4	$22\bar{4}0$, $21\bar{3}3$	3·31, 3·29
		$11\bar{2}4$	3·28
3·15	4B	$31\bar{4}0$, $31\bar{4}1$	3·19, 3·12
		$20\bar{2}4$	3·16
2·92	1—	$31\bar{4}2$	2·91
2·84	**10B**	$40\bar{4}0$, $40\bar{4}1$	2·87, 2·82
		$21\bar{3}4$	2·85
2·68	4	$40\bar{4}2$, $31\bar{4}3$	2·68, 2·69
2·50	7B	$41\bar{5}0$, $41\bar{5}1$, $32\bar{5}2$	2·51, 2·47, 2·48
		$40\bar{4}3$, $22\bar{4}4$, $21\bar{3}5$	2·49
2·36	1—	$32\bar{5}5$	2·33
2·28	1—	$50\bar{5}0$, $50\bar{5}1$, $41\bar{5}3$	2·30, 2·28, 2·25
		$40\bar{4}4$	2·28
2·21	4	$33\bar{6}0$, $50\bar{5}2$	2·21
2·12	2	$33\bar{6}2$, $30\bar{3}6$	2·12, 2·11
2·08	2	$51\bar{6}0$, $42\bar{6}2$, $50\bar{5}3$	2·06, 2·08, 2·09
2·04	1—	$51\bar{6}1$	2·04
1·99	1	$51\bar{6}2$, $32\bar{5}5$, $31\bar{4}6$	1·98, 1·99, 1·98

* Reflections observed on the fibre rotation patterns, but too weak to be seen on the powder patterns.

TABLE I (*cont.*)

$d_{obs.}$	*I.*	*hkil*	$d_{calc.}$
1·95Å.	1	$50\bar{5}4$	1·96Å.
	—	$51\bar{6}3$, $33\bar{6}4$, $(60\bar{6}0$ *	1·91
1·88	2	$43\bar{7}0$, $43\bar{7}1$, $40\bar{4}6$	1·89, 1·87, 1·89
		(0008)	1·89
1·84	2	$52\bar{7}0$, $43\bar{7}2$, $51\bar{6}4$	1·84, 1·83, 1·81
		$50\bar{5}5$	1·83
1·77	4	$43\bar{7}3$, $60\bar{6}3$, $41\bar{5}6$	1·77, 1·79, 1·78
1·75	1	$61\bar{7}0$, $40\bar{4}7$	1·75, 1·73
1·70	1	$61\bar{7}2$, $50\bar{5}6$	1·70
1·65	7	$44\bar{8}0$, $61\bar{7}3$, $52\bar{7}4$	1·66, 1·65, 1·65
		$60\bar{6}5$, $33\bar{6}6$, $32\bar{5}7$	1·62, 1·66, 1·67

$d_{obs.}$	*I.*	$d_{obs.}$	*I.*	$d_{obs.}$	*I.*
1·59	5	1·37	3B	1·19	1
1·51	3B	1·34	3	1·14	2
1·46	2	1·27	3	1·06	1
1·43	1	1·24	2	1·04	1
1·41	1—	1·21	2		

* Reflections observed on the fibre rotation patterns, but too weak to be seen on the powder patterns.

odd values of l. Reflections with odd l-indices are completely absent from the pattern shown in fig. 5, indicating a systematic absence of $hh\bar{2}\bar{h}l$ reflections for odd values of l. Other reflections with l odd, which have since been observed on fibre rotation patterns taken with much longer exposures, are in accord with this systematic absence, and have been interpolated in table I. $\{10\bar{1}0\}$ glide planes with component $c/2$ are therefore present, and the space-group is $P31c$, $P\bar{3}1c$, $P6_3mc$, $P\bar{6}2c$, or $P6_3/mmc$. The reciprocal and unit cells derived from the X-ray and electron data are summarized in fig. 6. It is interesting to note that whereas fibre rotation patterns do not distinguish between the apparent and true unit cells, single-crystal patterns are unequivocal. Fig. 5 also shows that $hh\bar{2}\bar{h}0$ reflections are much weaker for odd values of h than for even values.

Electron micrographs of fibres do not appear markedly hexagonal. It has already been stated that only a few electron-diffraction patterns show clear Laue zones. The angle between adjacent $\{10\bar{1}0\}$ and $\{11\bar{2}0\}$ planes is 30°, and in each case where Laue zones were present it was necessary to tilt the specimen stage up to 5° in order to centre the zero-order zone. This suggests that orientation of the fibres around their axes is random, and that there are no good cleavages in the zone parallel to c.

Chemical analysis and atomic cell contents.

A semi-quantitative spectrographic analysis of erionite gave: Si greater than 10 %; Al, Ca, Na, K, 10 to 1 %; Mg 1 to 0·1 %; Fe, Mn, Ba, Sr, 0·1 to 0·01 %; Cr, 0·01 to 0·001 %; and Zr, V, Cu, Ag, Ni, B, below 0·001 %.[1]

A new chemical analysis was made on 2 g. of selected and purified material. The results checked Eakle's analysis very closely, but with slightly higher water content and lower alkalis. Atomic cell contents

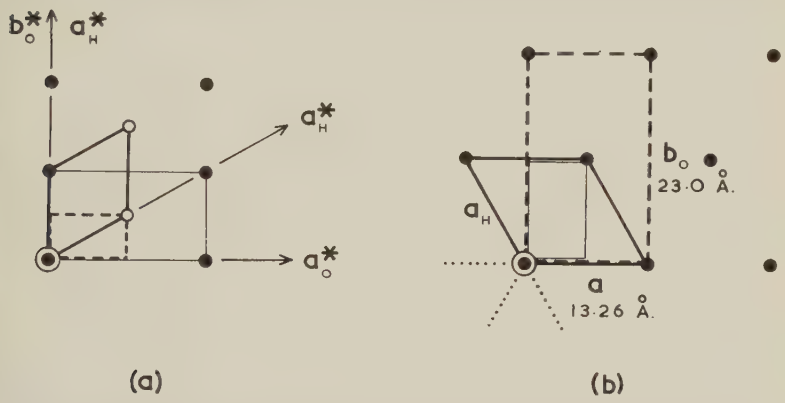

FIG. 6. Parts of the *c*-faces of (*a*) reciprocal and (*b*) real lattices of erionite. In (*a*) black circles represent the reciprocal lattice points derived from the X-ray data, and open circles the extra points revealed by electron diffraction. In both (*a*) and (*b*) thin lines outline the orthorhombic cell indicated by the X-ray data, broken lines the larger *C*-centred orthorhombic cell indicated by electron diffraction, and heavy full lines the equivalent hexagonal cell. Dotted lines in (*b*) show the positions of the [10$\bar{1}$0] glide planes.

were calculated for both analyses, assuming the highest experimental value for the specific gravity, 2·02. Results (table II) indicate the general formula $(Ca,Mg,Na_2,K_2)_{4\cdot5}Al_9Si_{27}O_{72}.27H_2O$. The specific gravity calculated from this formula is 2·07, which is slightly higher than the experimental value. The formula differs from that suggested by other writers, but indicates the presence in the unit cell of 36 $(Si,Al)O_4$ tetrahedra, which is more in accord with the hexagonal symmetry.

After submission of this paper, K. S. Deffeyes (1959) has published a single-crystal X-ray study on erionite from Nevada that indicates a hexagonal unit cell, density, and atomic cell contents similar to those

[1] Spectroscopist: T. C. Matthews, Oregon State Department of Geology and Mineral Industries, 9 Feb. 1954.

given above. $hh\bar{2}hl$ reflections were also missing for l odd. These data confirm those on which the crystal structure proposed in the following section is based.

Eakle noted that erionite contains ammonia and found 0·22 % present. Newly collected erionite was tested with freshly prepared Nessler reagent and gave a strong positive reaction, confirming Eakle's

TABLE II. Atomic cell contents for erionite, calculated on the basis of a hexagonal unit cell with a 13·26, c 15·12 Å. (unit-cell volume 2300 Å^3) and specific gravity 2·02.

	1.	2.		3.	4.	5.
SiO_2 ...	57·16	57·40	Si ...	26·68	26·80	27 } 36
Al_2O_3 ...	16·08	15·60	Al ...	8·82	8·57	9 }
CaO ...	3·50	2·92	Ca ...	1·75	1·46	}
MgO ...	0·66	1·11	Mg ...	0·45	0·77	} 9†
K_2O ...	3·51	3·40	K ...	2·09	2·02	}
Na_2O ...	2·47	1·45	Na ...	2·23	1·31	}
			O ...	71·0	70·3	72
			(not as H_2O)			
H_2O* ...	17·30	17·58	H_2O...	26·9	27·4	27
	100·68	99·46	† Calculated as monovalent ions.			

* H_2O at 100° C., 7·69 %; H_2O at 400° C., 15·44 %; total H_2O at 820° C., 17·58 %.

1. Chemical analysis by A. S. Eakle (1898).
2. Chemical analysis by L. L. Hoagland, Oregon State Department of Geology and Mineral Industries (1954).
3. Atomic cell contents calculated from 1.
4. Atomic cell contents calculated from 2.
5. Idealized atomic cell contents.

Idealized cell contents $(Ca,Mg,Na_2,K_2)_{4\cdot5}Al_9Si_{27}O_{72}.27H_2O$.
Calculated specific gravity, 2·07.

result. Ammonium ions may partly account for the small discrepancy (equivalent to 0·46 % NH_3) between the molar proportions of alumina and total alkalis and alkaline earths in the new chemical analysis. Ammonium zeolites have been prepared artificially (see Hey, 1955), but erionite is the only natural zeolite reported that contains a significant proportion of ammonia.

Structure.

Zeolites contain anionic frameworks in which all the oxygen atoms are shared between two $(Si,Al)O_4$ tetrahedra, and which are traversed by channels large enough to accommodate the cations and water molecules. Erionite is unusual among the zeolites in having hexagonal, but not rhombohedral, symmetry. It also differs from the other fibrous zeolites (see A. F. Wells, 1950, p. 589), which have columns with a

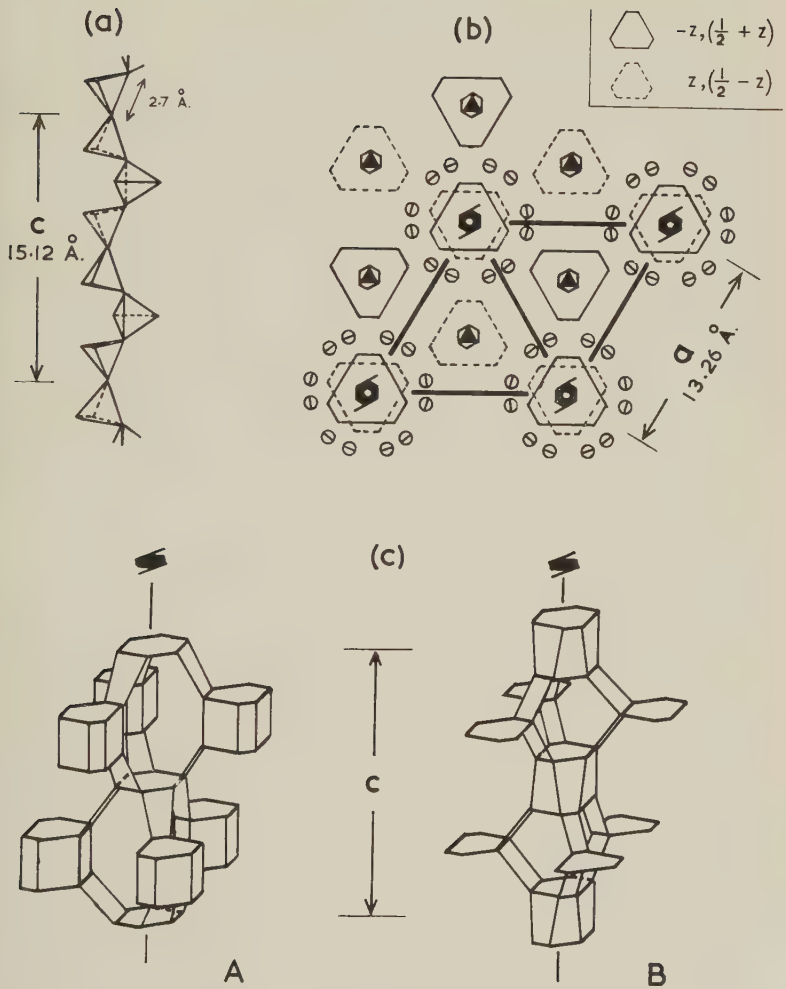

FIG. 7. (*a*) The 15·12 Å. *c*-spacing of erionite can accommodate 6 $(Si,Al)O_4$ tetrahedra, which form part of a continuous chain. (*b*) By suitable choice of *x*- and *y*-coordinates, the 24 general positions in the space-group $P6_3/mmc$ may be linked to form 6-membered rings. (*c*) The two possible ways of stacking six such rings. Comparison of calculated and observed structure factors shows that 'B' represents the correct structure.

repeating unit of five tetrahedra, cross-linked to give near-tetragonal symmetry; the fibre spacing is either about 6·6 or 13·2 Å., compared with 15·12 Å. for erionite. These distinctive characteristics of erionite make it interesting to speculate on its possible structure.

J. V. Smith (1954) has shown that the mean value for (Si,Al)–O bond lengths is 1·645±0·01 Å. for aluminosilicates in which the Al:Si ratio is 1:3, as in erionite, giving a mean value of 2·69 Å. for the edges of the $(Si,Al)O_4$ tetrahedra. The fibre spacing of 15·12 Å. could accommodate 6 such tetrahedra, each with one edge almost parallel to the *c*-axis, linked to form a continuous chain as in fig. 7*a*, in accordance with the fibrous nature of erionite; 6 such chains would be present in the unit cell. $P6_3/mmc$ appears to be the most probable space-group, as it would allow the maximum number, 24, of the 36 (Si,Al) atoms to occupy general positions, of which there are 6 in each plane normal to *c* at heights z, $(\frac{1}{2}-z)$, $(\frac{1}{2}+z)$, $-z$. Fig. 7*b* shows that suitable choice of x and y-co-ordinates would permit cross-linkage through oxygen bonds into rings containing 6 (Si,Al) atoms. Further bonding in the *c*-direction would give 'double-decker' rings, either with one centred on each of the $\bar{6}$-axes at (1/3, 2/3, z) and (2/3, 1/3, z), or with both centred on the 6_3-axis at (0,0,z). The remaining 12 (Si,Al) atoms must occupy special positions, and could form two 6-membered rings acting as links between the double rings. Thus, the two types of structure "A" and "B" shown in fig. 7*c* are possible; "B" is unambiguous, but the unit-cell parameters permit two variations of "A" differing only in orientation of the tetrahedra in the double rings. The X-ray powder pattern contains only 10 unambiguous reflections, too few to test the validity of the structures. Intensities were therefore estimated from the fibre rotation patterns by visual comparison with a standard exposure strip, and structure factors ($|F_0|$) were derived by application of polarization, Lorenz, and Cox and Shaw factors. Correlation with calculated structure factors ($|F_c|$) of *hki*0 reflections was poor for structures "A1" and "A2", but was satisfactory for "B", even when the comparison was extended to the other 8 recorded layer lines. The structure factors are shown in fig. 8 on a scale that represents values of $|F_c|$, but as no correction was made for absorption, comparison is only reliable within each layer, and values of $|F_0|$ have been adjusted therein so that $\Sigma|F_0| = \Sigma|F_c|$. The validity of structure "B" was confirmed by calculation of reliability factors $R = \Sigma(|F_0|-|F_c|) \div \Sigma|F_0|$, which are listed in table III. The rather poor correlation for *hki*1 reflections is due to an anomalously high value of $|F_c|$ for $10\bar{1}1$.

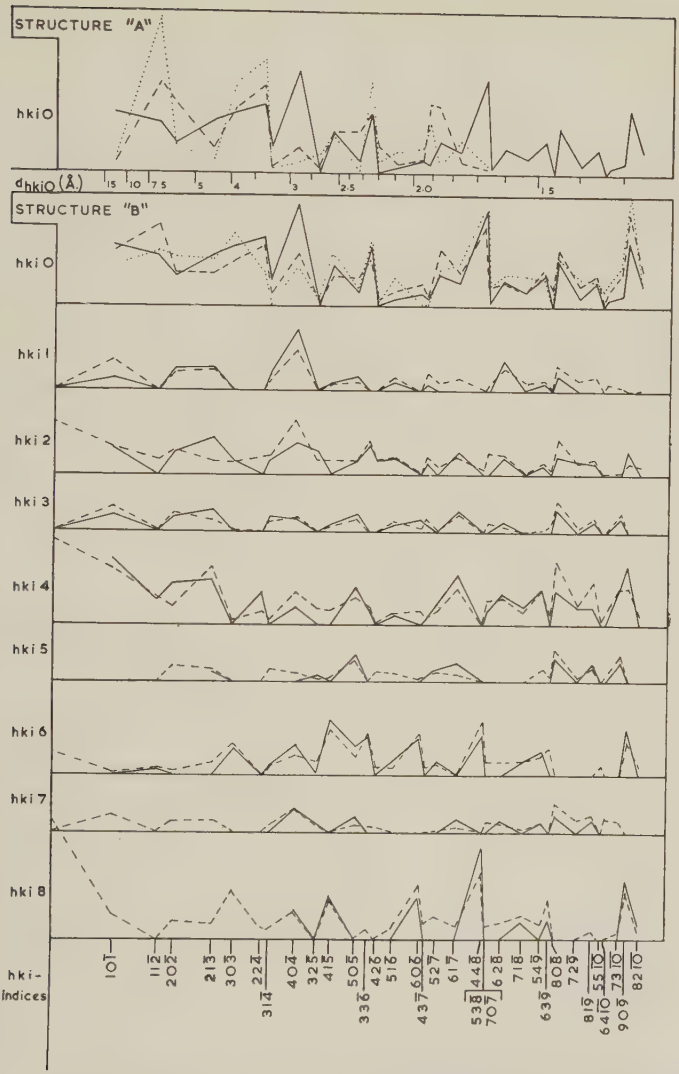

FIG. 8. Observed structure factors ($|F_0|$, represented by full lines) derived from the X-ray data, compared with those calculated ($|F_c|$, represented by broken lines) for the possible frame structures of erionite shown in fig. 7*c*. Correlation was poor for both of the minor variations of "A" (represented by broken and dotted lines in the upper graph), but was satisfactory for "B" for all recorded layer lines. The dotted line in the zero layer of "B" represents $|F_c|$ when the cations were assumed to be situated at (2/3, 1/3, *z*) and (1/3, 2/3, *z*). Correlation was slightly poorer than for the frame alone.

In an attempt to locate the approximate positions of the cations, they were provisionally assumed to be situated with random distribution on the principal axes of the cavities, i.e. at (2/3,1/3,z) and (1/3,2/3,z).

TABLE III. Reliability factors $R = \Sigma(|F_0|-|F_c|) \div \Sigma|F_0|$ for reflections observed in X-ray fibre rotation patterns of erionite and the two types of structure shown in fig. 7c. Value of $|F_0|$ were normalized so that $\Sigma|F_0| = \Sigma F_c|$ within each layer. Correlation was so poor for structures A1 and A2 that values of F_c were not calculated for reflections with d-spacings less than 1·65 Å.

1.	2.	3.	4.	1.	2.	3.	4.
A1	0	19	0·80	B	3	15	0·35
A2	0	19	0·88	B	4	21	0·36
B	0	28	0·30	B	5	8	0·28
B+ cations*	0	28	0·34	B	6	12	0·25
B	1	12	0·46	B	7	8	0·34
B	2	19	0·31	B	8	9	0·30

1. Type of structure shown in fig. 7c.
2. l-index.
3. Number of reflections with calculated or observed structure factors above the observable minimum.
4. Reliability factor (R).

* The cations were assumed to be situated with random distribution on the principal axes of the cavities, i.e. at (2/3, 1/3, z) and (1/3, 2/3, z).

TABLE IV. Atomic coordinates for the aluminosilicate frame of erionite.

1.	2.	3.	x.	y.	z.
Si_I	24	l	0·000	0·237	0·106
Si_{II}	12	j	0·088	0·421	0·250
O_I	24	l	0·017	0·350	0·162
O_{II}	12	k	0·106	0·212	0·128
O_{III}	12	k	0·123	0·246	−0·133
O_{IV}	12	i	0	0·262	0
O_V	6	h	0·217	0·434	0·250
O_{VI}	6	h	0·450	0·900	0·250

1. Atoms, numbered as in fig. 9.
2. Number of equivalent atoms in one unit cell.
3. Type of atomic site (Wyckoff notation, International Tables for X-ray Crystallography, vol. 1, p. 304).

Structure factors were again calculated for the $hki0$ reflections, but correlation with $|F_0|$ values gave $R = 0·34$, rather higher than for the frame alone (table III), showing that the assumption was probably incorrect.

Projections of the structure of the erionite frame are shown in fig. 9, and atomic coordinates are listed in table IV. The mean (Si,Al)–0 bond

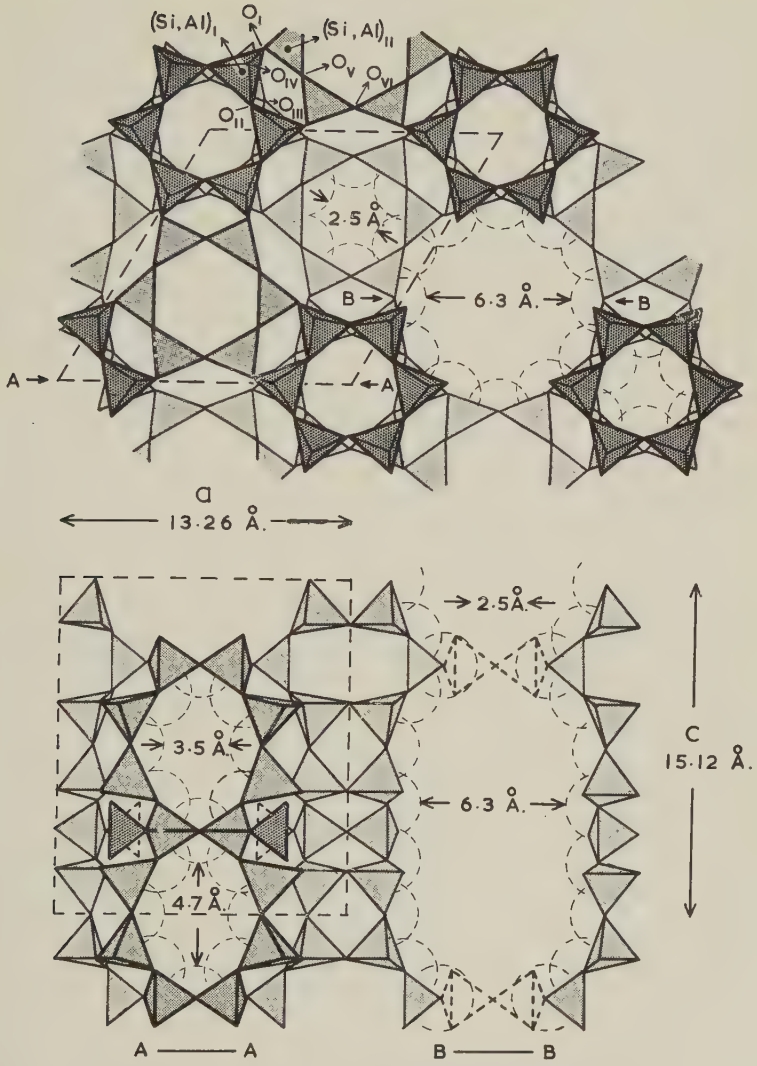

FIG. 9. Above, (0001) projection of erionite frame, showing the disposition of the $(Si,Al)O_4$ tetrahedra. Typical atoms are numbered as in Table III. Single rings are at $z = \frac{1}{4}$ (thin lines) and $z = \frac{3}{4}$ (heavy lines). Each has a 'window' with a free diameter of 2·5 Å.; one has been removed to show the free space at the centre of a cavity. Below, $(10\bar{1}0)$ projection, showing on the left the larger windows through 8-membered rings. These have been removed on the right to show a section of a cavity.

length is 1·635 Å., which is within the limits given by Smith (1954); Si–O–(Si,Al) bond angles vary between 137 and 170°. Fig. 10 shows views of a model of the aluminosilicate frame, in which the corners of polyhedra represent Si or Al atoms. It is characterized by columns in the *c*-direction, separated by cavities with a free diameter of about 6·3 Å., and a total length of 15·12 Å. Each column contains 6 chains of tetrahedra which are strongly cross-linked, but other bonds are comparatively few, explaining the fibrous nature of erionite and the absence of a distinct cleavage in the (*hki*0) zone. Each cavity is connected with six others through windows with a minimum free span of 3·5 Å., and with two others in the [0001] directions through smaller windows with a free diameter of 2·5 Å. The contents of each cavity thus have access to all others through the larger windows, suggesting that erionite should have a good capacity for base exchange, and that it could be used as a molecular sieve (see, for example, D. W. Breck and J. V. Smith, 1959).

Discussion.

Correlation between observed and calculated structure factors indicates that the structure shown in figs. 9 and 10 is substantially correct for the erionite frame. The presence of some anomalous values for F_c may be due to the effect of cations and water molecules, or to minor inaccuracies in the positions of the atoms of the frame. Fourier synthesis could assist in defining the complete structure. The X-ray data are adequate for refinement of the (0001) projection, but not of the *z*-coordinates. It has been shown (figs. 4 and 5) that electron-diffraction patterns can be recorded corresponding to $(11\bar{2}0)$ and $(10\bar{1}0)$ sections of the reciprocal lattice, raising the possibility of refinement of these projections, but the measurement of intensities presents a major difficulty. However, Burge *et al.* (1957) have described a modification to the electron microscope that spreads each spot into a rectangle of even optical density, which is claimed to facilitate accurate measurement of intensities.

Since this paper was read, L. S. Dent and J. V. Smith (1958) have proposed a new structure for chabazite, which makes an interesting comparison with that of erionite.[1] Chabazite is trigonal with a_H 13·78, c_H 15·03 Å. As in erionite, the *c*-spacing contains chains of 6 tetrahedra, and there are 6 rings in the unit cell each with 6 (Si,Al) atoms. In

[1] The authors are grateful to Dr. J. V. Smith for indicating the resemblance between the structures of chabazite and erionite, and to Dr. I. S. Kerr for pointing out the relation between the unit cells of levyne and erionite.

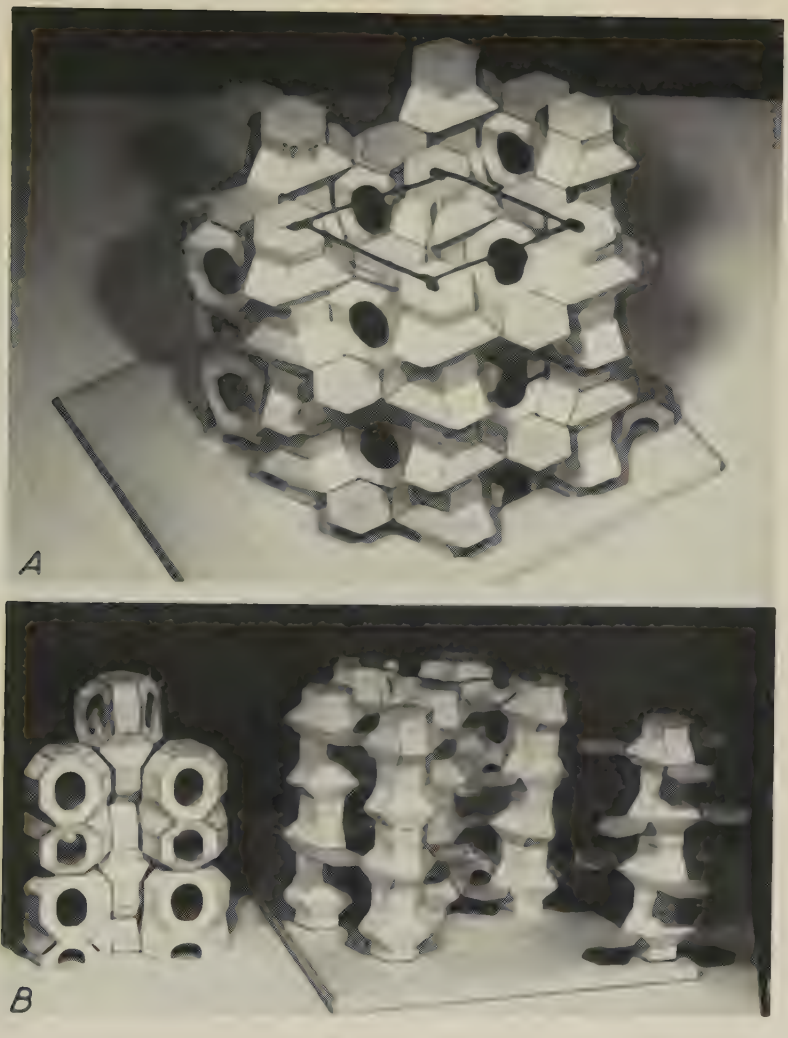

FIG. 10. Views of a model of the erionite frame, in which oxygen atoms are ignored, and corners represent (Si,Al) atoms. It is two unit cells high, with the fibre (*c*-) direction vertical, and the (0001) face on the base. The compact columns parallel to *c* are shown, and the cavities which carry the cations and water. Each cavity connects to six neighbouring ones through 'windows', and there are continuous channels in the [1120] and approximate [1121] directions. The compact columns are cross-linked by more widely spaced bonds, explaining the fibrous nature. In (*A*) the cavities are stacked in place between the compact columns; in (*B*) they are stacked separately, but in the same orientation, and one column has been detached from its neighbours.

chabazite, however, they are all linked in double rings situated at the corners of the rhombohedral cell. The cavities in chabazite are slightly smaller but more numerous, in the ratio 3:2, than those in erionite. Each cavity in both structures has windows formed from 8-membered rings. Levyne[1] (H. Strunz, 1956) is another zeolite that may have a structure related to that of erionite. It is hexagonal, with a 13·3, c 22·5 Å., so that the unit cell may contain nine 6-membered rings.

Synthesis of erionite is probably difficult to achieve, as it has only once been reported (Breck *et al.*, 1956; no details were given). It also occurs rarely in nature, which suggests that highly specific conditions are necessary for its formation. In order to explain the regular manner in which complex aluminosilicates crystallize, R. M. Barrer *et al.* (1959) have proposed that the first stage is the formation in solution of anionic units, comprising rings or polyhedra of linked $(Si,Al)O_4$ tetrahedra. Preservation of order during condensation of these complex units is easier to visualize than a similar process with tetrahedra as the building units. The simplest recurring unit into which the erionite frame can be divided is a polyhedron containing 18 (Si,Al) atoms, two of which occur between the (0001) unit-cell faces centred on the 6_3 axis (fig. 7*c*, "B"), and which in turn could be formed by condensation of the three 6-membered rings which lie roughly parallel to the c-axis. The unit of the chabazite structure could be the double 6-membered ring, formed by condensation of either two 6-membered or three 4-membered rings. The comparative simplicity of the repeat unit in chabazite may explain why that mineral is more abundant in nature and easier to synthesize than erionite.

Acknowledgements. The authors wish to thank Prof. R. M. Barrer, Dr. H. F. W. Taylor, and Dr. F. W. Bultitude for discussions that assisted greatly in elucidation of the proposed structure.

Thanks are also to be given to Prof. A. Pabst of the University of California, Berkeley, for supplying some of Eakle's original specimen material and for use of laboratory facilities and assistance in the work. Material from the U.S. National Museum was supplied by Dr. G. Switzer. The chemical analysis was made by L. L. Hoagland, and the spectrographic analysis by T. C. Matthews, both of the Oregon State Department of Geology and Mineral Industries.

References.

Barrer (R. M.), Baynham (J. W.), Bultitude (F. W.), and Meier (W. M.), 1959. Journ. Chem. Soc., p. 195.

Breck (D. W.), Eversole (W. G.), Milton (R. M.), Reed (T. B.), and Thomas (T. L.), 1956. Journ. Amer. Chem. Soc., vol. 78, p. 5963.

—— and Smith (J. V.), 1959. Scientific American, vol. 44, p. 85.

[1] See footnote on p. 278.

Burge (R. E.), Munden (H. R.), and Curling (M. A.), 1957. Journ. Sci. Instr., vol. 34, p. 305.
Deffeyes (K. S.), 1959. Amer. Min., vol. 44, p. 501.
Dent (L. S.), and Smith (J. V.), 1958. Nature, vol. 181, p. 1794.
Eakle (A. S.), 1898. Amer. Journ. Sci., ser. 4, vol. 6, p. 66.
Fernquist (C.), 1937. The Mineralogist (Portland, Oregon), vol. 5, p. 18.
Fitzsimmons (J. P.), 1949. Doctoral Dissertation, Univ. of Washington.
Gard (J. A.), 1956*a*. Journ. Sci. Instr., vol. 33, p. 307.
—— 1956*b*. Brit. Journ. Appl. Phys., vol. 7, p. 361.
Haine (M. E.), Page (R. S.), and Garfitt (R. G.), 1950. Journ. Appl. Phys., vol. 21, p. 173.
Hey (M. H.), 1932. Min. Mag., vol. 23, p. 51.
—— 1955. An Index of Mineral Species and Varieties, 2nd edn, British Museum, London.
—— 1959. Min. Mag., vol. 32, p. 343.
Larsen (E. S.), 1921. U.S. Geol. Surv., Bull. 679.
Lindberg (M. L.), Pecora (W. T.), and Barbosa (A. L. de M.), 1953. Amer. Min., vol. 38, p. 1126.
Lindgren (W.), 1901. U.S. Geol. Surv., 22nd Ann. Rep., Pt. 2, p. 553.
Morse (H. W.) and Donnay (J. D. H.), 1936. Amer. Min., vol. 21, p. 391.
Reed (J. C.), 1937. Trans. Amer. Geophys. Union, Pt. 1, p. 239.
Regnier (J.), 1958. Ph.D. Thesis, Columbia Univ., New York; Bull. Geol. Soc. Amer., in the press.
Smith (J. V.), 1954. Acta Cryst., vol. 7, p. 479.
Strunz (H.), 1956. Neues Jahrb. Min. (Monats.), vol. 11, p. 250.
Thugutt (S. J.), 1948. Rocz. Polsk. Tow. Geol., vol. 18, p. 5.
Warren (B. E.) and Biscoe (J.), 1938. Journ. Amer. Ceram. Soc., vol. 21, p. 49.
Wells (A. F.), 1950. Structural Inorganic Chemistry, 2nd edn, Oxford University Press, London.

Yoderite, a new hydrous magnesium iron aluminosilicate from Mautia Hill, Tanganyika.

(With Plate XI.)

By Duncan McKie, M.A., B.Sc., A.R.I.C., F.G.S.
Dept. of Mineralogy and Petrology, Downing Place, Cambridge.

With chemical analyses by A. J. Radford, B.Sc., F.R.I.C.
Geological Survey, Causeway, Salisbury, Southern Rhodesia.

[Read 6 November 1958.]

Summary. Yoderite occurs as a major constituent in a quartz–kyanite–talc schist, and is a high-pressure phase formed by the reaction Ky + Tc→Yd + Qu. The monoclinic unit-cell, a 8·10 Å., b 5·78 Å., c 7·28 Å., β 106°, space-group $P2_1$ or $P2_1/m$, contains approximately $(Mg_{2\cdot0}Ca_{0\cdot2}Fe_{0\cdot5}Al_{5\cdot3})Si_{4\cdot0}O_{17\cdot6}(OH)_{2\cdot4}$. The structure appears to be related to that of kyanite, with which the mineral is intergrown; it is not an analogue of staurolite. The three strongest powder lines are 3·50 Å. vvs, 3·03 Å. vs, 2·61 Å. s. Specific gravity 3·39. Subsidiary reflections, similar to those of the intermediate plagioclases, have indices with non-simple fractional values of k. Optical properties are α 1·689 pale Prussian blue, β 1·691 indigo, γ 1·715 light olive-green, absorption $\beta > \alpha > \gamma$, $2V_\gamma$ 25°, optic axial plane {010}, γ:[001] $\approx 7°$ in the obtuse angle β. An interpretation of the colour on the electron-exchange hypothesis $Fe^{2+} \rightleftharpoons Fe^{3+} + e^-$, is suggested. A kinetic study has been made of the disappearance of the subsidiary reflections in the range 700° C. to 820° C.; further heating to 850° C. produces the metastable appearance of mullite, and at temperatures above 1100° C. the equilibrium anhydrous assemblage indialite + sapphirine appears.

YODERITE, a spectacular purple mineral, occurs in a quartz–yoderite–kyanite talc schist at Mautia Hill (6° 8½′ S., 36° 29′ E.), 6 miles north-east of the former Groundnut Scheme headquarters at Kongwa, Mpwapwa District, Central Province, Tanganyika Territory. The general geology of the district has been described by Temperley (1938), who regarded (p. 40) the yoderite-bearing rocks as glaucophane–kyanite–magnetite–muscovite–quartz schists and observed that 'glaucophane' always surrounds kyanite; a more detailed account of the petrology of Mautia Hill is in course of preparation by the author and J. R. Harpum. Mautia Hill is an east–west ridge, 2 miles long by ½ mile wide, of metamorphic rocks of the Usagaran System (Archaean), consisting of steeply dipping units of east–west striking crystalline lime-

stone, quartzite, piemontite–quartzite, kyanite–biotite gneiss, quartz–yoderite–kyanite–talc schist, and amphibolite, the whole completely surrounded by the poorly exposed migmatites of the Kongwa plains. No recognizable continuation of the distinctive Mautia succession appears to occur either to the east or the west.

The mineral is named in honour of Dr. H. S. Yoder, Jr., of the Geophysical Laboratory, Carnegie Institution of Washington, who first studied experimentally the central part of the MgO–Al_2O_3–SiO_2–H_2O system, within which 92 % of the composition of yoderite lies.

Yoderite has in the past been mistaken for glaucophane and for dumortierite, the characteristic pleochroism of which is closely similar; it was first recognized as a distinct mineral by its X-ray powder pattern.

Petrography. The quartz–yoderite–kyanite–talc schist is composed of coarse interlocking, often curved, flakes of talc with interstitial patches of quartz, exhibiting strain shadows; large irregularly margined grains of yoderite enclose random flakes of talc and some quartz. The general aspect of the rock is shown in pl. XI, fig. 1. A constant feature is the presence within each yoderite grain of relicts of kyanite (pl. XI, fig. 3), and kyanite occurs rimmed by yoderite (pl. XI, fig. 4). Quartz and talc occur on the outer margins of yoderite grains; the replacement of talc by yoderite is shown in pl. XI, fig. 2. Small rounded grains of hematite are randomly distributed through all other minerals. Yoderite and kyanite both contain large rounded quartz inclusions (pl. XI, figs. 3, 4); less regular patches of quartz also occur within yoderite grains. Every yoderite grain, however large and poikiloblastic, is optically a single crystal and all the kyanite relicts within it are in parallel orientation. Yoderite invariably separates talc from kyanite; assemblages present are quartz–yoderite–kyanite–hematite and quartz–yoderite–talc–hematite.

The proportions of quartz and talc vary markedly from the common talc-rich schistose type to a talc–yoderite–kyanite–quartzite. Yoderite has been studied from two specimens, a talc-rich type bearing the Geological Survey of Tanganyika number JH 2563/2 and a quartz-rich type numbered JH 2563/14.

Chemical composition.

Yoderite from specimen JH 2563/2 was freed from talc and quartz by centrifugal separation of −60 mesh +120 mesh material in methylene iodide, followed by electromagnetic removal of hematite, repeated electromagnetic separation of weakly magnetic yoderite from kyanite,

and finally hand-picking. Some 2 g. were available for the main analysis and a further portion, crushed to −90 mesh +120 mesh, was very carefully picked free of hematite-contaminated grains for the iron determinations.

The analysis is set down in table I and corresponds to the formula $(Mg_{2\cdot0}Ca_{0\cdot2}Fe_{0\cdot5}Al_{5\cdot3})Si_{4\cdot0}O_{17\cdot6}(OH)_{2\cdot4}$. H_2O+ was determined by direct weighing of the water evolved on ignition at 1100° C. in a tube furnace. The marked insolubility of yoderite made the determination of FeO

TABLE I. Chemical composition and unit-cell contents of yoderite.

		1.	2.			3.	4.	
SiO_2	...	36·12	36·07	Si^{4+}	...	0·6006	4·00	4·03
TiO_2	...	0·35	0·35	Ti^{4+}	...	0·0044	0·03	
Al_2O_3	...	41·06	41·00	Al^{3+}	...	0·8041	5·35	8·06
Fe_2O_3	...	0·50	0·50	Fe^{3+}	...	0·0063	0·04	
FeO	...	4·82	4·81	Fe^{2+}	...	0·0670	0·45	
MnO	...	0·32	0·32	Mn^{2+}	...	0·0045	0·03	
MgO	...	12·23	12·21	Mg^{2+}	...	0·3028	2·02	
CaO	...	1·48	1·48	Ca^{2+}	...	0·0262	0·17	
Na_2O	...	0·01	0·01	Na^{+}	...	0·0003	—	
K_2O	...	0·05	0·05	K^{+}	...	0·0011	—	
H_2O+	...	3·20	3·20	OH^{-}	...	0·3552	2·36	20·00
H_2O-	...	0·05	—	O^{2-}	...	2·6495	17·64	
		100·19	100·00					

1. Analysis of yoderite from specimen JH 2563/2. Analyst: A. J. Radford.
2. Analysis 1 recalculated to 100 % on an H_2O- free basis.
3. Atomic ratios.
4. Unit-cell contents corresponding to 20 anions per unit cell.

difficult; the method of Groves (1951, p. 183) proved unsatisfactory and I am indebted to Mr. J. H. Scoon[1] for a redetermination using Hey's (1941) micro-method, the result of which is quoted in table I. Cu, Pb, Co, Ni, B, and P were sought and found not to be present in significant amounts. Dr. S. R. Nockolds[1] confirmed the absence of Cu, Co, F, and B spectrographically.

Physical properties.

Yoderite occurs in anhedral, irregularly lath-shaped grains up to $\frac{1}{2}\times\frac{1}{4}\times\frac{1}{8}$ inches. Its hardness is 6 on Mohs' scale. Measurements of specific gravity by displacement of methylene iodide from a specific gravity bottle gave a value of 3·39. Refractive indices at 20° C. are α 1·689, β 1·691, γ 1·715 (all ±0·002); and $2V_\gamma$ 25° (±2°). The pleochroic

[1] Department of Mineralogy and Petrology, University of Cambridge.

scheme is α pale Prussian blue, β indigo, γ light olive-green, with absorption $\beta > \alpha > \gamma$. In the absence of crystal faces and good cleavages the orientation of the optical indicatrix had to be determined by direct reference to the chosen monoclinic crystallographic axes; optical directions in a grain were labelled by attaching glass fibres and the grain was then completely oriented by a zero-layer *b*-axis Weissenberg photograph. The optic axial plane is {010}, $\alpha \wedge a \approx 9°$ and $\gamma \wedge c \approx 7°$, both in the obtuse β-angle. Parting directions are [001] moderately good and {100} poor. Grains are elongated parallel to [010] and longitudinal sections can therefore be length fast or length slow.

Table II. X-ray powder data for yoderite.

d, Å.	*I.*	*d*, Å.	*I.*	*d*, Å.	*I.*	*d*, Å.	*I.*
4·64	w	1·97	m	1·219	vw	0·909	vvw
4·18	vvw	1·89	w	1·210	vw	0·893	vvw
3·87	vw	1·84	vvw	1·202	vw	0·891	vvw
3·83	vw	1·82	s	1·197	vw	0·888	vvw
3·63	w	1·752	vvw	1·175	vvw	0·883	vvw
3·50	vvs	1·727	m	1·166	vvw	0·863	vvw
3·34	vvw	1·698	vw	1·101	vvw	0·861	vvw
3·23	ms	1·647	vw	1·076	vwB	0·845	vvw
3·19	ms	1·610	w	1·058	vvw	0·843	vvw
3·07	vw	1·596	w	1·054	vvw	0·8375	vvw
3·03	vs	1·561	vvw	1·041	vvw	0·8360	vvw
2·91	ms	1·547	w	1·038	vvw	0·8306	vvw
2·72	vw	1·534	w	1·033	vw	0·8284	vvw
2·68	m	1·515	w	1·007	vw	0·8256	vvw
2·65	vw	1·499	wB	1·005	vvw	0·8232	vw
2·61	s	1·473	wB	0·999	w	0·8184	vvw
2·58	ms	1·451	m	0·997	vw	0·8165	vvw
2·46	ms	1·437	vw	0·985	vw	0·8142	vvw
2·41	vvw	1·415	w	0·983	vvw	0·8131	vvw
2·39	mw	1·399	mw	0·977	vvw	0·8110	vvw
2·36	w	1·382	vwB	0·973	vvw	0·8085	vvw
2·32	w	1·356	m	0·967	vw	0·8051	vvw
2·27	vw	1·340	vw	0·964	vvw	0·8029	vvw
2·24	msB	1·328	m	0·945	vw	0·8005	vvw
2·16	vw	1·298	vw	0·943	vvw	0·7979	vvw
2·11	vw	1·286	vvw	0·939	vw	0·7957	vvw
2·06	vvw	1·265	vvw	0·925	vvw	0·7865	vvw
2·00	s	1·240	vvw	0·915	vvw	0·7785	vvw

X-ray powder data for the analysed sample of yoderite (JH 2563/2). Relative intensities *I* were estimated visually. A camera of 19 cm. diameter and Cu-$K\alpha$ radiation were used.

X-ray powder data for yoderite are presented in table II; 112 lines were measured. The three strongest lines are: 3·50 Å. vvs, 3·03 Å. vs,

2·61 Å. s. The iron content of the mineral is not high enough to produce any serious fluorescent fogging with Cu-$K\alpha$ radiation.

X-ray crystallography.

In the single-crystal study of yoderite grains were used from specimens JH 2563/2 and JH 2563/14; no differences were observed in the diffraction patterns. The symmetry of a *b*-axis oscillation photograph and that of a zero-layer Weissenberg photograph about the *b*-axis show that the mineral is monoclinic. The unit-cell dimensions and space-group were determined from oscillation photographs about the *a*, *b*, and *c* axes, and from zero and fourth layer Weissenberg photographs about the *a*-axis. The unit-cell dimensions are *a* 8·10 Å., *b* 5·78 Å., *c* 7·28 Å. (all $\pm$0·05 Å.), and β 106° ($\pm$1°); $a:b:c = 1{\cdot}402:1:1{\cdot}259$. The only systematic absences were $0k0$ with k odd. Certain extra weak reflections that cannot be indexed on the lattice described above were observed on all overexposed photographs and will be discussed below. The space-group of the pseudo-lattice is therefore $P2_1$ or $P2_1/m$; a positive pyroelectric effect suggests that $P2_1$ is the more likely.

The unit-cell volume 328 Å.^{3} corresponds to the unit-cell contents shown in column 4 of table I, or to $\{X_2Si(O,OH)_5\}$, analogous to the aluminium silicate formula Al_2SiO_5 with some replacement of Al and O, all positions being occupied and no Si replaced. Al^{3+} is replaced essentially by Mg^{2+}, Fe^{2+}, Fe^{3+}, and Ca^{2+}, one-third of the Al^{3+} ions being replaced; the charge deficiency is compensated by the substitution of 2·35 OH^- for O^{2-}. The volume per oxygen atom is 16·4 Å.^{3}, compared with 14·2 Å.^{3} in kyanite (where the oxygen ions are approximately in cubic close packing), 16·2 Å.^{3} in sillimanite, 15·2 Å.^{3} in staurolite, and 17·1 Å.^{3} in mullite increasing to 17·5 Å.^{3} in synthetic iron-rich mullites.

Yoderite is seen in thin-section to contain relicts of kyanite in constant optical orientation. An oscillation photograph of a composite grain about the *b*-axis of yoderite indicated *b* (yoderite) || *c* (kyanite), and a zero layer Weissenberg photograph about this common axis gave a complete account of the relative orientation, which is shown in fig. 1. Extra reflections on the Weissenberg photograph show that kyanite in this grain is twinned about the normal to {100}, a not uncommon twin law in kyanite. *b* 5·78 Å. of yoderite is similar and parallel to *c* 5·56 Å. of kyanite, representing the length of two octahedral groups in the aluminium-oxygen chains, a common feature of the unit cells of all the aluminium silicates; *a* 8·10 Å. for yoderite is similar and parallel to *b* 7·72 Å. for kyanite; *c* 7·28 Å. for yoderite is not dissimilar to $a \sin \beta$

6·96 Å. for kyanite. Thus the yoderite unit cell is expanded by about 5 % in the a and c directions relative to kyanite, and by 4 % in the direction of the aluminium-oxygen chains, b_Y being similar to the corresponding parameter a 5·74 Å. of sillimanite. Considerable structural similarity may thus be expected between yoderite and kyanite; chains of aluminium coordinated octahedrally to oxygen may be expected to

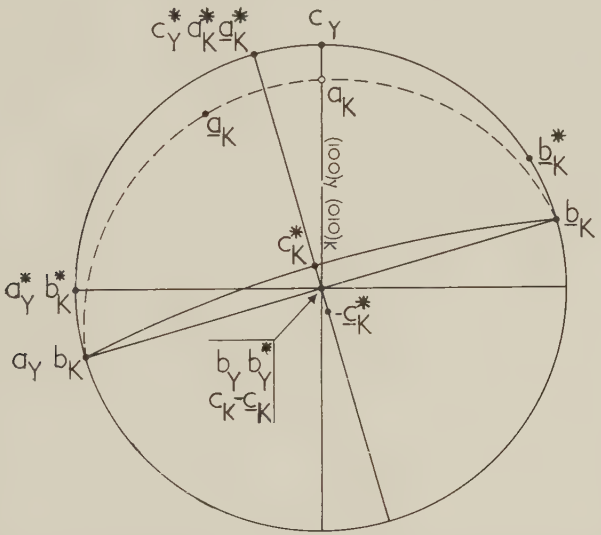

Fig. 1. Stereogram showing the relative orientation of yoderite (Y) and kyanite (K). Underlined symbols refer to the second individual of the kyanite twin.

run parallel to b, the chains being linked laterally by silicon in fourfold coordination and by aluminium probably in sixfold coordination as in kyanite. Aluminium, exhibiting sixfold coordination in both positions, may be designated Al_I in the chains and Al_{II} in the cross-linkages; the cations substituting for Al in yoderite all normally exhibit sixfold coordination and might therefore appear to replace Al in either position. The distribution of the 2·4 OH^- ions per unit cell may be random, but if the explanation of the colour of yoderite given below is correct and Weyl's (1951) interpretation of the pleochroic scheme of biotite is of general application the OH^- ions should be concentrated on planes perpendicular to the direction of minimum absorption γ, that is near $(\bar{1}06)$, which is parallel to $(6\bar{1}0)$ of kyanite, a plane, however, of no special significance in the kyanite structure.

Consideration of the atomic coordinates in kyanite (Naray-Szabo, Taylor, and Jackson, 1929) clarifies the structural relationship between yoderite and kyanite. Small displacements in the positions of atoms in the kyanite structure can give rise to a monoclinic $P2_1$ lattice, the largest adjustments being in the z-coordinates of Al in cross-linkages, Al_{III} and Al_{IV} of Naray-Szabo *et al.* The dimensions of the resultant unit-cell would be a' 6·96 Å., b' 7·72 Å., c 5·56 Å., β' 106°; it would be oriented with respect to the triclinic kyanite lattice in precisely the same way as yoderite was observed to be oriented in yoderite-kyanite intergrowths. The partial substitution of Mg^{2+} for Al^{3+} would appear to produce the requisite distortion, accompanied by an overall linear expansion of 4–5 %.

The orientation of staurolite with respect to kyanite (Naray-Szabo *et al.*, 1929) contrasts with that of yoderite in intergrowth with kyanite; c is a common direction in both cases, but the common plane is (100) of kyanite in the former and (010) in the latter instance. Fe^{2+} and OH^- ions lie on {010} planes in staurolite, which are parallel to the AlO_6 chains and therefore there is no significant (1 %) increase in chain length. The repeat distance normal to the $Fe(OH)_2$ layers, b_s 16·52 Å., is however of the order of 18 % greater than the corresponding dimension for two units of kyanite structure. The absence of such a strongly directed expansion, the difference in relative orientation, and crystallochemical considerations indicate that yoderite is not analogous to staurolite in its relationship to the kyanite structure.

Subsidiary reflections.

Sharp weak extra reflections occur between the layer lines on heavily exposed b- and c-axis but not on a-axis oscillation photographs. The separation of the subsidiary reflections from the principal layer lines was determined accurately and corresponds to $k = n \pm 0{\cdot}165$, $n \pm 0{\cdot}417$ and $l = n + \frac{1}{2}$; the values of the fractional indices may be expressed approximately, though perhaps without much significance, as $\frac{2}{12}$ ($= 0{\cdot}167$) and $\frac{5}{12}$, corresponding to twelvefold multiplication of the b parameter with systematic absence of all but the $12n$ (strong), $12n \pm 2$, $12n \pm 5$ layer lines. Weissenberg photographs of the zero and fourth layers about the a-axis and of the k 1·417 layer about the b-axis were used to determine the positions of the subsidiary reflections in reciprocal space. Two types of reflections occur, type I with indices $n.\ n' \pm 0{\cdot}417.\ n'' \pm \frac{1}{2}$, and type II with indices $n.\ n' \pm 0{\cdot}167.\ n''$. The diffraction pattern of yoderite is thus characterized by pairs of subsidiary reflections sym-

metrically separated by a translation corresponding to 0·083 b^* from absent reflections which would represent halving of b^* and c^*, and by pairs of subsidiary reflections disposed in an identical manner about the strongest principal reflections; the resemblance of this pattern to that exhibited by intermediate plagioclases and investigated in detail by Cole, Sörum, and Taylor (1951), and Gay (1956), is marked. Any dependence of the separation of the subsidiary reflections on composition cannot be investigated at present as all specimens of yoderite from Mautia Hill produce identical diffraction patterns. Any convincing attempt at explanation of the subsidiary reflections is difficult in a mineral whose structure is undetermined and in which possibilities of the occurrence of ordered sequences in the distributions of Al and Si, Mg and Al, OH and O occur. The very small atomic scattering factor of H, however, makes it unlikely that ordering of the OH distribution could give rise to the observed effects.

The assignment of Al atoms exclusively to sixfold positions and Si atoms to fourfold positions in kyanite provides a completely ordered structure in which no extensive substitution by other cations is known to occur, and it is not surprising to find a complete absence of subsidiary reflections on heavily overexposed c-axis oscillation photographs of kyanite. In staurolite Fe^{2+} and OH^- ions separate blocks of kyanite structure to produce a completely ordered structure, and subsidiary reflections failed to appear on a c-axis oscillation photograph heavily overexposed to Fe-$K\alpha$ radiation. Subsidiary reflections are lacking too on c-axis oscillation photographs of lusakite, which has a structure analogous to staurolite (Skerl and Bannister, 1934). Agrell and Smith (1957) have observed in mullite diffraction patterns certain weak non-integral reflections, which are similar to those of the intermediate plagioclases; such subsidiary reflections may be tentatively related to either the presence of Si and Al in ordered sequences in fourfold positions, or to some degree of ordering in the distribution of 39 O^{2-} between forty available positions, or both.

If the analogy between the inferred structure of yoderite and that of kyanite is as good as has been suggested, the possibility of the subsidiary reflections being due to Si–Al ordering may be ruled out because subsidiary reflections are not observed and such ordering cannot occur in kyanite; thus the subsidiary reflections observed in yoderite may be regarded as related to the presence of ordered sequences in the distribution of Mg and Al in equivalent or nearly equivalent positions.

Heat treatment. Single crystals were subjected to successive heatings so that each crystal had an effectively isothermal history. Temperatures were controlled by a platinum resistance thermometer and continuously recorded by a chromel-alumel thermocouple; a constancy of $\pm 5^\circ$ C. was maintained between successive heatings. Quenching by cooling in air to room temperature took < 3 minutes. After each heating the crystals were examined by oscillation photographs (15° oscillation) about the b-axis with the X-ray beam, accurately set by Laue photograph, in a standard orientation $\perp(403)$; this orientation causes the reciprocal lattice point corresponding to one of the strongest of the subsidiary reflections $1.1{\cdot}417.\bar{\frac{1}{2}}$ to be intersected by the sphere of reflection near the middle of the oscillation. The intensities of this reflection and of two principal reflections (assumed to be unaffected by heating) were measured by visual comparison with a linear intensity scale and the intensity I of reflection $1.1{\cdot}417.\bar{\frac{1}{2}}$ after heating at T° C. for t hours was expressed as a fraction of its initial intensity I_0. As a check on the generality of the intensity variation of $1.1{\cdot}417.\bar{\frac{1}{2}}$, measurements were made of the intensity of the other strong subsidiary reflection $0.1{\cdot}417.\frac{1}{2}$ for heatings at 730° C., and a similar variation was found. No study has been made of the behaviour of type II reflections.

The experimental data can be fitted empirically to a rate law of the form $i-1 = kt$, where $i = \sqrt{I_0/I}$ and k is a constant. Such a law cannot be rationalized until a structure determination and an interpretation of the subsidiary reflections become available; however, if the process by which the subsidiary reflections decrease in intensity is one of disordering, and if the degree of long-range order α is given by an expression of the form $I/I_0 = (1-\alpha)^2$, as it is in the rather simpler case of order–disorder transitions in cubic alloys (Wilchinsky, 1944), then the rate law would represent second order kinetics for a disordering process. At 795° C. the data clearly fit the second order better than the first order law $\log i = kt$, but at other temperatures either law will fit the experimental data within the rather large limits of error imposed by the inaccuracy of intensity measurement. The nature of the problem precludes the application of more sensitive kinetic criteria for the order of reaction. Since there is no reason to suppose that any change of mechanism occurs with variation in temperature a second order law will be assumed to apply to the process (fig. 2 (i)). At temperatures investigated in the range 700° C. to 817° C. the subsidiary reflections decrease in intensity and vanish if the heating is sufficiently prolonged; they maintain their position, sharpness, and shape unchanged. Below 700° C. the rate of change of intensity was

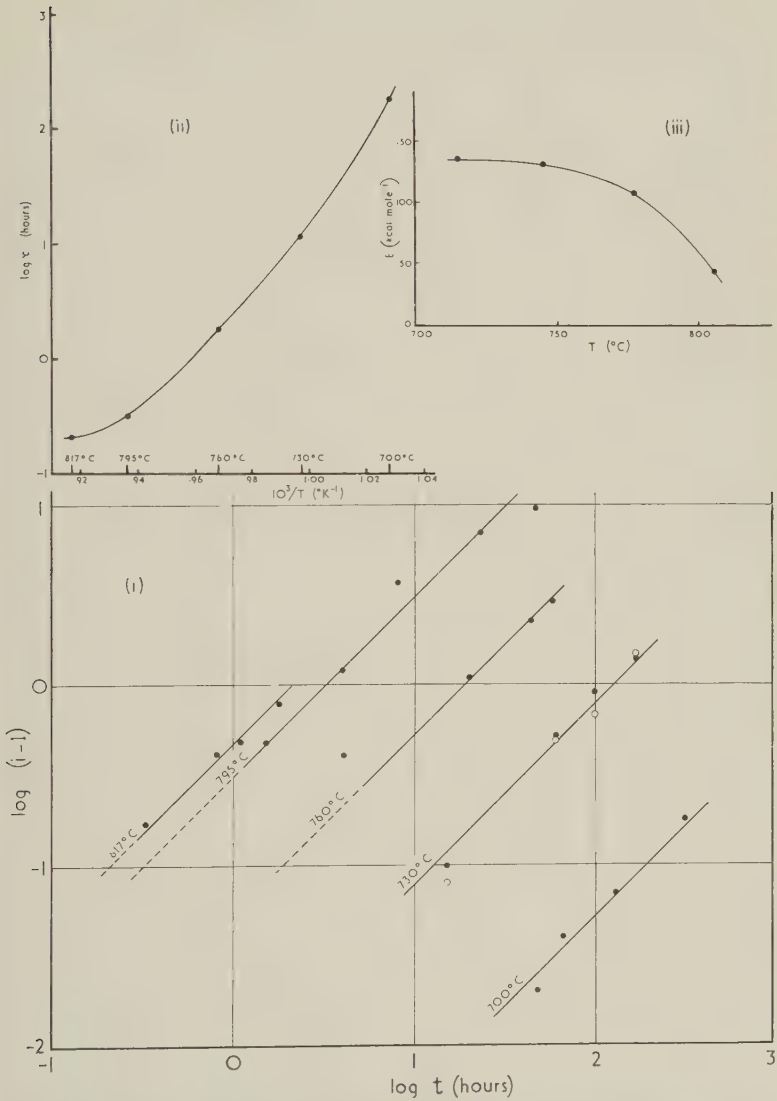

FIG. 2. (i) Plot of $i-1 = kt$; • refers to 1.1·417.$\frac{1}{2}$, ◦ refers to 0.1·417.$\frac{1}{2}$. (ii) Plot of $\log \tau = E/RT + B$. (iii) Plot of activation energy against temperature.

too slow for convenient observation, and at 850° C. slow decomposition of the yoderite structure had begun.

It is convenient to designate the state of yoderite without subsidiary reflections, which is stable above some critical temperature less than 700° C., as high-yoderite, and to refer to yoderite with subsidiary reflections as low-yoderite. All kinetic observations have thus been made in the region in which low yoderite is metastable, and the rate of the transformation process at 700° C. is so sluggish that it would seem that transitional thermal states corresponding to subsidiary reflections of diminished intensity are inaccessible to kinetic observation, in contrast to order–disorder transitions in certain alloys, where transitional states of partial ordering rapidly approach equilibrium. That the kinetic observations have been made for transition from a metastable to a stable state does not invalidate the conclusions drawn from those data in the next paragraph, but does preclude any inferences about the thermodynamic equilibrium between the high and low thermal states.

In considering the temperature coefficient of the rate of reaction it is convenient to assume a relationship of the form $\tau = Ae^{E/RT}$, where τ is the time required for a given fraction of the transformation to take place isothermally at $T°$ K., i.e. the time corresponding to a given value of i, and A is a constant.[1] A plot of this expression in the form $\log \tau = B + E/RT$ is shown in fig. 2 (ii). If the observed process is an order–disorder transition, E may be taken to represent the energy barrier which an ion must surmount to pass from a position of order to become part of a disordered array. The value of E will be expected (Bragg, Sykes, and Bradley, 1937) to decrease as T rises, since each ion will then have more of its neighbours in the disordered state; such a decrease is observed (fig. 2 (iii)) from values in the region of 140 kcal. per gram-ion at 700° C. to 40 kcal. per gram-ion at 817° C.

Values of the activation energy E of the process will be independent of the correctness of any order–disorder interpretation of I/I_0 and of the right choice of rate law. Such activation energies, for which no more than approximate accuracy is claimed, should correspond to those characteristic of the diffusion of cations through a silicate lattice, since in each case momentary displacement of ions from lattice positions must occur. No comparable data are available for the diffusion of cations

[1] This expression is a form of the Arrhenius equation $k = Ae^{-E/RT}$, familiar in gas and solution kinetics, where it has a theoretical basis. It can readily be seen that $k\tau$ = constant. By considering τ instead of k, uncertainty about the precise significance of i is eliminated.

through silicate lattices, but in metals a large collection of data covers the range 10 to 100 kcal. per gram-atom and in salts, other than those of abnormally high conductivity, conductivity measurements lead to values of the activation energy for diffusion from 10 to 50 kcal. per gram-ion (Barrer, 1951, p. 275).

The effect of a non-oxidizing atmosphere, that is nitrogen with a low oxygen content corresponding to $p_{O_2} \sim 10^{-20}$ atm. (i.e. in the presence of metallic iron at the same temperature as the specimen), on the rate of decrease of intensity of $1.1{\cdot}417.\frac{1}{2}$ was found to be negligible within the limits of experimental error in one heating at 760° C. at 1 atm. total pressure.

Discussion. The subsidiary reflections in yoderite are sharp, consistent in position and intensity with the monoclinic symmetry of the pseudo-lattice, and have constant separation in the b^* direction of reciprocal space from principal reflections (type II) or from absent reflections (type I), such parent reflections corresponding to an A-centred lattice of dimensions a, $2b$, $2c$, β; they remain unchanged in position and their sharpness persists until they vanish on heating. Neither type appears to exhibit any systematic absences. Members of each pair of type I reflections, $h.(2k+1)/2 \pm 0{\cdot}083.l + \frac{1}{2}$, commonly differ in intensity, and even on heavily exposed photographs in some cases only one member of a pair may be detectable. Asymmetry is likewise observed in the intensity of pairs of type II reflections, $h.k \pm 0{\cdot}167.l$, except for k zero. No regularity is discernible in the occurrence of one or both members of split reflection pairs, nor in the variation of intensity with h, k, or l. Type II reflections are always associated with principal reflections of higher intensity, the strongest principal reflections tending in general to have relatively strong satellites; reflections $h.0 \pm 0{\cdot}167.l$ may be of non-zero intensity and are then symmetrical as required by the monoclinic symmetry. The form of the variation of intensity of type I reflections with temperature has been indicated in the preceding section.

The properties of type I reflections are very like those of normal type (*b*) subsidiary reflections in the intermediate plagioclases, especially in the more An-rich part of the series (Gay, 1956), except that on heating in the range 950° C. to 1200° C. the latter become diffuse before they finally disappear (Gay and Bown, 1956). Type II reflections correspond likewise to satellites well known in the intermediate plagioclases (Bown and Gay, 1958). The subsidiary reflections in mullite (Agrell and Smith, 1957) are split in directions other than that of the AlO_6 octahedral chains and consequently differ from those in yoderite in their orientation

relative to the presumed common elements of the mullite and yoderite structures. No adequate explanation of the plagioclase and mullite phenomena has yet been given.

Lipson (1950) has reviewed the several types of superlattice produced by ordering in alloys and their diffraction effects; none gives rise to subsidiary reflections analogous to those of yoderite.

Chayes (1958) has discussed the subsidiary reflections of intermediate plagioclase in terms of a simple statistical model of short-range disorder, without attempting to explain how the observed diffraction pattern is produced. In explaining the diffraction effects characteristic of the intermediate plagioclases and yoderite the essential problem is, however, not one of statistics but of diffraction theory. Megaw (1957) has approached this aspect of the problem with a model involving the presence of stacking faults; while the diffraction theory of such a structure has not yet been fully explored, some measure of explanation has been achieved.

An analogy may be drawn between the subsidiary reflections in yoderite and the effects produced by two common types of ruling error in optical diffraction gratings. A periodic error in spacing gives rise to Rowland ghosts, which are subsidiary spectra situated symmetrically close to principal spectra; they correspond to the subsidiary reflections due to periodic variation of lattice spacing observed for instance in Cu_4FeNi_3. Lyman ghosts lie far from the parent line, being nth harmonics of a fundamental period of error N, where N is large and n/N is close to some simple fraction; they occur in small groups n, $n+1$, $n+2$, &c., and are very weak. The appearance of Lyman ghosts is due to an error involving two periods that are incommensurate with each other (Meyer, 1934) or a single error of very short period. The attribution of type I subsidiary reflections in yoderite to such a variation in atomic scattering factor, perhaps combined with a like variation in lattice parameter, would seem reasonable, although simple calculation fails to produce significant results for the periods of variation.

The solution of the problem of the subsidiary reflections in yoderite must await a complete structure determination. It would appear, however, that since the reflections are split in the direction of the dyad axis the problem represents a simplification of that of the intermediate plagioclases.

Thermal decomposition.

Powder data. Finely ground specimens of yoderite were heated in unsealed platinum envelopes in alumina crucibles at various tempera-

tures. After being held at the requisite temperature for a convenient time, the specimen was allowed to cool in air to room temperature and then examined on the X-ray diffractometer with Cu-$K\alpha$ radiation. A series of traces for the range 2θ 20° to 40° is shown in fig. 3.

After 72 hours at 950° C. the yoderite pattern, fig. 3 (i), has completely disappeared and given way to mullite and an unidentified phase, fig. 3 (ii), the very strong mullite peak at 2θ 26·2° being present as a weakened broadened peak, which may also involve the second phase; oxidation has occurred and the mauve colour of yoderite powder has become dull yellow. The formation of mullite at this temperature is not indicated by the phase diagram and must be regarded as a kinetically controlled reaction leading to a metastable product; the structure of yoderite becomes unstable at 840° C. (±20°) (inferred from single crystal data) and portions of the structure undergo slight rearrangement to form metastable mullite, a process involving a lower activation energy than the formation of the assemblage, 68 % cordierite+32 % sapphirine, that would be thermodynamically stable but which, inheriting no structural elements from yoderite, would require a higher activation energy for its formation. After a further 75 hours at 1100° C. the pattern has again altered fundamentally; indialite and sapphirine are accompanied by a small amount of mullite. Single crystal data indicate that the formation of indialite begins at 1040° C. The indialite peaks are displaced slightly to the high θ side of those, fig. 3 (vi), of indialite (Miyashiro *et al.*, 1955). That indialite rather than cordierite is present is shown by the shape of the critical peak at 2θ 29½°; the metastable formation of indialite is usual at temperatures greater than 830° C. At 1180° C. (70 hours) the same pattern was observed, with increase in the strength of the sapphirine peaks relative to indialite, At 1270° C. (120 hours), fig. 3 (iii), and 1345° C. (90 hours) indialite and sapphirine are present and evidence of a small content of mullite persists. The relative strength of the sapphirine peaks increases steadily, producing a step on the high θ side of the 2θ 29½° indialite peak. The colour of the powder gradually changed from dull yellow at 950° C. to medium brown at 1345° C., where considerable contraction occurred to produce a hard cake; incongruent melting may be presumed to begin between 1270° C. and 1345° C. After a further 12 hours at 1415° C., fig. 3 (iv), the indialite pattern disappears; sapphirine and mullite are present and the specimen is in the form of a hard green cake.

Single crystal data. In heating experiments below 850° C. no change was discernible in the quality of the principal reflections. Incipient

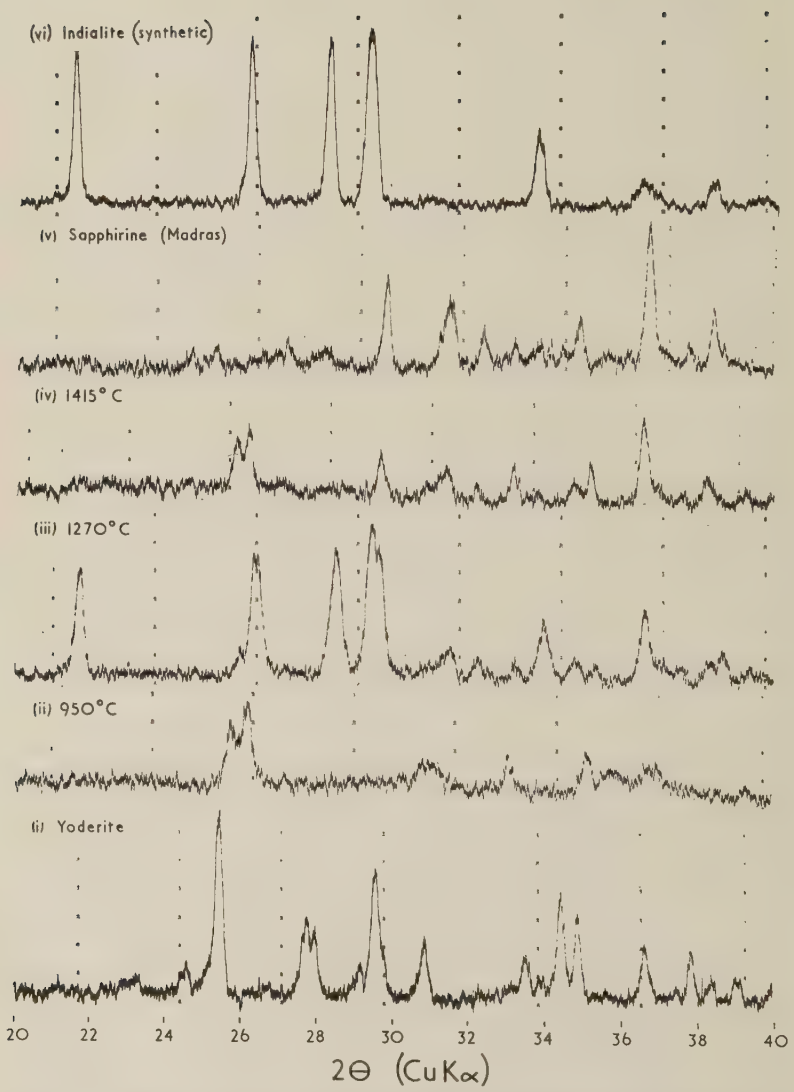

FIG. 3. Diffractometer traces of yoderite and the products of its thermal decomposition.

thermal decomposition of yoderite, indicated by the increased size of Laue reflections, was observed in a crystal heated for about 150 hours at 850° C.; similar effects were observed after about 80 hours at 900° C. At 1000° C., however, decomposition has become much more rapid, and after 1 hour no yoderite reflections persist on *b*-axis oscillation photographs. Partial decomposition to mullite was observed in a crystal heated for 10 minutes at 1000° C. and the relative orientation of the mullite and yoderite lattices was obtained from zero, first, and second layer Weissenberg photographs about the *b*-axis of yoderite. The AlO_6 chain direction, *b* in yoderite and *a* in mullite, is common and the *a*-axis of mullite is 4° (±2°) from the *c*-axis of yoderite; in part at least the AlO_6 chains would thus appear to remain nearly constant in orientation, while cross-linkages are rearranged and part of the unit-cell contents of yoderite diffuse out of the domains of the new mullite lattice. Mullite reflections are streaked along θ curves and their relatively high intensity centres occupy a large volume in reciprocal space, consistent with the expected small size and departure from perfect orientation of the units of mullite structure. The Weissenberg photographs also exhibit reflections that can be indexed on an orthorhombic lattice of dimensions *a* 5·78 Å., *c* 5·72 Å. (±0·05 Å.), with $a||b$ of yoderite and $b||a$ of yoderite, not corresponding to any known phase in the MgO–Al_2O_3–SiO_2–H_2O system.

At 1040° C. powder lines of indialite showing no preferred orientation appear. The rate of formation of units of indialite structure large enough to give sharp powder lines appears to be rapid, in that 20 minutes at 1045° C. are adequate to produce a sharp pattern, whereas 1 hour at 1035° C. produces no indialite pattern at all. The process is envisaged as the formation of nuclei of indialite among the disorganized array of cations distributed through the oxygen lattice outside the mullite crystallites; at temperatures above the critical temperature for nucleation of indialite, 1040° C., grain growth is so rapid that no intermediate stages with broadened powder rings are observed. Single crystal reflections of mullite and of the orthorhombic phase persist for at least 17 hours at 1100° C. and were observed on a zero layer Weissenberg photograph about the *c*-axis of mullite; the reflections are more markedly streaked along θ curves than at lower temperatures.

The formation of mullite is accompanied by the oxidation of Fe^{2+} ions, indicated by the development of a dull yellow colour in the crystal; Fe^{3+} can substitute readily for Al^{3+} in the mullite lattice. Heating at atmospheric pressure in N_2 with a low oxygen content corresponding to the

iron–iron-oxide equilibrium ($p_{O_2} \sim 10^{-15}$ atm.) facilitates the thermal decomposition of yoderite. Mullite and indialite are present and yoderite persists after 21 hours at 900° C.; yoderite, however, is completely decomposed to mullite and indialite in 1 hour at 1000° C. In both experiments the crystal became dull grey in colour. It is inferred that reduction of Fe^{3+} takes place simultaneously with dehydration, a process which involves the thorough disruption of the yoderite structure to produce an environment more favourable for the nucleation of indialite than that provided by the material expelled from the relatively large units of mullite structure under oxidizing conditions, where an approximately close-packed oxygen lattice may persist and give rise to a high energy of nucleation of indialite; at low p_{O_2}, however, the critical temperature for indialite nucleation is lowered by $> 140°$ C. and mullite crystallites are smaller and less well oriented.

Differential thermal analysis and thermogravimetric analysis. Differential thermal analyses in oxygen and in nitrogen at atmospheric pressure have very kindly been made for me by Dr. R. C. Mackenzie.[1] The run in oxygen was made on 30 mg. yoderite mixed with 10 mg. calcined kaolinite sandwich-packed in a nickel holder, and exhibited significant endothermic peaks at 500° C. and 917° C.; a strong exothermic peak begins above 950° C. at the end of the trace. The run in nitrogen was made on 47 mg. yoderite mixed with 10 mg. calcined kaolinite sandwich-packed with 140 mg. calcined kaolinite in a ceramic holder, and exhibited significant endothermic peaks at 486° C. and 888° C. and a strong exothermic peak beginning above 900° C. near the end of the trace. There is thus no marked difference between the runs and it is inferred that oxidation of Fe^{2+} is one of the reactions represented by the exothermic peak above 900° C., which is incompletely displayed on the traces.

In an attempt to elucidate the endothermic peak at 486–500° C. a thermogravimetric analysis was very kindly made for me by Dr. J. R. Butler[2] on an 884·7-mg. sample of yoderite. No significant weight loss ($< 0{\cdot}1$ %) occurred between 20° C. and 1050° C.; at 1050° C. the sample began to lose weight rapidly and reached a constant weight at 1125° C., where the weight loss amounted to 2·96 %. No further change in weight occurred between 1125° C. and 1200° C., and no increase in weight was observed on cooling overnight to room temperature. If the loss in weight above 1050° C. represents dehydroxylation and oxidation

[1] The Macaulay Institute for Soil Research, Aberdeen.

[2] Department of Geology, Imperial College of Science and Technology, London.

of Fe^{2+}, the analysis of table I indicates that it should amount to 2·65 %; the FeO determination is however subject to some uncertainty and a loss of 2·96 % would correspond to a rather lower FeO content of 2·25 %, or to incomplete oxidation.

Differential thermal, thermogravimetric, and X-ray data indicate that oxidation must accompany dehydroxylation and nucleation of metastable mullite, a complicated process giving rise to the strong exothermic peak above 950° C., correlated with the rapid weight loss beginning at 1050° C. and the appearance of reflections due to mullite on single crystal photographs after brief heating at 1000° C. or after prolonged heating as low as 850° C. The small endothermic peak (at 915° C.) preceding this exothermic change has some counterpart in kaolinite, where the third endothermic peak (Mackenzie *et al.*, 1957, p. 107) immediately precedes the main exothermic peak and may be interpreted in terms of an entropy increase due to a structural rearrangement; alternatively the peak at 915° C. in yoderite may correspond to endothermic dehydroxylation, followed by exothermic nucleation of mullite above 950° C.

For the small endothermic peak at 486–500° C. no explanation can be offered.

The colour of yoderite.

The intense colour of yoderite requires explanation in the absence of a significant content of any simple ionic chromophore such as Cu or Co. The blue colour of minerals containing iron in two valence states is well known and has been reviewed by MacCarthy (1926), Weyl (1951*a*), and others; it appears to be due to the presence of a chromophore group Fe^{3+}–O–Fe^{2+} in which electron exchange $Fe^{2+} \leftrightharpoons Fe^{3+} + e^-$ is facilitated by the high polarizability of O^{2-}. Such exchange is inhibited by anions of low polarizability, and the presence of layers of OH^- or F^- ions in a structure will give a strongly directional character to the absorption, as Weyl (1951*b*) has observed in biotite. Familiar examples of blue ferrous–ferric compounds are Prussian Blue and the alkali amphiboles with a wide range of FeO/Fe_2O_3 values and total iron contents; compounds of very high iron content such as magnetite exhibit very strong absorption and appear black. Yoderite has a high FeO/Fe_2O_3 value of 9·6 and low total iron calculated as FeO 5·27 %. On heating in an oxidizing atmosphere above 950° C. it becomes pale yellow, the colour change moving inwards from the margins of the grain as the time of heating is increased; at 900° C. in nitrogen at low p_{O_2} yoderite becomes greenish grey and it is inferred that reduction has accompanied dehydration.

The blue colour of glasses in which di- and tri-valent iron are in equilibrium has been the subject of a considerable amount of experimental study, summarized by Weyl (1951*a*). Such glasses are characterized by a strong absorption minimum in the region 550–700 mμ, bounded by the Fe^{3+} absorption band in the near ultra-violet and violet end of the visible range and by the 1100 mμ absorption band of Fe^{2+}.

Paragenesis and stability relations.

The chemical analysis of a talc-rich specimen of quartz–yoderite–kyanite–talc schist is shown in table III; the composition of the yoderite-

TABLE III. Chemical composition of quartz–yoderite–kyanite–talc schist and of talc.

	1.		2.		3.		
SiO_2 ...	74·54	SiO_2 ...	63.49	Si^{4+} ...	3·98		
TiO_2 ...	0·27	Al_2O_3 ...	3·95	Al^{3+} ...	0·29	}	
Al_2O_3 ...	8·13	FeO ...	0·56	Fe^{2+} ...	0·03	}	
Fe_2O_3 ...	1·92	MnO ...	0·06	Mn^{2+} ...	—	}	2·85
FeO ...	0·90	MgO ...	26·66	Mg^{2+} ...	2·49	}	
MnO ...	0·11	CaO ...	0·64	Ca^{2+} ...	0·04	}	
MgO ...	12·33	H_2O+ ...	4·64	O^{2-} ...	10·00		
CaO ...	trace	H_2O- ...	0·12	OH^- ...	1·94		
Na_2O ...	0·14		100·12				
K_2O ...	0·03						
CO_2 ...	nil						
P_2O_5 ...	trace						
H_2O+ ...	1·59						
H_2O- ...	0·28						
	100·24						

1. Analysis of quartz–yoderite–kyanite–talc schist, Mautia Hill, Tanganyika. JH 2563/2. Analyst: W. H. Herdsman.

2. Analysis of talc, Mautia Hill, Tanganyika. JH 2563/2. Total iron recorded as FeO. Analyst: A. J. Radford.

3. Unit-cell contents of talc, corresponding to 10 O^{2-} per unit cell, calculated from analysis of column 2 omitting H_2O-.

bearing rocks ranges from that of the analysed specimen towards quartz. The analysis essentially represents a high silica composition in the MgO–Al_2O_3–SiO_2–H_2O system (fig. 4) and is characterized by a virtually complete lack of Ca and alkalis, high Mg/Fe, and the presence of 8 % corundum and 31 % enstatite in the norm. Such a composition differs markedly from that of any igneous rock or common sediment; three rather specialized possibilities remain: the rock may result from the metamorphism of a tectonic mixture of quartz with an igneous ultra basic rock, or may be a product of magnesian metasomatism, or of the

isochemical metamorphism of a saponitic bentonite. The first is improbable on the grounds that no source of ultrabasic material is discernible and that it is difficult to reconcile the high alumina content with absence of Ca and Na. The second would require magnesian metasomatism of an

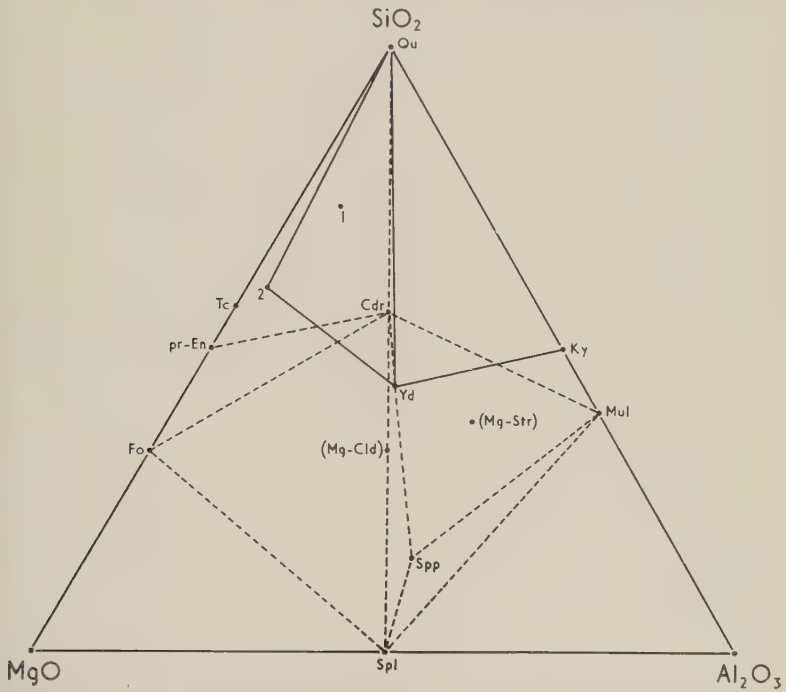

FIG. 4. Projection of the MgO–Al_2O_3–SiO_2–H_2O system from the H_2O apex. Solid lines show phase assemblages at Mautia Hill. Dashed lines show phase assemblages at the solidus in the dry system. Key: 1, quartz–yoderite–kyanite–talc schist; 2, talc from 1; Cdr, cordierite; Fo, forsterite; Ky, kyanite; (Mg-Cld), hypothetical magnesian chloritoid; (Mg–Str), hypothetical magnesian staurolite; Mul, mullite; pr-En, proto-enstatite; Qu, quartz; Spl, spinel; Spp, sapphirine; Tc, talc; Yd, yoderite.

argillaceous sandstone, the introduction of Mg being associated, as is usual (Eskola, 1914), with loss, in this case complete, of Ca and alkalis. The occurrence of an argillaceous sandstone interstratified with a manganiferous sandstone and a limestone is stratigraphically consistent; that Mg should have been fixed in this semi-pelite but not in the adjacent piemontite–quartzite might well have been controlled, or at least facilitated, by the prior existence of a high content of phyllosilicate

minerals, at once providing a local concentration of slip-planes during tectonic movement, and therefore channels for the admission of Mg-bearing solutions, and on a molecular scale a structural framework sufficiently similar to that of talc for the replacement of Ca and alkalis by Mg to occur under conditions favouring the nucleation of talc, excess Al being segregated in kyanite or some other aluminous mineral that became kyanite during subsequent metamorphism. The source of the Mg would appear to have been entirely external and unrelated to the dolomite-free character of the adjacent crystalline limestone, which therein differs from most Archaean limestones in Tanganyika. The third possibility perhaps provides the fewest difficulties; the present composition of the rock lies at low temperatures in the field of synthetic montmorillonite–quartz–talc (Roy and Roy, 1955) and is approximately analogous to natural chert-bearing saponitic bentonites, which may be produced under a variety of conditions from basic pyroclastics by weathering *in situ* (Ross and Hendricks, 1945, p. 64), the peculiarity of this occurrence being the very low calcium content. The work of Roy and Roy (1955) has shown that montmorillonite decomposes at temperatures less than 500° C. to give rise at this composition to a quartz–talc–pyrophyllite assemblage stable up to 530° C. at p_{H_2O} 667 bars, where cordierite formation begins, accompanied at 575° C. by the decomposition of pyrophyllite to cristobalite and mullite. If these two latter reactions are inhibited, as would seem probable, by increased pressure, and pyrophyllite decomposes, without the prior formation of cordierite, to silica and kyanite, the assemblage that apparently existed before the formation of yoderite will have been developed.

The yoderite-bearing rocks are composed principally of talc and quartz with some 10 % of yoderite-rimmed kyanite and accessory hematite. The chemical analysis of talc from the analysed rock is set down in table III; with an alumina content of 3·95 %, corresponding to 15 % of the pyrophyllite molecule in solid-solution, it is one of the most aluminous natural occurrences of talc known and reflects the relatively aluminous nature of the environment. Yoder (1952) has observed that synthetic talc growing in aluminous media can apparently take a considerable amount of pyrophyllite into solid solution. The talc is pale flesh-pink in hand-specimen and has $2V_{\alpha}$ 6°, β 1·592 ($\pm$0·002). The kyanite is remarkable for its light brown colour in hand-specimen, contrasting with the grass-green colour of kyanite in the kyanite–biotite gneiss at Mautia Hill. The brown kyanite contains[1] a marked content of

[1] Qualitative spectrographic analysis by Dr. S. R. Nockolds.

Mn, a small content of Fe, about 100 p.p.m. Cr, about 100 p.p.m. Zr, a trace of Ti, and about 20 p.p.m. Ga, with Ni, Co, V, Na below the limits of sensitivity. The green kyanite contains rather less Mn, Fe, Ti, about 50 p.p.m. Cr, and about 20 p.p.m. Ga, with Zr, Ni, Co, V, Na below the limits of sensitivity. The colour of the brown kyanite may be tentatively attributed to the presence of Mn^{3+}, while the green colour may be due to Fe in the presence of a rather lower Mn content. The identification of hematite was confirmed by its X-ray powder pattern.

Whatever may have been the early history of the rock, the assemblage talc–kyanite-quartz was eventually generated, presumably in the presence of excess water vapour. However, according to Yoder's (1952) experimental work, talc and kyanite can have no stable coexistence at pressures below 1000 bars. Kyanite may perhaps have formed metastably at low temperatures in the presence of talc, perhaps in the manner suggested in a previous paragraph. When the temperature subsequently increased, talc and kyanite reacted to produce, not cordierite and water vapour as might be expected, but the hydrous mineral yoderite. In seeking an explanation of this it may be instructive to consider the volume change for the relevant reactions:

(i) $\underset{140\text{ c.c.}}{\text{Tc}} + 3\,\underset{135\text{ c.c.}}{\text{Ky}} + 0{\cdot}5\,\underset{11\text{ c.c.}}{\text{Qu}} \rightleftharpoons 1{\cdot}5\,\underset{337\text{ c.c.}}{\text{Cdr}} + \underset{34\text{ c.c.}}{\text{H}_2\text{O}}$ $\quad \Delta V = +85$ c.c.

(ii) $\underset{140\text{ c.c.}}{\text{Tc}} + 3\,\underset{135\text{ c.c.}}{\text{Ky}} + 0{\cdot}3\,\underset{10\text{ c.c.}}{\text{H}_2\text{O}} \rightleftharpoons 1{\cdot}1\,\underset{216\text{ c.c.}}{\text{Yd}} + 2.5\,\underset{65\text{ c.c.}}{\text{Qu}}$ $\quad \Delta V = -13$ c.c.

The gram-formula volume indicated beneath each solid phase will be independent to a first approximation of pressure and temperature. The conditions represented are T 500° C., p_{H_2O} 1000 bars, the corresponding density of water, 0·532 g./c.c., being taken from Kennedy (1950); under these conditions equation (i) represents the formation of cordierite with a volume increase of 30 %, and equation (ii) the formation of yoderite with a volume decrease of 5 %. The magnitude of these volume changes will decrease with declining temperature and increasing pressure, but ΔV for equation (i) will remain positive and for equation (ii) negative at all temperatures and pressures; thus throughout the petrogenetically interesting PT range the formation of cordierite by equation (i) will be inhibited and that of yoderite by equation (ii) facilitated by high pressure. An upper limit to the temperature at which yoderite can form is set by the univariant curve of talc decomposition (Bowen and Tuttle, 1949) reproduced in fig. 5. At p_{H_2O} 1000 bars talc is stable below 795° C. and at least as low as 400° C. Temperatures in excess of 850° C.

cannot therefore have prevailed at Mautia Hill and would not in any case be expected. A minimum pressure limit is set by the univariant curve of the kyanite–sillimanite transition (Clark, Robertson, and Birch, 1957), also shown in fig. 5. It should be noted that the attainment of equilibrium at the Al_2SiO_5 composition even in the presence of significant p_{H_2O} is remarkably sluggish; however, at high temperatures kyanite inverts rapidly to sillimanite and therefore the region below the

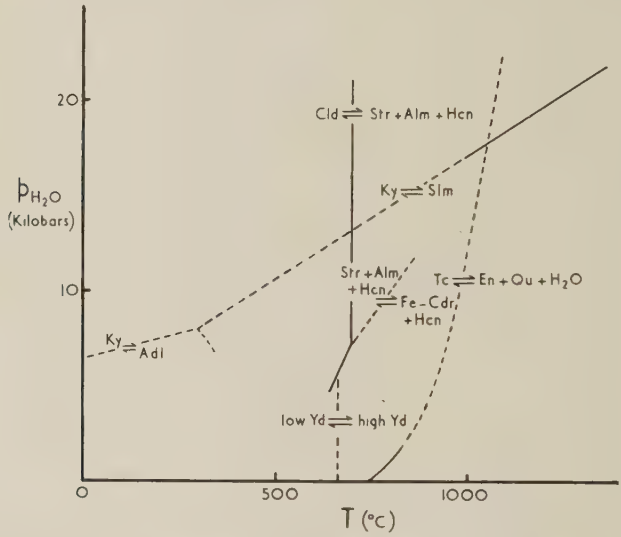

FIG. 5. p_{H_2O}–T diagram illustrating the stability relations of yoderite. Key: Adl, andalusite; Alm, almandine; Cld, chloritoid; En, enstatite; Fe-Cdr, iron-cordierite; Hcn, hercynite; Ky, kyanite; Qu, quartz; Slm, sillimanite; Str, staurolite; Tc, talc; Yd, yoderite.

kyanite curve beyond about 500° C. may be regarded as outside the likely *PT* conditions at Mautia Hill during the formation of the talc–quartz–kyanite assemblage.

The existence of subsidiary reflections in yoderite indicates that the yoderite-bearing rocks must have cooled slowly through the range immediately below the lower limit of stability of high-yoderite, as the rate of the transition process must soon become prohibitively slow as temperature falls. Alternatively the transition from high-yoderite to low-yoderite may well have no significant rate under any conditions and low-yoderite may be able to form only during crystallization. The low→high transition temperature in yoderite appears to be just below

700° C. at 1 atm., and no data are yet available on its pressure coefficient; crystallization of yoderite in the range immediately below 700° C. would not be inconsistent with any of the factors discussed in the previous paragraph. Gay and Bown (1956) have considered the analogous problem of thermometric inferences from the structural state of intermediate plagioclase, where transitional states are also observed.

That the formation of yoderite will be favoured by high p_{H_2O} can be seen from fig. 4. At low p_{H_2O} the assemblages talc–cordierite–quartz and kyanite–cordierite–quartz are stable. At higher total pressure and presumably at high values of p_{H_2O} the assemblages talc–yoderite–quartz–water and kyanite–yoderite–quartz–water become stable. Assemblages containing yoderite and cordierite have not been observed at Mautia Hill; they would be presumed to correspond to relatively low values of p_{H_2O}. Yoder (1952) studied the cordierite composition at various temperatures and p_{H_2O} 1000 bars, and Roy and Roy (1955) studied the composition $23MgO:28Al_2O_3:49SiO_2$ at 515° C. and p_{H_2O} 667 bars; neither studied any composition nearer that of yoderite, $27MgO:29Al_2O_3:44SiO_2$ and therefore it cannot be inferred that the lower stability limit of yoderite is as high as 667 bars.

Recent experimental work on the stability relations of staurolite (Halferdahl, 1957) may throw some light on the stability field of yoderite; although their structures are distinct, both minerals may be regarded as hydrous modifications of the kyanite structure. Staurolite is stable at all $p_{H_2O} > 7000$ bars and temperatures greater than about 700° C., below which chloritoid is a stable phase, and lower than a largely undetermined univariant curve which represents the decomposition of staurolite into anhydrous phases. Moreover an upper p_{H_2O} limit emerges for the stable existence of iron-cordierite, represented by the equilibrium Fe-cordierite + hercynite + $H_2O \rightleftharpoons$ staurolite + almandine. Halferdahl's curves, shown in fig. 5, apply only to the iron-chloritoid composition and may be expected to be modified in position, if not in general form, towards the composition corresponding to the iron analogue of yoderite. Structural differences between yoderite and staurolite, and the non-existence of the magnesian chloritoid end-member will further modify the position of the yoderite field in relation to that of staurolite; that yoderite is stable only at p_{H_2O} in excess of about 10 000 bars, and has a lower temperature limit of stability certainly less than 1000° C. and perhaps no greater than 500° C., would be consistent with what evidence there is.

It is difficult to comment adequately on the p_{O_2} conditions under

which yoderite crystallized at Mautia Hill. Hematite inclusions occur in yoderite, which contains iron dominantly in the ferrous state, with $Fe^{3+}/Fe^{2+} = 0{\cdot}09$. Preliminary experimental work suggests that completely ferrous minerals are not stable at higher partial pressures of oxygen than are represented by the equilibrium $2Fe_3O_4 + \frac{1}{2}O_2 \leftrightharpoons 3Fe_2O_3$ at any temperature and any total pressure (Eugster, 1956; Halferdahl, 1957). Its Fe^{3+} content, though small, may enable yoderite to extend into the hematite field, so that over a small range of p_{O_2} at any temperature yoderite and hematite may be in equilibrium in accordance with the petrographic observation at Mautia Hill.

In conclusion it should be stressed that this discussion of the paragenesis of yoderite is speculative. The final elucidation of the metamorphic history of the yoderite-bearing rocks at Mautia Hill must await more detailed study of the petrology of the associated rocks, search for and study of other yoderite occurrences, and an experimental study of the stability relations of yoderite.

Acknowledgements. My thanks are due to Professor C. E. Tilley, F.R.S., for constant advice and encouragement during this work and to Dr. S. O. Agrell, Dr. P. Gay, Dr. J. D. C. McConnell, and Dr. S. R. Nockolds for advice and many helpful discussions. I am indebted to Dr. J. R. Butler for the thermogravimetric analysis, to Dr. R. C. Mackenzie for differential thermal analyses, to Dr. S. R. Nockolds for spectrographic determinations, to Dr. S. O. Agrell for making available to me before publication the text of a further communication by himself and Dr. J. V. Smith on mullite, to Mr. J. H. Scoon for the ferrous oxide determination, and to Mr. K. O. Rickson for taking some of the X-ray photographs. I acknowledge the grant of a Research Studentship by the Department of Scientific and Industrial Research.

References.

Agrell (S. O.) and Smith (J. V.), 1957. Abstracts Fourth Internat. Congr. of Cryst., Montreal, p. 32.

Barrer (R. M.), 1951. Diffusion in and through solids. Cambridge University Press.

Bowen (N. L.) and Tuttle (O. F.), 1949. Bull. Geol. Soc. Amer., vol. 60, p. 439.

Bown (M. G.) and Gay (P.), 1958. Zeits. Krist., vol. 111, p. 1.

Bragg (W. L.), Sykes (C.), and Bradley (A. J.), 1937. Proc. Phys. Soc., vol. 49, extra part, p. 96.

Chayes (F.), 1958. Acta Cryst., vol. 11, p. 323.

Clark (S. P.), Robertson (E. C.), and Birch (F.), 1957. Amer. Journ. Sci., vol. 255, p. 628.

Cole (W. F.), Sörum (H.), and Taylor (W. H.), 1951. Acta Cryst., vol. 4, p. 20.

Eskola (P.), 1914. Bull. Comm. Géol. Finlande, no. 40.

Eugster (H. P.), 1956. Ann. Rept. Geophys. Lab. 1955–6, p. 158.

Gay (P.), 1956. Min. Mag., vol. 31, p. 21.

—— and Bown (M. G.), 1956. Ibid., vol. 31, p. 306.

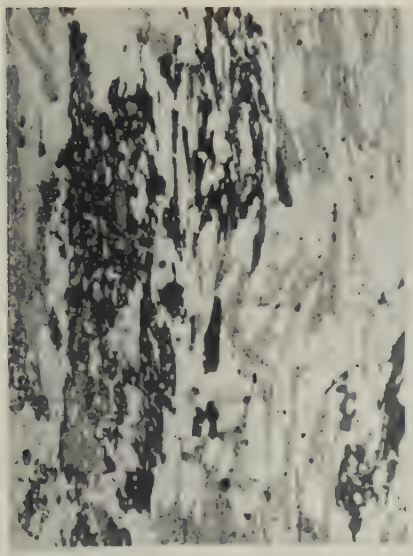

1

2

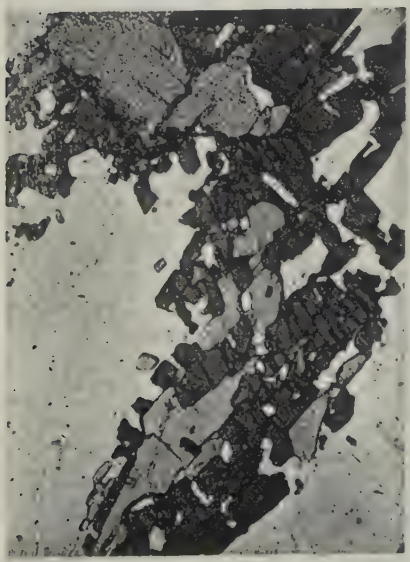

3

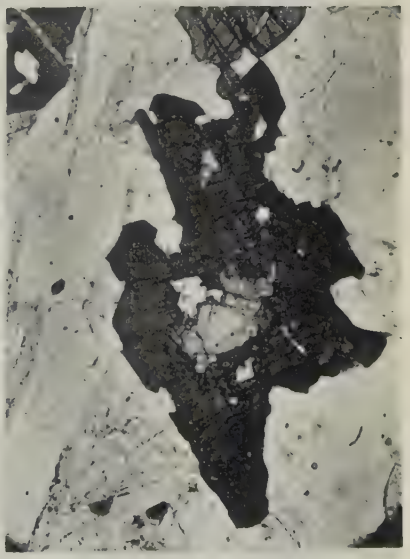

4

Duncan McKie: Yoderite

Groves (A. W.), 1951. Silicate Analysis, 2nd edn, London.
Halferdahl (L. B.), 1957. Ann. Rept. Geophys. Lab. 1956–7, p. 225.
Hey (M. H.), 1941. Min. Mag., vol. 26, p. 116.
Kennedy (G. C.), 1950. Amer. Journ. Sci., vol. 248, p. 540.
Lipson (H.), 1950. Progress in Metal Physics, vol. 2, p. 1.
MacCarthy (G. R.), 1926. Amer. Journ. Sci., ser. 5, vol. 12, p. 17.
Mackenzie (R. C.) *et al.*, 1957. The Differential Thermal Investigation of Clays. Mineralogical Society, London.
Megaw (H. D.), 1957. *In* Conference Report, Brit. Journ. Appl. Physics, vol. 8, p. 427.
Meyer (C. F.), 1934. The diffraction of light, X-rays, and material particles. University of Chicago Press.
Miyashiro (A.), Iiyama (T.), Yamasaki (M.), and Miyashiro (T.), 1955. Amer. Journ. Sci., vol. 253, p. 185.
Naray-Szabo (St.), Taylor (W. H.), and Jackson (W. W.), 1929. Zeits. Krist., vol. 71, p. 117.
Ross (C. S.) and Hendricks (S. B.), 1945. U.S. Geol. Surv., Prof. Paper 205-B.
Roy (D. M.) and Roy (R.), 1955. Amer. Min., vol. 40, p. 147.
Skerl (A. C.) and Bannister (F. A.), 1934. Min. Mag., vol. 23, p. 598.
Temperley (B. N.), 1938. Geol. Surv. Tanganyika, Short Paper 19.
Weyl (W. A.), 1951*a*. Coloured Glasses. Soc. of Glass Technology, Sheffield.
—— 1951*b*. Journ. Phys. Chem., vol. 55, p. 507.
Wilchinsky (Z. W.), 1944. Journ. Appl. Phys., vol. 15, p. 806.
Yoder (H. S.), 1952. Amer. Journ. Sci., Bowen vol., p. 569.

Explanation of Plate XI.

Fig. 1. General aspect of quartz yoderite-kyanite–talc schist. JH 2563/2. Ordinary light, ×4.

Fig. 2. Replacement of talc along cleavage planes by yoderite. JH 2563/2. Plane polarized light, ×110.

Fig. 3. Kyanite relicts in parallel orientation in a grain of yoderite. JH 2563/14. Plane polarized light, ×16.

Fig. 4. The development of yoderite rims to kyanite grains. JH 2563/2. Plane polarized light, ×14.

Delorenzite is tanteuxenite.

By J. R. Butler, M.A., Ph.D.
Imperial College, London
and P. G. Embrey, B.Sc., M.A., A.R.I.C.
Dept. of Mineralogy, British Museum (Natural History).

[Read 29 January 1959.]

Summary. Specimens of delorenzite from the type locality, Craveggia, Val Vigezzo, Piemont, have been examined and found to be close to tanteuxenite from Australia. The X-ray powder patterns are virtually the same, and the chemical analyses (including the relative abundances of the rare earths) are closely similar.

Zambonini's original (1908) specimens have not been re-examined, but are without reasonable doubt the same as the specimens now described; the considerable discrepancies between the old and new analyses can be explained by the difficulty of the separations. It is suggested that the name delorenzite be abandoned despite its priority because of its association with an incorrect analysis.

C. M. GRAMACCIOLI (1958) has described his rediscovery in 1957 of delorenzite at the type locality, Piano del Lavonchio, Craveggia, Val Vigezzo, Piemont. He submitted a specimen to the British Museum (Natural History) for exchange, and later kindly presented the fragments of a large crystal, which had broken on removal from the matrix; the present paper is based on this latter material (B.M. 1958,397).

Delorenzite was originally described by Zambonini (1908), and the new material agrees very well with his description except for the chemical composition and the specific gravity. A pyknometric determination on the new material gave 5·68, which is close to the published specific gravity (5·77) of tanteuxenite from Cooglegong, Western Australia, but differs considerably from Zambonini's value of about 4·7; this latter value was obtained by comparing the rates of fall of delorenzite fragments in a column of acetylene tetrabromide with those of similar fragments of xenotime, and the inaccuracy of the method could easily account for the difference.

As noted by Zambonini, delorenzite crystals are deeply striated in the prism zone; measurement of many fragments of the new material yields interfacial angles in agreement with the originally described values, but also shows that several vicinal forms are developed and hence that no

reliance may be placed on any crystallographic distinction drawn between the present material and euxenite as was done by Zambonini for the type delorenzite. Delorenzite and tanteuxenite are both metamict, but X-ray powder photographs of heated specimens of the two are virtually the same—as may be expected from their similarity of com-

TABLE I. Analytical data for delorenzite and tanteuxenite.

	1.	2.	3.
Na_2O	—	*	tr.
MgO	—	0·19	—
FeO	4·25	M	—
MnO	—	m	·35
CaO	—	2·17	2·22
PbO	—	tr.	tr.
Al_2O_3	—	m	nil
Fe_2O_3	—	1·8	1·18
$(Yt,Ln)_2O_3$	14·63	24·35	24·70
SiO_2	—	M	0·90
TiO_2	66·03	16·2	14·17
SnO_2	4·33	tr.	0·14
ThO_2	—	*	tr.
UO_2	9·87	—	—
UO_3	—	—	3·35
U_3O_8	—	7·75	—
Nb_2O_5	—	4·45	3·83
Ta_2O_5	—	36·4	47·31
Ign	—	n.d.	2·40
	99·11	(92·3)	100·55

1. Delorenzite, Piano del Lavonchio, Craveggia, Val Vigezzo, Piemont, Italy. Anal. Štěrba, in Zambonini, 1908. State of oxidation of U and Fe not known.

2. Delorenzite, locality as 1. Anal. Butler and Hall. Total iron as Fe_2O_3 determined by D. I. Bothwell. Optical spectrographic data indicate that Fe and Si exceed 1 %, Al exceeds 0·1 %, and Mn exceeds 0·01 %; Pb and Sn are below 0·01 %; *=not detected spectrographically. (B.M. 1958,397.)

3. Tanteuxenite, Eleys, 10 miles south of Cooglegong, Pilbara goldfields, W. Australia. Anal. Simpson, 1928. (B.M. 1928,341, type material.)

position. The type tanteuxenite consists of worn fragments with no measurable faces, and so its morphology cannot be compared with euxenite on the one hand or delorenzite on the other.

On the basis of the analysis of Štěrba (Zambonini, 1908) there is no doubt that delorenzite was rightly considered to be a new mineral (table I, col. 1); present-day correlation of that analysis reveals some *chemical* similarity between delorenzite and davidite in terms of Ti, Ln, and U contents, but the presence of Sn in delorenzite is a contrasting property. It is not clear what methods were used in the original analysis

but it seems certain that chemical precipitates were not checked spectrographically for purity. Ti, Nb, and Ta occurring together presented many difficulties to analysts in the early part of the century, and it is suggested that Štěrba's TiO_2 value is one that should be correlated with the value of $TiO_2+Nb_2O_5+Ta_2O_5$ now found (table I, col. 2). If oxalate ion was originally used to keep the decomposed mineral in solution then part of the rare-earths will have been reckoned as TiO_2, and this may explain the discrepancy between the old and new values for the rare-earths. Thus Štěrba's summation of TiO_2 and Ln_2O_3 approximates within 1 % to our value of $TiO_2+Nb_2O_5+Ta_2O_5+Ln_2O_3$. The figures for U are not too dissimilar; delorenzite was noted to be the only radioactive mineral at the type locality and it is suggested that the identity of the mineral now analysed is certainly delorenzite.

Analytical methods. About 600 mg. of the mineral was decomposed by prolonged attack with conc. HNO_3–40 % HF mixtures and the rare-earth oxides plus thoria separated via the fluorides and oxalates (Butler, 1957*a*); individual rare-earths were determined on these separated oxides using optical spectrographic methods (Butler, 1957*b*). $(Ta,Nb)_2O_5$ was determined in the filtrate from the Ln+Th fluoride precipitation by evaporating down to dryness twice with conc. HNO_3, taking up in NH_4F and water, and treating chromatographically (Mercer and Wells, 1954). Ti and W were confirmed as below 0·1 and 0·5 % respectively on the separated $(Ta,Nb)_2O_5$ by normal optical spectrographic methods; the spectrogram showed clearly enough the preponderance of Ta over Nb. Ta and Nb were determined on the separated $(Ta,Nb)_2O_5$ by the pyrogallol method (Hunt and Wells, 1954). Ti was determined by the peroxide method on a separate portion of the mineral (10 mg.). U was determined on 100 mg. mineral using the colorimetric ascorbic acid method. A radiometric assay by Mr. E. F. Bunt of the Geological Survey (Atomic Energy Division) gave eU_3O_8 = 7·3 %. Optical spectrography was used to determine elements in the mineral; conditions were as for the rare-earths determination except for the recording range (3600–2700 Å.) and the spectrograph (Hilger no. 471; quartz prism). Sn and Pb were judged to be below 0·01 %, Mn and Al below 0·2 %, and Si above 1 %.

Relationship of delorenzite to tanteuxenite. Table I (cols. 2 and 3) shows the new analysis of delorenzite compared with that for the type tanteuxenite (Simpson, 1928). The total for the new analysis is below 100 in that Mn, Al, Si, and H_2O were not determined. It will be seen that total rare-earths, CaO, and TiO_2 are closely similar in both minerals; Nb values are reasonably similar and Ta values somewhat different. U differs by a factor of two and is lower in the type tanteuxenite. Despite the Ta and U differences the new analysis of delorenzite is difficult to reconcile with that of any mineral other than tanteuxenite. Additional evidence for the identity of delorenzite with tanteuxenite is the remarkable similarity of their rare-earth distribution patterns. The

rare-earths may be nominally described as Yt-earths as Yt comfortably exceeds the sum of the lanthanons. The lanthanons, however, instead of being Dy-rich (on the basis of Yt and Dy having identical radii) are Nd-rich (fig. 1). It is quite abnormal for Nd to exceed other individual lanthanons in minerals containing essential rare-earths. Lyndochite (Butler, 1957*c*), and æschynite from an alkali syenite pegmatite (Semenov and Barinsky, 1958), show Nd peaks in their lanthanon distribution

TABLE II. Individual rare-earth concentrations in $(Yt,Ln)_2O_3$ separated chemically from the minerals. Eu_2O_3 below 0·1 %; no data for Ho_2O_3. σ, percentage standard deviations of individual rare-earths from duplicate spectrograms.

	1.	2.	σ.
Yt_2O_3	44·5	56·8	5
La_2O_3	0·83	0·51	8
CeO_2	5·76	4·60	7
Pr_6O_{11}	1·45	1·37	8
Nd_2O_3	11·7	9·05	5
Sm_2O_3	6·30	6·10	5
Gd_2O_3	9·70	6·30	6½
Tb_4O_7	1·82	1·33	6
Dy_2O_3	8·85	5·71	5
Er_2O_3	4·68	2·34	13
Tm_2O_3	0·48	0·4	10
Yb_2O_3	2·94	1·60	5
Lu_2O_3	0·46	0·4	35
Sum	99·47	96·51	

1. $(Yt,Ln)_2O_3$ from delorenzite.
2. $(Yt,Ln)_2O_3$ from tanteuxenite. Localities in table I.

pattern but the former has total lanthanons exceeding Yt in atomic ratio 2:1, and presumably the latter is also Yt-poor (otherwise it might have been described as priorite or æschynite-priorite). Similarly the Ce-poor rhabdophane from Salisbury, Connecticut, U.S.A. (Hildebrand *et al.*, 1957) has Nd the most abundant rare-earth with the atomic ratio Yt:Ln approximately 1:4. The only mineral showing Yt predominating in the rare-earths and Nd predominating in the lanthanons is yttrotungstite (Butler, 1957); Ce is almost as abundant as Nd. Other complete-assemblage type rare-earth minerals would be expected to have the possibility of containing high concentrations of Nd but with other *Z*-even lanthanons almost equally abundant; one gadolinite has been reported to contain 14 % Nd_2O_3 in total Ln_2O_3 (Semenov and Barinsky, 1958). The lanthanon distributions in delorenzite and tanteuxenite are to be regarded as uncommon; certainly the distribution pattern is

distinct from those shown by members of the euxenite-polycrase series which are Nb- rather than Ta-rich (Butler, 1958).

Conclusions. It is clear from the foregoing paragraphs that the mineral now described as delorenzite agrees with the original descrip-

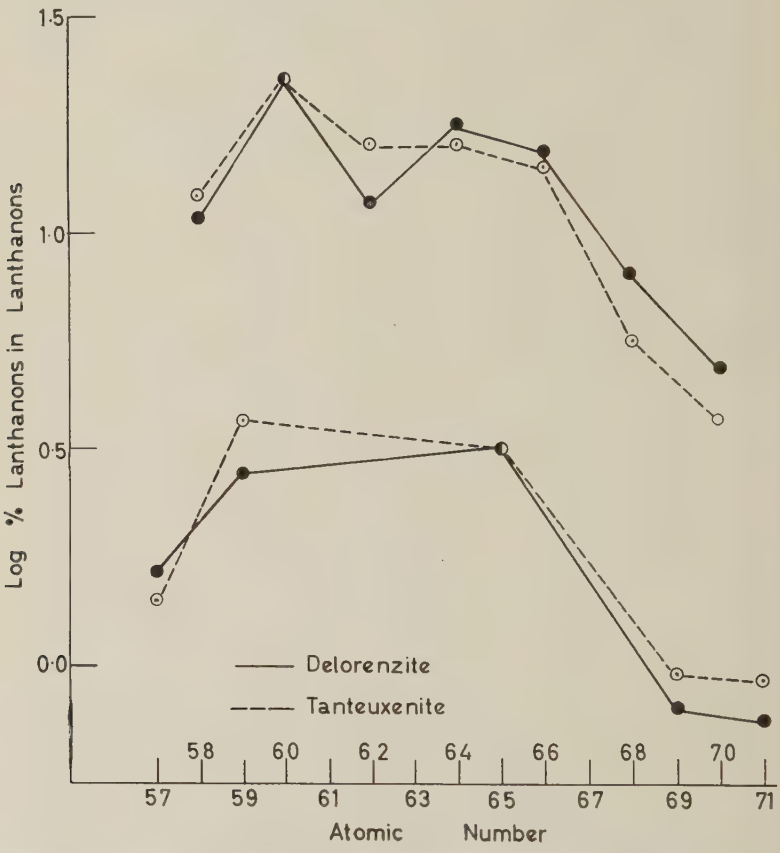

Fig. 1. Lanthanon distribution in delorenzite and tanteuxenite (Ho excluded).

tion, and that the discrepancies have a straightforward explanation. Moreover, no other radioactive mineral has been reported from Craveggia with which the old or the new delorenzite could be confused. The identity of delorenzite with tanteuxenite is certain, and Craveggia is thus the only known locality for tanteuxenite outside Western Australia. We recommend that the name delorenzite be abandoned in favour of tanteuxenite, despite its priority, both to make clear the close

relationship to euxenite (of which it is a variety) and because of its association with an incorrect chemical analysis.

Acknowledgement. We wish to thank the Director of Rothamsted Experimental Station for permission to use the Mannkopff optical spectrograph there.

References.

Butler (J. R.), 1957*a*. Geochimica Acta, vol. 12, p. 190.
—— 1957*b*. Spectrochimica Acta, vol. 9, p. 332.
—— 1957*c*. Amer. Min., vol. 42, p. 67.
—— 1958. Min. Mag., vol. 31, p. 763.
Gramaccioli (C. M.), 1958. Natura (Milan), vol. 49, p. 110.
Hildebrand (F. A.), Carron (M. K.), and Rose (H. J., Jr.), 1957. Bull. Geol. Soc. Amer., vol. 68, p. 1744.
Hunt (E. C.) and Wells (R. A.), 1954. Analyst, vol. 79, p. 345.
Mercer (R. A.) and Wells (R. A.), 1954. Ibid., p. 339.
Semenov (E. I.) and Barinsky (R. L.), 1958. Geochemistry, no. 4, p. 398.
Simpson (E. S.), 1928. Proc. Roy. Soc. Western Australia, vol. 14, p. 45.
Zambonini (F.), 1908. Zeits. Kryst. Min., vol. 45, p. 76.

A dickite with an elongated crystal habit and its dehydroxylation.

By E. R. Schmidt, M.Sc., Senior Research Officer,
and R. O. Heckroodt, M.Sc., Assistant Research Officer,
National Building Research Institute, Pretoria, Union of South Africa.

[Taken as read 5 November 1959.]

Summary. Dickite from a new occurrence at Barkly East, Cape Province, is described and compared with a previously unreported dickite from Postmasburg and a dickite from Ouray, Colorado. The Barkly East dickite crystals are elongated in the direction of the *a*-axis; the ratio of length to width of crystals varies from 3:1 to 16:1. Optical, electron microscopic, X-ray, and thermal data and a chemical analysis are given. The thermogram of the fraction smaller than 2 μ e.s.d.[1] is characterized by a single peak at 600° C., while that of fractions larger than 2 μ e.s.d. shows a double endothermal effect. This two-stage dehydroxylation of dickite on heating is attributed to a particle size effect.

THE only dickite occurrences so far reported in South Africa are those in the Witwatersrand system (Whiteside, 1941; Frankel, 1949). In the latter paper mention is also made of a dickite from the Middelburg district, Transvaal, but only refractive indices are given.

In this paper a dickite occurring near Barkly East in the Eastern Cape Province is described and compared with a dickite from Postmasburg in the northern Cape Province as well as with the dickite from Ouray, Colorado (Clay Mineral Standard, H–14).

The sample received from *Barkly East* is a white glittering powder. Large calcite crystals and portions of vugs lined with calcite crystals were found in the material. Although nothing more is known of the geological associations it is assumed that the dickite is closely associated with the vugs found in the sample bag and that it is, therefore, of hydrothermal origin. The most outstanding feature of this dickite is the fact that the particles have a very pronounced elongated crystal habit. Except for slightly elongated particles shown in electron micrographs (Davis *et al.*, 1950), dickites with such a pronounced elongation have not yet been described in the literature. According to Grim (1953, p. 108) dickite occurs in well-formed, six-sided, flake-shaped particles,

[1] e.s.d.—effective spherical diameter.

frequently showing a definite elongation in one direction, but in the electron micrograph of dickite (Grim, 1953, p. 114) elongation is not very marked. The only other reference to elongated dickite crystals which could be found in the literature is that by Mezösi (1957) who described a dickite occurrence from Mád, Hungary. This dickite is closely associated with kaolinite in cavities in porous rhyolite tuffs. The crystals are from 15 to 20 μ long and 3 to 8 μ wide and the elongation is in the direction of the *a*-axis. As will be seen below, this elongation is much less than that of the Barkly East dickite.

The *Postmasburg* specimen is in the form of a lump with quartz crystals and specularite adhering to it. The dickite in a hand specimen is very light greenish in colour and is slightly transparent. When pulverized, the material is pure white. According to Dr. L. G. Boardman,[1] from whom the sample was received, it occurs in the highly altered Gamagara shales associated with iron ores, especially where diaspore and zunyite have also been found. It is found as fillings in cavities in the ore bodies on Kapstewel although some cavities contain only quartz or calcite crystals. According to Boardman, the iron ore bodies have been formed by the replacement of the Gamagara shales which were infolded in the lower Griquastad beds. Remnants of the original shales are often found in the quarries.

In view of the fact that this dickite occurs in cavities associated with the iron ore bodies, one must conclude that it also was formed as a result of hydrothermal activity.

Microscopical examination.

The Barkly East dickite was sieved through a 200-mesh (74 μ) Tyler sieve, without grinding, to eliminate all the coarse calcite crystals and other contaminants. This sieved material, when examined under the microscope, was found to be exceptionally free from contaminants and was fractionated into three sizes of fractions by sedimentation in water, viz. $< 2\ \mu$, 2 to 6·3 μ, and 6·3 to 20 μ. It did not contain any particles larger than 20 μ equivalent spherical diameter (e.s.d.) and only a very small percentage (1·3 %) less than 2 μ.

In fig. 1 the elongated habit of the particles can be clearly seen. The length:width ratio of the plates varied from 3:1 to 16:1. The width of the particles varied from 6·6 to 13·2 μ and the length from 33 to 105 μ. The plates were elongated in the direction of the *a*-axis. Refractive indices were determined in sodium light at 23° C. using phase contrast

[1] Geologist, c/o African Metals Corporation, P.O. Box 8186, Johannesburg.

equipment. Plates lying on (001) gave α' 1·566 and γ 1·569. Fig. 2 is an electron micrograph of the dickite. Here again the elongated habit of the plates can be clearly seen.

The Postmasburg sample was ground to pass a 200-mesh (74 μ) screen. Under the microscope some plates were more or less regular hexagons but most had rounded outlines, which was probably due to the grinding. Plates lying on (001) gave α' 1·565 and γ 1·568.

Fig. 1

Fig. 2

Fig. 1. Dickite in 6·3 to 20 μ fraction from Barkly East ($\times$400).

Fig. 2. Electron micrograph of Barkly East dickite showing euhedral crystals with elongated outlines ($\times$3000). (Electron micrograph by Dr. J. T. Fourie, National Physical Research Laboratory, South African Council for Scientific and Industrial Research.)

A chemical analysis of the 6·3 to 20 μ fraction of the dickite from Barkly East gave: SiO_2 46·43, Al_2O_3 39·54, Fe_2O_3 0·15, MgO 0·17, CaO nil, K_2O 0·02, Na_2O 0·03, TiO_2 nil, loss on ignition 14·20, total 100·54 (Analyst: Miss R. Rethemeyer, National Chemical Research Laboratory, C.S.I.R.). No impurities were detected by X-rays, and the SiO_2:Al_2O_3 ratio, 1·996, confirms the purity of the material.

X-ray examination.

X-ray powder diffraction patterns were obtained with a Phillips high-angle goniometer, using Cu-$K\alpha$ radiation and a speed of one degree 2θ

per minute. To minimize preferred orientation the samples were first mixed with an equal volume of fine cork powder before loading the aluminium sample holders. One side of the sample holder was cut away so that the samples could be loaded from the side according to the method described by von Engelhardt (1955). The spacings and intensities of the two South African dickites were compared with those of dickite from Ouray, Colorado (Clay Mineral Standard H–14), obtained under the same conditions, and with the spacings published by Smithson and Brown (1957).

The average values of the first five basal spacings are 7·152, 7·156, and 7·152 for the dickites from Barkly East, Ouray, and Postmasburg respectively. These values compare well with the average value of 7·154 found by Smithson and Brown (1957).

The intensities of the basal reflections of the Barkly East dickite were lower relative to those of the other two dickites, but it is possible that there could still have been some preferred orientation in the latter samples. The long needle-like plates of the Barkly East sample would not show such a strong tendency to orientate themselves parallel to $\{001\}$ as would plates with equant outlines. Apart from slight variations in the intensities of the reflections, the spacings are identical, within experimental error, and correspond very well with the values of Smithson and Brown (1957).

The Barkly East dickite also developed a 14 Å. reflection after heating at 600° C. and 650° C. for one hour and therefore shows the same phenomenon as that reported by Hill (1955) for the dickite from Ouray. The 2 to 6·3 μ and 6·3 to 20 μ fractions both developed a 14 Å. reflection after heating at 600° C. and 650° C. for one hour. For material heated to 550° C. this reflection did not form and for material heated at 700° C. it disappeared. After heating at 600° C. the reflections at 7·2, 3·57, and 2·33 Å. had not completely disappeared. According to Roy and Brindley (1955) these reflections must not be regarded as the higher orders of the 14 Å. line, since they are almost certainly due to incomplete conversion of the ordinary dickite structure and indicate only a mixture of phases.

Differential thermal analysis.

Differential thermal analysis curves were obtained using a two-well nickel block and a heating rate of 10° C. per minute. The temperature was measured in the inert material (calcined α-alumina, -74 μ).

In fig. 3 the curves for the various dickites are shown. These curves were made using the sieved materials. The curves for the Ouray and

Postmasburg dickites are nearly identical and correspond closely to the published curve for dickite from Ouray (Kerr *et al.*, 1949). In the Ouray and Postmasburg dickites, dehydration starts at about 500° C., taking place slowly at first as indicated by the shallow inflexion between about

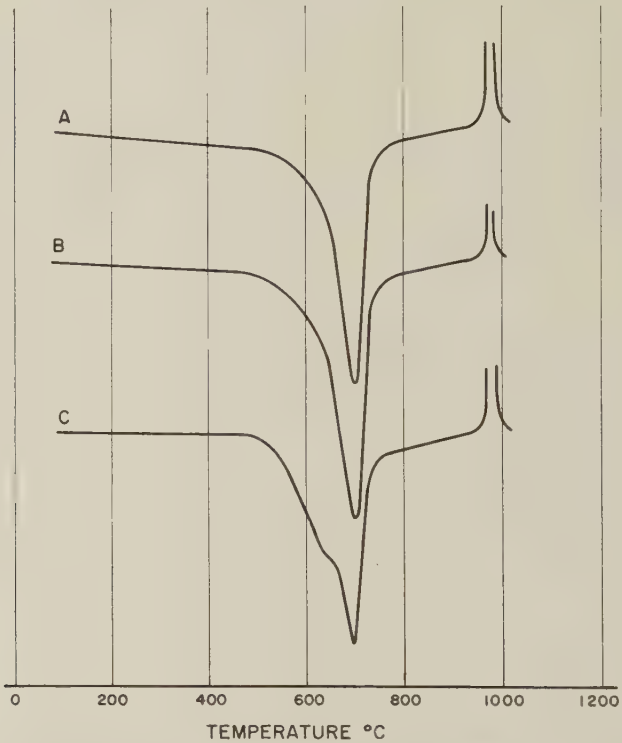

Fig. 3. Differential thermal analysis curves of various dickites. A. Ouray, Colorado (C.M.S. H.14). Amplification ×5. B. Postmasburg, Northern Cape Province. Amplification ×5. C. Barkly East, Eastern Cape Province. Amplification ×5.

500° C. and 610° C. At the latter temperature the curve turns down sharply. The curve for the Barkly East dickite shows a better defined, although only partially resolved, double endothermic peak, similar to the curve for dickite from Anglesey (Kerr *et al.*, 1950, p. 66) and the curve published by Smithson and Brown (1957). In the Barkly East dickite, dehydration also starts at about 500° C. but takes place more rapidly than in the Ouray and Postmasburg dickites.

According to Smithson and Brown (1957) there are two possible reasons for the double peak in dickite; either both peaks are due to

dickite and are shown because of the particular conditions, e.g. small ranges of crystal size with well-developed crystals, or the first peak is due to an impurity, the most likely being kaolinite. On the basis of X-ray and optical evidence, Smithson and Brown decided that the double endothermic peak must be tentatively attributed to dickite only.

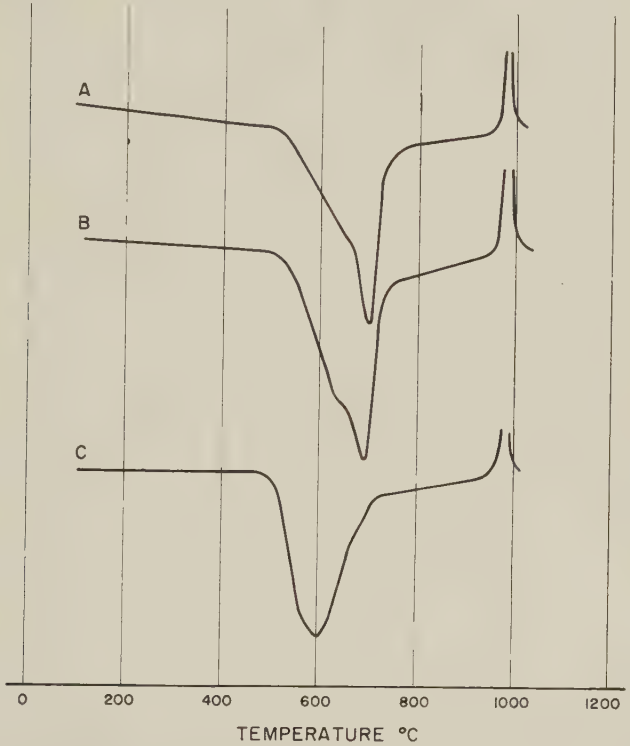

Fig. 4. Differential thermal analysis curves of various size fractions of the Barkly East dickite. A. 6·3–20 μ. Amplification $\times 5$. B. 2–6·3 μ. Amplification $\times 5$. C. $< 2\ \mu$ (Sandwich). Amplification $\times 20$.

In fig. 4 the differential thermal analysis curves of the fractionated Barkly East dickite are shown. The high-temperature portion of the double peak becomes smaller with a decrease in particle size. In the $< 2\ \mu$ fraction, only a slight inflexion remains on the high-temperature side of the peak. The curve for the $< 2\ \mu$ fraction in fig. 4 cannot be directly compared with that of the coarser fractions because insufficient material was available to fill the well in the sample holder. In this case the material was sandwiched between calcined alumina and the ampli-

fication was increased. In fig. 5, however, the curves are directly comparable; these curves were obtained for samples which were diluted with calcined α-alumina (10 % dickite, 90 % Al_2O_3). For the $< 2\ \mu$ fraction the main peak is at about 600° C. instead of 690° C. for the coarser

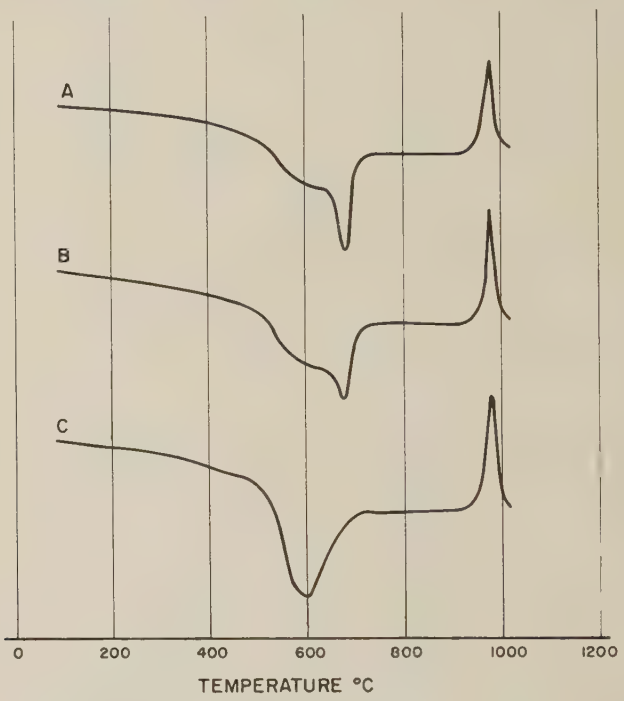

Fig. 5. Differential thermal analysis curves of various size fractions of the Barkly East dickite diluted with calcined alumina (10 % dickite, 90 % alumina). A. 6·3–20 μ. Amplification ×20. B. 2–6·3 μ. Amplification ×20. C. $< 2\ \mu$. Amplification ×20.

particle size fractions. As would be expected, the effect of the dilution was to improve the resolution of the two poorly-resolved peaks of the undiluted samples. Microscopical examination of the $< 2\ \mu$ fraction showed that it consisted of very fine elongated dickite particles only. No contaminants could be detected.

Discussion and conclusions.

With coarse-grained dickites such as those from Ouray and Postmasburg it would be very difficult to obtain a size fraction $< 2\ \mu$ e.s.d.

without resorting to grinding, but it is assumed that similar results will be found with these materials. McLaughlin (1955) studied the effects of grinding on the Ouray dickite. After two hours dry grinding he obtained a material which yielded a double endothermic peak. After 60 hours wet grinding, only one peak remained at a temperature lower than 600° C. McLaughlin states that the double peak is probably due to differences in reactivity between ground and unground material. It is, however, more probable that the particle size distribution of the sample after dry grinding for two hours was such that a double peak was formed. Unfortunately, McLaughlin did not report the particle size after 60 hours wet grinding but his curve is similar to the $< 2\ \mu$ fraction in fig. 4, although the peak temperature is somewhat lower. According to Murray and White (1955, p. 147), when fine particle size is produced by grinding it is not certain that the lowering of decomposition temperature is due to particle size alone, since fine grinding causes considerable disturbance in the surface layers of minerals, particularly if they are soft. It must be pointed out, however, that the actual temperature where decomposition started in the wet-ground material is not significantly lower than the corresponding temperature in the unground material, viz. 500° C.

The evidence presented shows that the double peak for some dickites must be ascribed to dickite only and not to the presence of contaminants. Furthermore, it is clear that in the particular dickite with elongated habit examined, the double peak is a particle size effect which practically disappears if all the particles are $< 2\ \mu$ e.s.d.

The mechanism of dehydroxylation in dickite.

The results of the present study enable some conclusions to be drawn as to the mechanism of dehydroxylation in dickite. Apart from the elongated habit of the Barkly East dickite, the only obvious difference between it and the Ouray and Postmasburg dickites appeared to be their different ranges of crystal sizes. It was also noticed that the latter dickites intumesced in the differential thermal analysis sample holder whereas the Barkly East dickite did not. In the Ouray and Postmasburg dickites, which have well-developed basal planes and equant outlines, one would expect the final dehydration to take place violently when the OH-groups in the interior of the particles escape, so that a portion of the material would be ejected from the holder, especially if the particles had acquired a preferred orientation as a result of being tamped into the holder. Roy and Osborn (1954), in a study of the temperatures of formation and temperature limits of stability of certain clay minerals, found

that kaolinite, halloysite, dickite, and nacrite all decomposed under equilibrium conditions at the same temperature of 405° C. They state (p. 863): 'The main difference in decomposition behaviour is the rate of decomposition with the larger particles of dickite and nacrite requiring longer periods of time to effect significant decomposition. Differences in the thermodynamic constants among these four phases must be slight.' Roy and Osborn conclude (p. 885): 'Thus the data from the present study would indicate that differential thermal analysis curves of dickite would approach more and more closely those of kaolinite as the particle shape and size were made more and more equal.'

For the Barkly East $< 2\ \mu$ fraction the peak temperature of about 600° C. corresponds to a peak temperature of 610° C. for well-crystallized kaolinite from Macon, Georgia (Clay Mineral Standard H4), obtained with the same differential thermal analysis apparatus under the same conditions. These findings support the conclusions of Roy and Osborn (1954) and confirm their deductions which were based on indirect evidence.

It is clear from the curves that the loss of water begins at a constant temperature of about 500° C. for different dickite samples and irrespective of particle size. It is thus reasonable to explain the double peak of dickite as follows: The first portion of the double peak is due to the loss of OH-groups from the surfaces and edges of the particles and the second to the loss of OH-groups situated in the interior of the particles. The intumescence noticed with the Ouray and Postmasburg dickites is especially indicative of the loss of OH-groups from the interior of the relatively large particles. In the Barkly East dickite the loss of such OH-groups does not take place so violently because they can escape more easily, owing to the thin elongated habit of the crystals. A higher temperature is, however, still necessary to eliminate them from the coarser particles as indicated by the curves. As the particle size diminishes, the number of OH-groups in the interior of the crystals decreases relative to the more loosely bound OH-groups on the surfaces and edges of the particles, and therefore less energy is needed for their elimination (see fig. 5). In the particle size fraction $< 2\ \mu$ e.s.d., practically all the OH-groups can escape easily, so that only one peak occurring at a relatively low temperature is registered on the differential thermal analysis curve.

Acknowledgement. The authors wish to thank Dr. T. L. Webb for his many helpful suggestions and the interest shown in the work. This paper is published with the permission of the South African Council for Scientific and Industrial Research.

References.

Davis (D. W.), Rochow (T. G.), Rowe (F. G.), Fuller (M. L.), Kerr (P. F.), and Hamilton (P. K.), 1950. Amer. Petr. Inst., Clay Mineral Standards. Prelim. Rep. No. 6, Columbia University, New York.

Engelhardt (W. von), 1955. Zeits. Krist., vol. 106, p. 430.

Frankel (J. J.), 1949. Min. Mag., vol. 28, p. 582.

Grim (R. E.), 1953. Clay Mineralogy (New York: McGraw-Hill).

Hill (R. D.), 1955. Acta Cryst., vol. 8, p. 120.

Kerr (P. F.), Kulp (J. L.), and Hamilton (P. K.), 1949. Amer. Petr. Inst., Clay Mineral Standards, Prelim. Rep. No. 3, Columbia University, New York.

Kerr (P. F.), Hamilton (P. K.), Pill (R. J.), Wheeler (G. V.), Lewis (D. R.), Burkhardt (W.), Reno (D.), Taylor (G. L.), Mielenz (R. C.), King (M. E.), and Schieltz (N. C.), 1950. Ibid., no. 7.

McLaughlin (R. J. W.), 1955. Clay Min. Bull., vol. 2, no. 14, p. 309.

Mezösi (J.), 1957. Acta Univ. Szeged. Acta Min.-Petr., vol. 10, p. 67.

Murray (P.) and White (J.), 1955. Trans. Brit. Ceram. Soc., vol. 54, p. 137.

Roy (R.) and Brindley (G. W.), 1955. Proc. Fourth Nat. Conf. Clays and Clay Minerals (Publ. 456, Nat. Acad. Sci.–Nat. Res. Council, Washington, D.C. 1956).

Roy (R.) and Osborn (E. F.), 1954. Amer. Min., vol. 39, p. 853.

Smithson (F.) and Brown (G.), 1957. Min. Mag., vol. 31, p. 381.

Whiteside (H. C. M.), 1941. Trans. Geol. Soc. South Africa, 1942, vol. 44 (for 1941), p. 121.

Pseudomorphs after olivine in Markle basalt.

By W. W. Smith, B.Sc., Ph.D.

The Macaulay Institute for Soil Research, Aberdeen, Scotland.

[Taken as read 5 November 1959.]

Summary. Pseudomorphs after olivine in Markle basalt from Holyrood Park, Edinburgh, consist of an intimate mixture of hematite and chlorite, along with a small percentage of quartz. A definite relationship exists between the orientations of the two main constituents and is dependent upon their structures.

THE Markle basalt, which forms part of the Whinny Hill Series of lavas in Holyrood Park, Edinburgh, is hydrothermally altered in that the original olivine phenocrysts are completely replaced. In the weathered rock, the resultant pseudomorphs are very conspicuous since they consist of a glittering red platy product which has at least one excellent cleavage or rather 'pseudocleavage'. In the past, material like this would probably have been described as a single mineral termed iddingsite. This name was originally applied by Lawson in 1893 following earlier descriptions of the material (from Carmelo, California) by Iddings in 1892. From the many chemical analyses of 'iddingsite' carried out by Ross and Shannon (1926) and Tomkeieff (1934), ten were selected by Wilshire (1958) to express a range of composition for this material. An average composition was calculated, and these results are compared with the analysis of the Markle basalt material in table I. The Markle sample differs, however, in having a comparatively high content of alumina and ferrous oxide.

Variations in chemical composition are not surprising, since recent X-ray investigations have revealed that the name 'iddingsite' has been used for at least two different mixtures. Sun (1957) identified 'iddingsite' from Carrizozo, New Mexico, and from Paton Peak, Colorado, as a mixture of goethite and amorphous material, and Wilshire (1958) identified material from various localities in California, including the type locality Carmelo Bay, also New South Wales and Hawaii, as mixed-layer montmorillonite–chlorite and goethite. The Markle basalt pseudomorphs after olivine were likewise found to contain more than one mineral, viz. hematite, chlorite, and a small quantity of quartz.

An attempt to determine the percentages of hematite and quartz by

X-ray powder methods with corundum as an internal standard was not very satisfactory, owing to the small quantity of material available for making specimens. Six results ranged from 33 to 42 % hematite, against 32·39 % total Fe_2O_3 by chemical analysis of the air-dried sample. By the dithionite method of determining free iron oxide (Mitchell and Mackenzie, 1954) it appeared that all the ferric oxide in the sample was in the free state and therefore the quantity of hematite was taken to be

TABLE I. Chemical analyses of 'iddingsite' and of the pseudomorphs from the Markle basalt.

	*Iddingsite**		*Material from Markle Basalt*
	Range	*Average*	
SiO_2	22·08–48·36	41·20	24·77
TiO_2	0·12–0·26	0·14	—
Al_2O_3	0·00–5·09	3·81	14·77
Fe_2O_3	25·48–60·13	35·42	34·09
FeO	0·00–1·97	0·38	4·50
MnO	0·00–0·11	0·05	—
MgO	0·60–12·71	6·85	13·27
CaO	1·72–3·26	2·35	0·73
Na_2O	0·12–0·13	0·12	—
K_2O	0·09–0·10	0·10	—
H_2O+	5·74–11·00	9·30	8·26
		99·72	100·39
H_2O- (300° C.) ...			5·04

* Analyses of ten iddingsite samples are represented and are quoted from Wilshire (1958). All analyses were recalculated to 100 % excluding H_2O before averages were computed.

32·39 % of the air-dried sample. Quartz was determined by X-ray methods as approx. 2 % of the mixture, whence the remainder of the sample was found to have the composition of a chlorite with formula $0{\cdot}22\ M^{+}[Si_{3\cdot27}Al_{0\cdot73}][Al_{1\cdot85}Mg_{2\cdot94}Fe^{2+}_{0\cdot55}]O_{10}(OH)_8$. The calculation of this formula was based on the assumption that each structural unit contained 10 oxygen and 8 hydroxyl ions. Since there was no shift in the 14·5 Å. basal spacing of this mineral after heat treatment at 600° C., it is considered to be a true chlorite and of the pennine species according to the classification proposed by Hey (1954). Its cation-exchange capacity is 24 m.e. per 100 g. with calcium as the exchangeable cation.

The *optical properties* of the combined product, as seen in thin section, tend to be similar to those of biotite, especially the pleochroic effect with strong absorption of the rays vibrating parallel to the main cleavage. The colour ranges from a pale straw yellow to a dark reddish brown,

as in biotite. An electron-micrograph of crushed fragments of this material shows transparent chlorite coated with iron oxide as pigment (fig. 1). The platy form of the chlorite and hematite and the manner in which these minerals aggregate result in a well-developed cleavage within the pseudomorphs (fig. 2). Where it is possible to obtain an interference figure along the normal to the cleavage planes, the material is always biaxial negative with 2V varying from 0° to 20°.

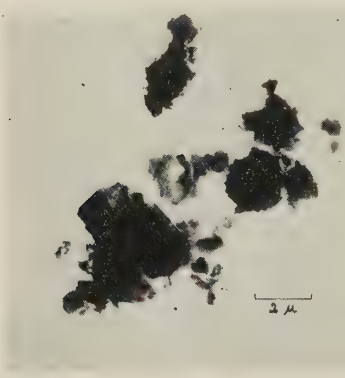

Fig. 1

Fig. 2

Fig. 1. Electron-micrograph of crushed fragments of pseudomorphs after olivine.
Fig. 2. Photomicrograph of thin section of rock showing well-developed cleavage of pseudomorph. ×43.

Orientation relationships. The hematite and chlorite exist as intimately mixed aggregates of very small crystals, as shown by the smoothness of the reflections in an X-ray diffraction photograph obtained from a stationary cleavage flake. The same photograph also shows that the crystals exist in a preferred orientation. The quartz occurs as very small mosaic-like patches within the pseudomorphs, as seen in thin sections using polarized light. The X-ray evidence shows that the individual crystals of quartz are in random orientation.

The orientation relationship between the hematite and the layer-silicate was studied by taking a series of X-ray rotation photographs. For convenience, the hematite is referred to hexagonal crystallographic axes x, y, u, and z while the monoclinic chlorite is assigned the axes a, b, and c. When the specimen was rotated about a vertical axis normal to the cleavage plane, the c-axes of the layer-silicate particles and the z-axes of the hematite particles were simultaneously vertical (fig. 3).

With the *a*-axes of the chlorite crystals vertical, the zero layer line contained the general 060 reflection and orders of the basal 00*l* reflection, while at the same time one of the three short axes of the hematite was vertical (fig. 4).

From the rotation photographs, the unit cell dimensions of the two components were calculated and a definite epitaxial relationship was

FIG. 3. Rotation photograph about the *z*-axis of the hematite (. *c*-axis of the chlorite).

established: *a* (5·20 Å.) of chlorite approx. parallel to *x* (4·97 Å.) of hematite, *c* (14·50 Å.) of chlorite approx. parallel to *z* (13·76 Å.) of hematite. The chlorite has *b* 9·18 Å., β approx. 97°.

The *a* and *b* unit-cell dimensions of the chlorite were also calculated from an electron diffraction pattern taken along the *c*-axis direction and these agreed well with the X-ray data.

Disorientation effects. Both the hematite and the chlorite gave some sharply defined spots and some elongated streaks in the rotation photographs.

When a cleavage flake of the pseudomorph was rotated with the *x*-axis of the hematite vertical the 03$\bar{3}$0 hematite and 060 chlorite reflections, which appeared on the zero layer line, were sharp and short,

whereas when the flake was rotated with the z-axis of the hematite vertical the same reflections, again on the zero layer line, were elongated (figs. 4 and 3). The streaking of the reflections must be due to slight disorientation of the crystals about a direction normal to their z- or c-axis, as this type of displacement would have almost no lengthening effect upon the $03\bar{3}0$ and 060 reflections with the flake adjusted for rotation about the x-axis. For the same setting, however, the $00l$ reflec-

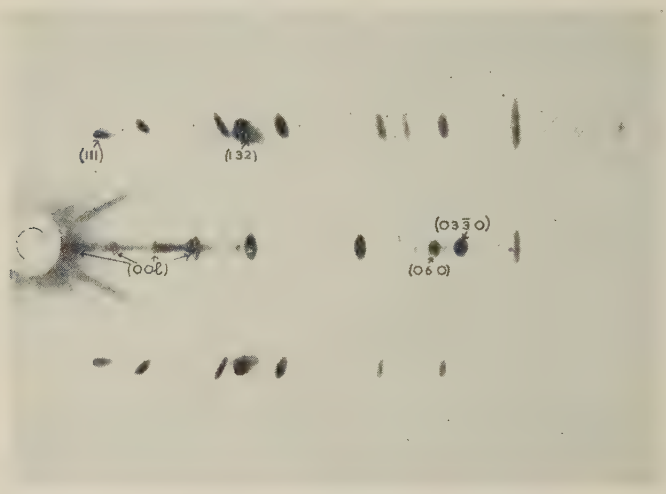

Fig. 4. Rotation photograph about the x-axis of the hematite (= a-axis of the chlorite).

tions of the chlorite are elongated as one would expect (fig. 4). Similarly, when the crystals were set up for rotation about their y*- or b-axes the reflections $2\bar{1}\bar{1}0$ and $4\bar{2}20$ were sharp and short compared with the $2h\bar{h}\bar{h}l$ and $00l$ reflections (fig. 5).

The conclusion that disorientation takes place in a direction normal to the c- or z-axis is confirmed by the radial streaking of all reflections in a Laue photograph taken with the X-ray beam parallel to the c- or z-axis. The fact that the streaking effect is of uniform length in all directions indicates that the disorientation occurs as a tilting of the crystal plates about any axis in the ab or xyu plane. In comparison, very little disorientation of the crystal plates occurs about the direction of the c- or z-axis. This has already been mentioned in connexion with the short reflections in the rotation photographs and is also demonstrated

by the absence of any marked circular spread of reflections in the Laue photograph.

An attempt was made to measure the extent of disorientation by taking Weissenberg photographs of the material rotated about each of the three principal chlorite axes. Most of the reflections appeared as straight lines on these photographs, their length depending on the

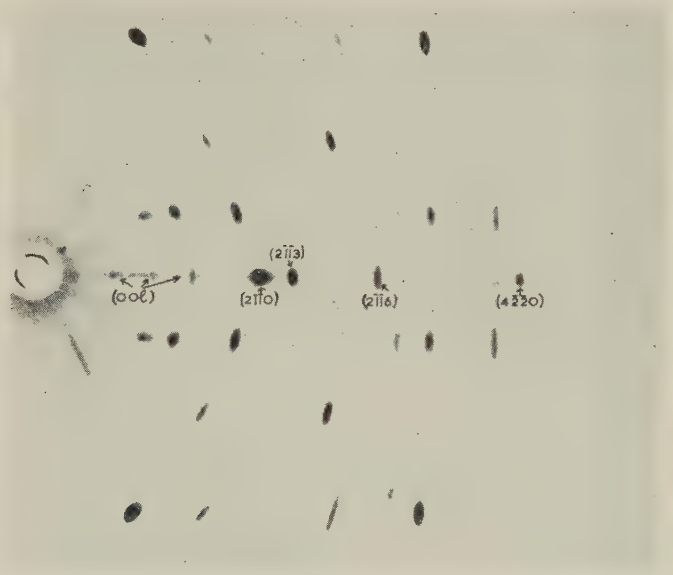

FIG. 5. Rotation photograph about the y^*-axis of the hematite (= b-axis of the chlorite).

amount of angular disorientation about the direction of the rotation axis. Intensity distribution for each spot was calculated using calibration curves which had been prepared from measurements of the optical density of films exposed to X-rays by a step sector arrangement. Optical density measurements were made in every case by a photometer with photo-electric cell and galvanometer. The curves shown in fig. 6 were drawn from average measurements of six reflections in each case, taking the maximum calculated intensity of each reflection to be 100 % and the film background intensity to be 0 %. The intensity profile of reflections from a quartz crystal (similar in size to the cleavage flake of the pseudomorph) is included in fig. 6, to show the angular

spread of intensity one would expect from a perfectly oriented aggregate of crystals.

In the Weissenberg photographs some chlorite reflections were represented by rods in reciprocal space passing through (ha^*,kb^*,0) parallel to c^*, indicating that the crystals of chlorite are extremely thin along the c-axis direction.

Discussion. Comparison of curves B and C in fig. 6 shows that disorientation of the crystals of hematite is less about the z-axis than about

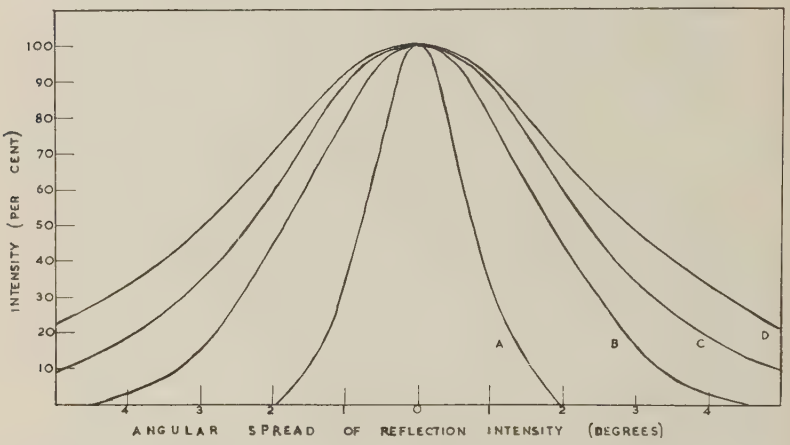

FIG. 6. Intensity profiles of Weissenberg zero-layer reflections. A, Quartz crystal rotated about the z-axis. B, Hematite crystals rotated about the z-axis. C, Hematite crystals rotated about the x- and y^*-axes. D, Chlorite crystals rotated about the b-axis.

any normal to this axis. The chlorite crystals behave in the same way.

Both minerals have sheets of oxygen atoms in hexagonal close packing, parallel to the (00l) and (000l) planes of chlorite and hematite respectively. These are the cleavage planes and are most likely to be the contact surfaces between the crystals. The superposition of the sheets of oxygen atoms brings the a- and x-axes into alignment with almost no disorientation about the z-axis direction. In the electron-micrograph, thin films of hematite are seen formed on the surfaces of chlorite plates.

The disorientation normal to the z- or c-axis direction may be due to bending of the chlorite plates, since they are extremely thin in the c-axis direction. Also, the thinness of the chlorite plates and the fact that the chlorite is twice as abundant as the hematite suggest that the basal surface area of the chlorite is much greater than that of the

hematite. The extent of hematite disorientation in comparison with chlorite (cf. curves *C* and *D*, fig. 6) may depend on the positioning of the hematite crystals upon the chlorite, e.g. they may be restricted to the flatter portions of the chlorite plates.

Some of the hematite reflections do not satisfy the conditions limiting possible reflections in the space-group $R\bar{3}c$ to which hematite belongs. Twinning could account for these reflections but a more obvious explanation is that the hematite may have more than one orientation on the chlorite plates. The apparent hexagonal symmetry of the hematite is probably due to the hexagonal symmetry inherent in the chlorite tetrahedral layer enabling the *x*-axis of the hematite to take up any one of six possible positions at 60° intervals of rotation about *z*.

Acknowledgements. The author is indebted to Miss C. I. Dickson for chemical analysis of the sample and also to Dr. R. C. Mackenzie for help in calculating the chlorite formula. Thanks are due also to Mr. W. A. Mitchell for helpful interest and encouragement during this work. The author is grateful to members of the Chemistry Department, University of Aberdeen, Dr. J. A. Gard for producing the electron-micrograph, and Dr. H. F. W. Taylor for discussion and granting the use of a Weissenberg camera.

References.

Hey (M. H.), 1954. Min. Mag., vol. 30, p. 277.
Iddings (J. P.), 1892. U.S. Geol. Survey, Monogr. 20, App. B, p. 388.
Lawson (A. C.), 1893. Univ. Calif. Publ. Geol. Sci., vol. 1, p. 1.
Mitchell (B. D.) and Mackenzie (R. C.), 1954. Soil Sci., vol. 77, p. 173.
Ross (C. S.) and Shannon (E. V.), 1926. Proc. U.S. Nat. Mus., vol. 67, art. 7, p. 1.
Sun (Ming-Shan), 1957. Amer. Min., vol. 42, p. 525.
Tomkeieff (S. I.), 1934. Geol. Mag., vol. 71, p. 501.
Wilshire (H. G.), 1958. Amer. Min. vol. 43, p. 120.

An X-ray study of manganese minerals.

By Bibhuti Mukherjee, M.Sc., D.Phil.
Geological Survey of India, Calcutta, India.

[Communicated by the Editor; taken as read 5 November 1959.]

Summary. Rhodonite, rhodochrosite, spandite, psilomelane, beldongrite, braunite, sitaparite, and vredenburgite from a collection by Fermor have been studied by the X-ray powder diffraction method. The cell dimensions of all forms of cryptomelane—massive, horny, botryoidal, reniform, mamillated, and stalactitic—are a 9.82 Å., c = 2.86 Å., whereas the cell dimensions of shiny pitch-like beldongrite are a = 9·85 Å., c = 2·87 Å. The amorphous admixture associated with cryptomelane is revealed by a broad halo, 4·60 Å. to 3·90 Å., in the powder pattern. Aminoff's crystal data for braunite are discussed with a different orientation, and a new space group, $I\ 4/mmm$ (D_{4h}^{17}), is assigned after indexing the powder pattern. Fermor's sitaparite (bixbyite) is assigned a new space group $I\ m3$ (T_h^7), different from that proposed by Pauling *et al.*, on the basis of a fresh indexing of the powder pattern. Manganese-garnet from the gondite series has a cell-size of the order of spessartine, whereas the cell-size of manganese-garnet from the kodurite series varies from 11·72 to 11·95 Å. Fermor's spandite from the kodurite series is a mixture of spessartine, grossular, and andradite garnet-molecules with almandine and pyrope as minor components. Ramsdellite and γ-MnO_2 or β-MnO_2 are found in a number of samples of manganese ores.

FERMOR (1909) classified manganese-ore deposits in India into three main groups: deposits interbedded with the Archeans, including the gondites; deposits associated with the kodurites; and lateritoid deposits or surface enrichments of a lateritic nature. Fermor's 'gondite series' of Central Provinces is characterized by the presence of various manganiferous silicates, chiefly spessartine and rhodonite. The ore body consists mainly of a banded quartzite–manganese-oxide–braunite rock. Associated manganese minerals are sitaparite, hollandite, jacobsite, hausmannite, psilomelane, and pyrolusite. Fermor's 'kodurite series' of Vizagapatam is characterized by spandite (a garnet intermediate in composition between spessartine and andradite), rhodonite, psilomelane, and pyrolusite with some braunite, manganmagnetite, and, in one locality, 'vredenburgite'. Other manganese ore deposits associated with Archean rocks, and the lateritoid deposits in parts of Orissa, Bombay, and Mysore, contain psilomelane and pyrolusite, with braunite and spessartine in a few localities.

The space-group and cell-dimensions of cryptomelane and psilomelane were previously reported by the author (Mukherjee, 1959).

Results and discussion.

The original type minerals from the collection in the Indian Museum made by Fermor were used for the X-ray study, and most of the specimens studied are described in the Memoirs of the Geological Survey of

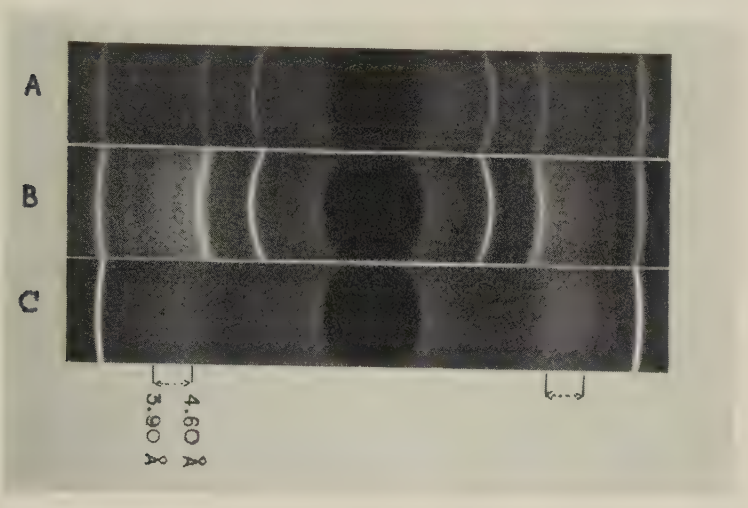

Fig. 1. X-ray powder diffraction photograph of Fermor's psilomelane. A, Cryptomelane (A385). B, Cryptomelane (1158) with amorphous admixture. C, Pyrolusite (A268, outer crust) with amorphous admixture.

India (1909, vol. 37, pts. i–iii) by Fermor. The powder photographs were obtained using Fe-$K\alpha$ radiation, and the relative intensities of powder lines were determined on a Moll recording microphotometer.

Cryptomelane and beldongrite. Almost all manganese ores of Indian deposits contain cryptomelane with more or less amorphous admixture. But the X-ray powder diffraction method gives practically no information concerning amorphous phases, which may sometimes be present as a major constituent along with the cryptomelane. Fleischer and Richmond (1943) pointed out that in an intergrowth of 50 % cryptomelane and 50 % amorphous material, the X-ray powder pattern would only be that of pure cryptomelane. In the present investigation the presence of amorphous admixture with cryptomelane was clearly revealed by a broad halo (4·60 Å. to 3·90 Å.) in the powder pattern (fig. 1).

The cell-dimensions of tetragonal cryptomelane (Fermor's 'psilomelane'—massive, horny, botryoidal, reniform, mamillated, pisolitic, and stalactitic[1]) are a 9·82 Å., c 2·86 Å., and c/a 0·291. Beldongrite, the smooth shiny pitch-like mineral from Beldongri quarry, Madhya Pradesh, described by Fermor (no. 1079, Indian Museum no. 18/922), was shown to be tetragonal on indexing the powder pattern by Hesse's method (1948) and the cell-dimensions are a 9·855 Å., c 2·869 Å. (±0·003), and c/a 0·291. Two samples of beldongrite from Mansar mine, Chargaon, Madhya Pradesh (Fermor's nos. 1026 and 1035), showed identical powder patterns. Beldongrite is isostructural with cryptomelane, and detailed work, including a chemical analysis, is in progress.

Monoclinic hollandite with well-developed crystal faces was found on a matrix of massive cryptomelane in Kajlidongri, Chhindwara, and Balaghat manganese ores. Ramsdellite was detected in Dongri Buzurg and Sandur manganese ores. γ-MnO_2 or β-MnO_2 of McMurdie[2] was found in Sandur and Belgaum ores in intimate association with pyrolusite.

Braunite. The powder spacing data of braunite from Kacharwahi, Nagpur (Fermor's no. B 1259), are similar to those reported by Harcourt (1942) for braunite (Harvard Museum no. 83692) from Vizagapatam, India. The cell-dimensions of tetragonal braunite were determined after indexing the powder pattern (table I) by Hesse's method as a 9·402 Å., c 18·740 Å. (c/a 1·994). The systematic absences indicate a space-group $I\,4/mmm$ (D_{4h}^{17}). With the above axial lengths and sp. gr. 4·8 for braunite the unit-cell contents are $8(3Mn_2O_3.MnSiO_3)$.

Aminoff (1931) determined the cell-dimensions of tetragonal braunite from Långban as a 13·28 Å., c 18·58 Å. from single crystal measurements. This cell is face-centred, and gives on conversion to the body-centred lattice a 9·39 Å., c 18·58 Å., z 8. Aminoff suggested a space-group D_{4h}^{20} on the basis of indexing of his photographs, but the conditions limiting possible reflections for the space-group D_{4h}^{20} are not satisfied by his index-

[1] The following specimens were examined (both Fermor's and the Indian Museum numbers are given, the latter in parentheses): A680 (J903) and A682 (J904) from Chikhli, Satara, Bombay; A705 (J905) from Yeruli, Satara, Bombay; A376 (J917), A377 (J918), and A385 (J921) from Tekrasai, Singhbum, Bihar; A267 (18/425) and A268 (18/426) from the Garbham mine, Vizagapatam; and 1158 (18/986) from Sonegaon, Guguldoho, Nagpur. A268 has an inner dull core of cryptomelane and an outer crust of pyrolusite.

[2] Byström (1950) concluded that the γ-MnO_2 of McMurdie and Golovato (1948) is not identical with the oxide called γ-MnO_2 by Cole *et al.* (1947) and by Byström (1949), but is a rather poor β-MnO_2 preparation.

ing; the definite existence of the powder line 130 excludes the space-group D_{4h}^{20}, and the possible presence of reflections 150, 053, and 039 cannot be ruled out.

Sitaparite. The powder spacing data of sitaparite (Fermor's no. B 322) from Sitapar, Chhindwara, are similar[1] to those of bixbyite from Simson, Utah, reported by Zachariasen (1928). The cell-size of sitaparite

TABLE I. X-ray powder data for braunite, Kacharwahi, Nagpur (Fermor's no. B1259).

d, Å.	I/I_0	$Sin^2\theta$ obs.	*hkl*	$Sin^2\theta$ calc.	*d*, Å.	I/I_0	$Sin^2\theta$ obs.	*hkl*	$Sin^2\theta$ calc.
5·360	10	0·0326	112	0·0319	1·681	5	0·3314	345	0·3317
4·655	20	0·0432	004	0·0427	1·659	80	0·3405	440	0·3392
3·470	30	0·0778	123	0·0770				048	0·3405
3·320	10	0·0850	024	0·0851	1.537	20	0·3965	347	0·3958
2·960	10	0·1069	130	0·1060				149	0·3965
2·830	5	0·1170	132	0·1167	1·501	25	0·4158	163	0·4162
2·710	100	0·1276	224	0·1275	1·464	20	0·4370	451	0·4373
2·508	15	0·1489	134	0·1487	1·418	60	0·4660	264	0·4667
2·405	5	0·1620	233	0·1618	1·412	30	0·4698	2·2·12	0·4693
2·345	40	0·1704	040	0·1696	1·368	15	0·5007	363	0·5010
			008	0·1709	1·355	25	0·5102	448	0·5101
2·141	45	0·2044	235	0·2045	1·265	20	0·5856	273	0·5858
1·915	10	0·2555	244	0·2547	1·175	20	0·6786	080	0·6784
			228	0·2557	1·164	20	0·6913	471	0·6917
1·871	20	0·2676	341	0·2677				181	0·6917
1·841	10	0·2764	150	0·2756	1·146	10	0·7134	565	0·7133
			138	0·2769	1·078	50	0·8062	664	0·8059
1·803	15	0·2883	053	0·2890	1·051	40	0·8483	480	0·8480
			343	0·2890				088	0·8493
1·735	20	0·3113	147	0·3110					
			039	0·3117					

was determined as a 9·40 $\pm$0·01 Å. Three original type samples of sitaparite from Fermor's collection showed identical powder patterns. After indexing all the powder lines of sitaparite (table II), the conditions limiting possible reflections are found to be those of a body-centred cubic lattice. These systematic absences indicate a space-group $Im3$ (T_h^5). The definite existence of the powder lines 310 and 510 excludes the possibility of the space-group $Ia3$ (T_h^7) for bixbyite, suggested by Pauling and Shappell (1930) from the study of Laue photographs.

With a 9·40 Å. and sp. gr. 5·0 for sitaparite, the unit-cell content is 16 ($FeMnO_3$), as found by Zachariasen (1928). Fleischer and Richmond (1943) reported in the powder data for bixbyite the spacings 4·204 (10), 1·075 (40), and 1·048 (20), but these lines could not be indexed on the

[1] Mason (1942) has also found sitaparite to be identical with bixbyite.

basis of a body-centred cubic lattice (table II); these lines, which are moderately intense in Fleischer's data, are not, however, present in the data of Zachariasen or of the present author. Evidently, they were due to some impurity in Fleischer's sample.

TABLE II. X-ray powder data for sitaparite, Sitapar, Chhindwara (Fermor's no. B322).

d, Å.	$h^2+k^2+l^2$	hkl	I/I_0	d, Å.	$h^2+k^2+l^2$	khl	I/I_0
4·700	4	200	10	1·257	56	642	10
3·837	6	211	60	1·195	62	732	10
3·327	8	220	5			651	
2·976	10	310	5	1·176	64	800	25
2·716	12	222	100			811	
2·513	14	321	20	1·158	66	741	25
2·354	16	400	40			554	
2·215	18	411	5	1·141	68	820	20
2·105	20	420	5			644	
2·006	22	332	40	1·125	70	653	15
1·921	24	422	10	1·109	72	822	10
1·846	26	510	40			660	
1·718	30	521	20			831	
1·662	32	440	90	1·094	74	750	10
1·614	34	530	10			743	
		433		1·079	76	662	60
1·567	36	600	5	1·065	78	752	5
		442		1·052	80	840	50
1·527	38	611	20	1·039	82	910	10
		532				833	
1·488	40	620	5	1·026	84	842	10
1·452	42	541	30			921	
1·419	44	622	70	1·015	86	761	30
1·387	46	631	30			655	
1·358	48	444	20	1·003	88	664	20
1·330	50	710		0·9917	90	930	
		550	5			851	20
		543				754	
1·305	52	640	10				
1·280	54	721					
		633	25				
		552					

Manganese-garnet. The cell-size of manganese-garnet was determined with an accuracy of ±0·003 Å. The manganese-garnet of Fermor's gondite series has a cell-size (11·615 Å.–11·642 Å.) near that of spessartine. In Fermor's kodurite series the cell-size of the manganese-garnet lies between 11·72 Å. and 11·95 Å. for different samples. The molecular percentage composition of four constituents in Fermor's spandite from Kotakarra, kodurite series (A233), was derived from the recorded chemi-

cal analysis[1] as: spessartine 37·65, grossular 34·87, almandine 16·82, andradite 10·66 %, and the cell-size was determined as 11·723 Å. from the powder pattern. The recorded chemical analysis[1] of Fermor's spandite from Garbham, kodurite series (A219), shows that the spandite is a mixture of spessartine (39.26 %) and andradite (46·23 %) with pyrope (14·51 %) as a minor constituent, and the cell-size was determined as 11·915 Å. from the powder pattern. The analytical data of Fe''' and Al''' for spandite, A219, are probably anomalous.

Jacobsite, hausmannite, and vredenburgite. Jacobsite was found as a major constituent in almost all specimens of ores from Tirodi, Dongri Buzurg, Balaghat, and Beldongri (Madhya Pradesh) and from Kodur, Devada, Garividi, and Avagudem (Vizagapatam). The cell-size of jacobsite lies between 8·42 Å. and 8·52 Å. for different samples from Tirodi and Kodur.[2] A pure sample of hausmannite was separated from the ore of Sitapar, Chhindwara. The cell-dimensions of the tetragonal mineral were determined after indexing the powder pattern by Hesse's method (1948) as a 5·75 Å., c 9·41 Å. ($\pm$0·01). Hausmannite was found associated with almost all specimens of jacobsite as a minor constituent.

Vredenburgite (Fermor's no. B1257) from Beldongri contains mainly jacobsite with a considerable amount of hausmannite.[3] The feebly magnetic fraction contains braunite, cryptomelane, and hausmannite, and the strongly magnetic fraction contains jacobsite and hausmannite. Vredenburgite from Garividi, Vizagapatam (Fermor's no. A346), contains jacobsite and a small amount of hausmannite.

Rhodonite and rhodochrosite. Rhodonites, of pink, greenish grey, and brown, were found in rocks of the gondite series associated with spessartine and quartz. The powder spacing data of pink rhodonite are similar to those reported by Mikheev and Dubinina (1948) for a sample from Sverdlovsk, Ural. The pink material of rhodonite rock (no. 23/364) from Bhandara, Madhya Pradesh, contains rhodonite, spessartine, and rhodochrosite, and the associated yellowish-white material contains quartz, feldspars, and fluorapatite. The dark brown (partly blackened) material of the rhodonite rock contains rhodonite, rhodochrosite, cryptomelane, and hematite. Fermor's pinkish-white rhodochrosite (no. B325) from Gaimukh, Chhindwara, is associated with rhodonite, braunite, and barite.

[1] Chemical analyses by Mr. T. R. Blyth, reported by Fermor in Mem. Geol. Surv. India, 1909, vol. 37, p. 168.

[2] Johansson (1928) found a 8·42 Å., and Passerini (1930) a 8·515 Å.

[3] Orcel and Pavlovitch, 1932; cf. Fermor, 1938, and Mason, 1947.

Various manganese ores. Nearly three hundred specimens of manganese ores from various deposits, collected by geologists of the Geological Survey of India and from Fermor's collection, were studied. An isodynamic separator was used to concentrate the minerals in a number of magnetic fractions, and the mineralogical composition of the ore was determined from the minerals identified in each fraction. In the manganese ores of Madhya Pradesh and Bombay (Jhabua, Kajlidongri, Sitapar, Chhindwara, Balaghat, Beldongri, Chargaon, Tirodi, Jagantola, Bharweli, Ramrama, Suteli, Bhandara, Chikhla, Sitasaongi, and Dongri Buzurg) the most common manganese minerals are braunite, spessartine, jacobsite, cryptomelane, pyrolusite, hausmannite, bixbyite, hollandite, and psilomelane. In the Vizagapatam deposits (Devada, Kodur, Garbham, Avagudem, Garividi, and Chipurupalli) jacobsite, spandite, pyrolusite, cryptomelane, braunite, and hausmannite occur in most specimens of ore. In Mysore (Sandur, Ramandrug, Shimoga, Belgaum, and North Kanara), Bombay (Panchmahals, Sivarajpur, Bamankua, Pani, Baria, Satara, Jambughoda, Chota Udaipur, and Baroda), Rajasthan (Banswara), and Orissa (Keonjhar, Koraput, Kalahandi, Bonai, and Bamra) deposits, pyrolusite and cryptomelane with amorphous admixture are the major constituents of ore; braunite, spessartine, and jacobsite are sometimes associated as minor constituents. Manganese-amphibole and -pyroxene are not included in the present investigation.

Acknowledgements. The author is most grateful to the Director of the Geological Survey of India for kind permission to publish these results, to Prof. B. S. Basak of the Presidency College, Calcutta, for useful discussion, and to Dr. B. Das Sarma, Chemist, G.S.I., for helpful suggestion on the composition of manganese-garnet.

References.

Aminoff (G.), 1931. Kungl. Svenska Vetenskapsakad Handl., ser. 3, vol. 9, p. 14 [M.A. **4**–461].
—— 1926. Zeits. Krist., vol. 64, p. 475 [M.A. **3**–342].
Byström (A. M.), 1949. Acta Chem. Scand., vol. 3, p. 163 [M.A. **11**–238].
Byström (A.) and Byström (A. M.), 1950. Acta Cryst., vol. 3, p. 153 [M.A. **11**–238].
Cole (W. F.), Wadsley (A. D.), and Walkley (A.), 1947. Trans. Electrochem. Soc., vol. 92, p. 133.
Fermor (L. L.), 1909. Mem. Geol. Surv. India, vol. 37, pts. i–iv.
—— 1938. Proc. Nat. Inst. Sci. India, vol. 4, p. 253 [M.A. **7**–169].
Fleischer (M.) and Richmond (W. E.), 1943. Econ. Geol., vol. 38, p. 269 [M.A. **9**–4.]
Harcourt (G. A.), 1942. Amer. Min., vol. 27, p. 74 [M.A. **8**–280].
Hesse (R.), 1948. Acta Cryst., vol. 1, p. 200 [M.A. **10**–527].
Johansson (K.), 1928. Zeits. Krist., vol. 68, p. 114.
Mason (B.), 1942. Geol. För. Förh., vol. 64, p. 117 [M.A. **8**–365].
—— 1947. Amer. Min., vol. 32, p. 426 [M.A. **10**–210].

McMurdie (H. F.) and Golovato (E.), 1948. Bur. Stand. Journ. Res., vol. 41, p. 589.

[Mikheev (V. I.) and Dubinina (V. N.)] Михеев (В.И.) и Дубинина (В.Н.), 1948. Зап. Всесоюз Мин. Общ. [Mem. All-Union Min. Soc.], vol. 77, p. 125.

Mukherjee (B.), 1959. Min. Mag., vol. 32, p. 166.

Orcel (J.) and Pavlovitch (S.), 1931. Bull. Soc. franç. Min., vol. 54, pp. 108 and 166 [M.A. **5**–206.]

Passerini (L.), 1930. Gazz. Chim. Ital., vol. 60, p. 397.

Pauling (L.) and Shappell (M. D.), 1930. Zeits. Krist., vol. 75, p. 128 [M.A. **4**–364].

Zachariasen (W.), 1928. Zeits. Krist., vol, 67, p. 455 [M.A. **3**–527].

A re-examination of uigite.

By Jessie M. Sweet, B.Sc.

Dept. of Mineralogy, British Museum (Natural History).

[Read 5 November 1959.]

Summary. Uigite from Uig in Skye described by M. F. Heddle in 1855 has proved on examination to be thomsonite (var. faröelite).

On 28 February 1855 M. F. Heddle described before the Royal Physical Society in Edinburgh[1] what he thought to be a new mineral, which he had collected near Uig in the Isle of Skye. It occurred in radiating sheafy plates, somewhat resembling the structure of a plumose mica, in vesicular basalt. In general appearance it was intermediate between faröelite and gyrolite; colour white, slightly yellowish; lustre 'tremulous and pearly'; hardness 5·5; brittle; density 2·284. In 1877 T. A. Readwin[2] listed uigite as a doubtful mineral. This brought a reply from Heddle in 1880[3] in which he pointed out that he had published full details of the occurrence of the mineral with two analyses in the 'Witness' newspaper[4] (a Free Church Edinburgh periodical originally edited by Hugh Miller) on 12 March 1856. Here he describes the exact spot at which he found it with faröelite and analcime: 'Sixteen miles north of Portree, in Skye, lies the "farm town" of Uig. At about the fifteenth mile-stone, the road makes an abrupt turn to the east, before descending the hill; and just at this spot a small quarry has been opened for the purpose of obtaining road-metal.'

As I was staying in Uig this summer I thought it would be interesting to find the old uigite locality and sure enough there was a milestone just outside the village on the road in from Portree. All signs of mileage were obliterated from the milestones, but this turned out to be the fourteenth milestone and there was no sign of any quarry nor did the road take an abrupt turn. The fifteenth milestone is in the village but at the

[1] M. F. Heddle, Proc. Roy. Phys. Soc. (Edinburgh) for Thursday, 28 Feb. 1855, printed in Edin. New Phil. Journ., 1856, vol. 4 (new ser.), p. 162.

[2] T. A. Readwin, Min. Mag., 1877, vol. 1, p. 90.

[3] M. F. Heddle, Min. Mag., 1882, vol. 5, p. 26 (read 23 Dec. 1880).

[4] M. F. Heddle, 'Witness' (Free Church periodical, Edinburgh), 12 Mar. 1856 (Report of the Proc. Roy. Phys. Soc.).

sixteenth milestone there is a sharp hairpin bend turning south-west and then north-east uphill. Here I found a tiny roadside cutting in which the rock was not noticeably vesicular and yielded nothing in the way of minerals. However other exposures in the neighbourhood showed pockets of zeolites and gyrolite and just below the Free Church I found a weathered vein from which I collected an amount of material. This consisted of radiating thomsonite (var. faröelite) with gyrolite, sometimes quite intimately intermixed; also analcime.

On my return through Edinburgh I was allowed to borrow the one and only specimen of uigite (456.24) from the Heddle collection in the Royal Scottish Museum. This is a vesicular basalt containing in the largest cavity radiating prisms, which tend to become acicular. The colour is white becoming cream on the weathered surface and the lustre somewhat pearly. On optical examination the mineral was seen to consist of needles and plates which gave straight extinction and a refractive index $1{\cdot}517 < \beta < 1{\cdot}524$. The plates were found to be biaxial positive. This agrees very well with faröelite and the identity was confirmed by an X-ray powder photograph, which is identical with one of thomsonite (B.M. 94978) from Old Kilpatrick, Dunbartonshire (the type locality). Other cavities in the specimen contain faröelite and analcime.

As this is the only specimen available it would appear that uigite is merely faröelite and Heddle himself throws considerable doubt on its validity as a species. He says:[1] 'Mineralogy is in that stage when men of the present age have to draw the sponge through many of the works of those who have gone before them, to have their own, in turn, expunged by those who follow after. Fearing that this might be the fate of *Uigite* I do not thrust it into the world as a new mineral.' I personally think there was another specimen on which he did his analyses and as gyrolite is so often intimately associated with the faröelite he may have been examining a mixture.

Heddle's analyses are given below (cols. 1 and 2); in col. 3 are the molecular ratios corresponding to the mean of the two analyses. Assuming that all the alumina belongs to a zeolite, the ratios for Al, Ca, and Na in col. 5 (faröelite) are obtained, leaving the Ca figure under col. 4 for gyrolite; taking gyrolite as $Ca_2Si_3O_7(OH)_2.H_2O$, col. 4 is completed and the ratios for Si and H_2O in col. 5 are obtained by subtraction. This corresponds to 25 % of gyrolite and 75 % of a faröelite of the composition given in col. 6, which is a highly siliceous faröelite, but corresponds

[1] 'Witness', 12 Mar. 1856 (but not copied in Min. Mag., vol. 5).

closely to Heddle's analysis[1] (1857) of a faröelite from Uig, 'associated with a (?) new mineral' (col. 7).

	1.	2.	3.	4.	5.	6.	7.
SiO_2... ...	46·320	45·980	0·7681	0·2300	0·5381	42·94	43·19
Al_2O_3 ...	21·348	21·928	0·4246	—	0·4246	28·74	29·16
CaO	16·361	16·150	0·2900	0·1533	0·1367	10·18	10·08
Na_2O ...	4·698	4·685	0·1513	—	0·1513	6·23	5·24
H_2O... ...	12·212	11·250	0·6516	0·1533	0·4983	11·91	12·43
	100·939	99·993				100·00	100·10

Acknowledgements. I am indebted to Dr. C. D. Waterston for much information and to the Director of the Royal Scottish Museum for permission to describe the type specimen; also to Dr. M. H. Hey for the comparison of analyses.

[1] M. F. Heddle, Phil. Mag., 1857, ser. 4, vol. 13, p. 53.

SHORT COMMUNICATIONS

A new occurrence of erionite.

While slip-cataloguing the zeolites in the British Museum collections, in 1938, I was unable to identify two specimens from the Allan-Greg collection (B.M. 96224 and 96225). These specimens are two very similar half-geodes (perhaps even two pieces of one geode) without matrix, and consist of a layer about 5 mm. thick of a white, compact fibrous mineral with low birefringence, straight extinction with positive elongation, and refractive index about 1·47, on which are crystals of chabazite; they were obtained by the eminent Scottish collector T. Allan before 1825, and are described by him: '27. Chabasie, in very perfect cristals, disposed in a geode of mesotype tinged on the surface of a bright orange. Faroe.' and '28. Chabasie, another similar geode, containing an irregular cristal of chabasie, ? or possibly a particular species. From Faroe.'

Dr. F. A. Bannister took an X-ray powder photograph of one of the specimens (B.M. 96225) in July 1939, but with the outbreak of war this film was set aside unexamined until this summer. We now find that it exactly matches a powder photograph of type erionite. The specimens differ markedly from those from the known erionite occurrences[1] where the mineral occurs in seams and not in geodes; the fibres are shorter and more firmly compacted, and although there is, unfortunately, no matrix present and the only associated mineral is chabazite, it is probable that the specimens are from the Faroese basalts and represent a very different paragenesis.

Department of Mineralogy, M. H. Hey
British Museum (Natural History)

[1] L. W. Staples and J. A. Gard, Min. Mag., 1959, vol. 32, p. 261; K. S. Deffeyes Amer. Min., 1959, vol. 44, p. 501.

Coronadite from Cumberland.

During a recent visit by students of this department to the Carrock–Caldbeck area of Cumberland, Mr. B. N. Twombley collected a specimen containing an unknown silver-white metallic mineral from the upper cross-cut dumps in Dry Gill. Very generously the specimen was placed at my disposal.

Data derived from X-ray powder photographs of the mineral agreed with the spacings given by Frondel and Heinrich[1] and by Neumann and Sellevoll[2] for coronadite, $MnPbMn_6O_{14}$. Material from Bou Tazoult, Imini, Morocco, kindly supplied by Dr. H. Neumann, of the Mineralogical Museum, Oslo, allowed a direct comparison of photographs to be made. There is no doubt that the Dry Gill mineral is coronadite.

Further confirmation was obtained from a qualitative spectrographic analysis of the material carried out by Miss J. M. Rooke in this department. Mn was present as a major element, Pb as a minor, with traces of Al, Ba, Ca, Co., and Fe.

The coronadite is found with massive quartz, psilomelane, and campylite, the well-known mineral association from the upper dumps in Dry Gill. It occurs in two forms:

As a silver-white, inclining to steel-grey, metallic mineral when fresh, tarnishing to a dull black. The habit varies from massive to fibrous, the fibres being especially well developed when the mineral is botryoidal, not only as radiating fibres within the body of the globules, but as minute acicular crystals on their surface giving the appearance of black velvet.

As a dull black, fibrous, botryoidal mineral, indistinguishable from psilomelane in the hand specimen. This form was X-rayed in the expectation of confirming the presence of psilomelane; obviously a re-examination of much of the psilomelane from Dry Gill might well be of interest.

The occurrence of coronadite in Dry Gill adds weight to the idea that the gill is part of a manganiferous outer zone, associated with the centre of tungsten mineralization in Grainsgill to the south. The manganese moved northwards along a series of north–south faults, which are especially well seen in Brandy Gill and fault the Dry Gill vein itself.

This is the first record of the occurrence of coronadite in the British Isles.

Dept. of Geology, J. Hartley
University of Leeds

[1] Amer. Min., 1942, vol. 27, p. 48.
[2] Vid.-Akad. Avh. Oslo. I. Mat.-Naturv. Kl. 1955, no. 3.

Molybdenite associated with Laxfordian gneisses at Loch Stack, Sutherlandshire.

An occurrence of molybdenite, associated with amphibolites adjacent to a quartz–albite–oligoclase pegmatite, has been found in a road cutting $1\frac{1}{4}$ miles north of Achfary, near the southern shore of Loch Stack, Sutherlandshire.

The pegmatites appear to be of two varieties, a pink quartz–microcline albite–muscovite type with accessory epidote and minor secondary chlorite and scapolite, and a white quartz albite–oligoclase type with minor biotite, chlorite, and epidote. The feldspars of each type are slightly altered.

Both varieties are seen to intrude the country rocks, which in this area consist of foliated quartzose rocks with biotite, hornblende, epidote, and sphene; plagioclase-amphibolites with epidote and sphene; and thick coarse-grained hornblendic rocks. In all of these types alteration of the feldspars and development of secondary chlorite are common.

The molybdenite is mainly concentrated in the hornblendic rocks, which are intruded by the white quartz–albite–oligoclase pegmatite; but locally small flakes of molybdenite associated with biotite are seen in the white pegmatite itself. In the hornblendic rocks molybdenite occurs as aggregates up to half an inch across and is locally associated with pyrites. Brown crystals of sphene are common. The amphibole is sometimes partly altered to a white, fibrous asbestiform mineral. A qualitative spectrographic analysis of the molybdenite indicated traces of the following elements: Ca, Al, Mg, Zr, Fe, Si, Co, Y, Ti, and Na.

Independently, Nutter (1953) noted molybdenite and traces of Mo in the quartzose veins, $\frac{1}{2}$ mile south-west of the house at Badnabay. The veins 'may represent a late stage differentiation from the Loch na Seilge sill' (Nutter, 1953, p. 291) which continues for 5 miles to the ESE. to Loch Stack, where the present molybdenite occurrence was found.

It may be that these isolated molybdenite occurrences are part of a more extensive, relatively molybdenum-rich, zone of pegmatitic or hydrothermal origin. It is hoped that a bio-geochemical investigation of this region can be undertaken in order to establish the extent of this molybdenum mineralization.

A somewhat similar type of molybdenite mineralization has been described by Thomson (1918, pp. 308–12) from Quebec. Molybdenite, pyrite, pyrrhotine, sphene, and scapolite are found in pyroxenites and are considered to be of pegmatitic origin.

Department of Geology,
The University,
Leeds, 2

O. von Knorring
R. Dearnley

Nutter (G.), 1953. A spectrographic and geochemical study of the trace elements in the Archaean pegmatites of NW. Sutherland. Ph.D. Thesis, University of Leeds.
Thomson (E.), 1918. Econ. Geol., vol. 13, p. 302.

BOOK REVIEWS

FRONDEL (Clifford). *Systematic Mineralogy of Uranium and Thorium.* Washington (U.S. Geol. Surv. Bulletin 1064), 1958. viii+400 pp., 1 pl., 24 text-figs. Price (paper cover) $1.50.

This is a comprehensive monograph on minerals containing uranium or thorium as 'essential constituents', which are described systematically in the following broad chemical categories: oxides, carbonates, sulphates, molybdates, phosphates and arsenates, vanadates, silicates, and niobate-tantalate-titanates. Within each category, minerals of analogous composition and crystal structure are grouped together, such as the torbernite group of phosphates and arsenates. No formal distinction is made in the classification between anhydrous species (primary in origin) and those containing water or hydroxyl (mostly secondary). The author has included some seventy uranium and six thorium minerals, as well as a few minerals whose status as separate species is uncertain and others in which the uranium or thorium content is regarded as non-essential.

Each species is described according to its synonymy, composition, crystallography and crystal habit, physical properties, optical properties, thermal behaviour, synthesis, identification, natural formation, and occurrence. Full X-ray powder data are listed whenever available. The treatment is critical and full; for example, 36 pages are devoted to uraninite alone. The descriptive mineralogy is followed by a series of determinative tables in which the mineral species are arranged according to their X-ray *d*-spacings, chemical composition, optical properties, colour, specific gravity, and fluorescence in ultra-violet light. The work is documented by 826 references to the world literature up to mid-1956. A short introduction gives some interesting historical matter, mentions some of the special difficulties in the identification of uranium and thorium minerals, and discusses briefly the subjects of age determination, autoradiography, and radiation damage, which arise from the radioactivity of these minerals. The book is well produced and the price of half-a-guinea is remarkably low.

There is no doubt that this is a work of the highest merit. The manner in which Dr. Frondel has met his own exacting standards of completeness, accuracy, clarity, and critical assessment compels whole-hearted admiration. Only a few errors have been noted. For example, on p. 155 it is stated that monazite is sometimes elongated along the *a*-axis when

b is meant. On p. 348, trögerite is inadvertently referred to as a phosphate. Cheralite is described with the silicates although it is essentially a phosphate and should follow monazite, not huttonite. The ångström unit is abbreviated A throughout, instead of Å as recommended by the International Union of Crystallography in 1951. In discussing the identification of monazite, mention might be made of the brilliant green colour assumed when viewed in visible light from a mercury-vapour lamp.[1]

The only significant criticism is of the choice of species described in the section on multiple oxides or niobate-tantalate-titanates. This comprises the fairly common or economically interesting minerals betafite, pyrochlore-microlite, brannerite, and davidite, together with two obscure species known only from single occurrences, písekite and delorenzite (the latter since discredited). The widespread species euxenite and samarskite, to take two conspicuous examples, are excluded on the grounds that their content of uranium or thorium is occasional or vicarious. Whatever may be their 'ideal' composition, in nature they invariably contain uranium or thorium, and the percentage is often considerable. With other less common species they are in fact classified as uranium and thorium minerals in U.S. Geological Survey Bulletin 1009-F, to which the reader is referred in the present work. Indeed, as every metamict mineral specimen contains at least some uranium or thorium, it follows that any species that habitually occurs in the metamict state is *ipso facto* a uranium or thorium mineral, and as such warrants a place in a monograph on the mineralogy of uranium and thorium.

A work of this length with tables on nearly every page is bound to take time to print, but two years or more in the press seems rather excessive. Progress in this field has been so rapid that the book is already out of date to a considerable extent. As it is not only an invaluable guide to identification but will also provide the background to detailed work on known and new species, it is important that it should not be allowed to lag too far behind research. Even between mid-1956, when the manuscript appears to have been completed, and April 1959, details of some three dozen allegedly new uranium and thorium minerals have been recorded in this Magazine, in Mineralogical Abstracts, and in the American Mineralogist. About two-thirds of these new mineral names are from Soviet sources. They are the first crop of material released for publication since the 1955 Geneva Conference and are one of

[1] K. J. Murata and H. Bastron, Science, 1956, vol. 123, p. 888.

the products of the intensive work in geology that has been taking place in the USSR since the war. In many cases there is considerable uncertainty as to whether the minerals are in fact new species or merely varieties of known ones. It is often impossible to decide such problems from the published data without direct comparison of actual specimens from the type localities. The free interchange of mineral specimens between East and West would do much to prevent the establishment of two rival nomenclatures.

J. E. T. Horne

Heinrich (E. W.). *Mineralogy and Geology of Radioactive Raw Materials.* New York, Toronto, and London (McGraw-Hill), 1958. xiv + 654 pp., 84 tables, 201 text-figs. Price 112*s.* 6*d.*

'It has been estimated', we are told in the preface, 'that since 1952 more man-hours have been spent in searching for uranium alone than had been spent in seeking all other metals in history.' One result of this unprecedented activity is the spate of publications on all aspects of the geology and mineralogy of uranium, and to a lesser extent of thorium, from which Professor Heinrich has endeavoured to distil the essence for the present survey. An idea of the magnitude of the task may be gained from the 58-page bibliography containing 1342 entries down to the end of 1957. The outstanding feature of the book is the comprehensive treatment of both mineralogy and geology in one volume. It is divided into two parts, of which Part I (149 pages) deals with descriptive mineralogy and Part II (406 pages) with ore deposits, actual or potential.

Part I begins with a rather sketchy chapter on radioactive minerals in general, which bears signs of hasty compilation. For instance, we are told (p. 21) that ^{40}K emits alpha as well as beta particles. U^{4+}, Th^{4+}, and other ions are described as isomorphous (pp. 8, 10) when it is meant that they undergo isomorphous replacement. As many age determinations are quoted later in the book, a section on the lead method could usefully have been included in this introductory chapter with some guidance on the selection of suitable material and the reliability of results. A discussion of the special difficulties encountered in the identification of uranium and thorium minerals would also have been helpful. This might have included such matters as the unreliability of optical data for identifying many uranium secondaries because of the varying content of zeolitic water; the ease with which some secondaries dehydrate to the meta form; the limitations of powder photographs in identifying

members of isomorphous groups; and the breakdown of normal methods for metamict minerals.

In chapter 2, minerals are classified broadly into uranium and thorium minerals, minerals with minor U, Th, or Ra, and minerals with radioactive impurities. Within each category species are grouped chemically. Doubtful or poorly defined species are relegated to the end of each group. A wider range of species is thus covered than in Frondel's Systematic Mineralogy reviewed above and the principal value of this chapter lies in the inclusion of species excluded from the more detailed work. Thus, amongst those classified here as uranium and thorium minerals are the metamict species fergusonite–formanite, samarskite–yttrotantalite, euxenite–polycrase, polymignite, æschynite–priorite, and zirkelite, together with thucholite and related hydrocarbon complexes. The section on minerals with minor U, Th, or Ra includes baddeleyite, perovskite, radiobaryte, apatite, wavellite, crandallite, xenotime, opal, zircon, allanite, gadolinite, chevkinite, sphene, and thalenite. Eight hydrated uranium minerals, described since Frondel's manuscript was completed, are also included, though the available data on most are scanty. The more important species are described under the headings composition, structure and form, occurrence, and identification. 'Structure' is used in the morphological sense. Chemical analyses are omitted, except for uranium and thorium. Occurrences are recorded very fully (an index of localities contains about 2130 place-names). In most cases physical properties are not described in the text, but are tabulated with those of related species. The notes on identification are not always adequate, for X-ray data, if given at all, comprise only the strongest three or four lines.

The second and larger part of the book covers the whole range of uranium and thorium deposits described in a very extensive literature. Uranium, in particular, occurs in many environments whose diversity has only become apparent in recent years. The complex geochemistry of uranium results from its ability to substitute extensively for thorium, rare earths, and calcium, to oxidize readily to the highly mobile uranyl ion, and above all to be precipitated as uraninite from hydrothermal solutions over a very broad range of temperature and pressure. The precise classification of deposits adopted in a book of this sort is perhaps of little consequence, since classification cannot be wholly divorced from genesis, over which controversy is as keen as ever. What is important is that the mineralogy and geology of the various deposits should be succinctly described and the theories of origin objectively stated. This the

author has done. Where he has no personal experience of the deposit, as with the Rand, he does not attempt to adjudicate, but where on familiar ground, as in the Colorado Plateau, he records his own conclusions. United States deposits perhaps have more than their fair share of attention on the grounds of economic or geological importance alone, but it would be ungracious to quarrel with that.

The book ends with the very full bibliography already mentioned and separate indexes for mineral species, localities, and subjects.

There are a few misspellings, notably 'thucolite' (no second h) throughout the book and 'montroesite' and 'paramontroesite' in chapter 10. Parentheses are used instead of braces to denote forms and cleavage, and instead of brackets to denote zone axes. The half-tone illustrations are excellent.

J. E. T. Horne

The Geology of Uranium. Translated from Вопросы геологии урана [Problems in the Geology of Uranium], Supplement no. 6 of the Soviet Journal of Atomic Energy, Atomic Press, Moscow, 1957. London (Chapman & Hall Ltd.) and New York (Consultants Bureau Inc.), 1958. vi+128 pp., 61 tables, 90 text-figs. Price (bound) 48*s*.

This is not an introduction to uranium ore deposits, as the title suggests, but a collection of a dozen unconnected papers. There are three on various aspects of uranium geology, six on uranium minerals, and three on radiometric techniques.

Two of the geological papers discuss the role of metamorphic processes in concentrating uranium in certain Palaeozoic sediments. A third is on the origin of uranium mineralization in coal and has appeared in somewhat different form in the proceedings of the second Geneva conference ;[1] comparison of the photomicrographs accompanying the two versions shows discrepancies in the magnifications quoted. These geological papers suffer from the usual Russian omission of localities and sketch-maps. The uranium content of coal is given only in relative units.

A paper by Polikarpova amplifies his earlier description of the uranium silicate nenadkevite,[2] rejected by Fleischer[3] as 'an unnecessary name for what is probably a variety of coffinite'. Several photomicro-

[1] Z. A. Nekrasova, Proc. 2nd U.N. Int. Conf. Peaceful Uses At. En., 1958, vol. 2, p. 412.

[2] See Min. Mag., 1958, vol. 31, p. 967, and M.A. **13**–385.

[3] M. Fleischer, Amer. Min., 1957, vol. 42, p. 441.

graphs are now given and from these and other data it seems likely that the mineral is indeed a new species. Thus some specimens at least are not deficient in silica and the dark varieties are amorphous, whereas coffinite contains (OH) in substitution for (SiO_4) and invariably yields a powder pattern. The powder pattern of light varieties of nenadkevite is certainly not that of coffinite; it shows some similarity to those of huttonite, monazite, and cheralite, but is not necessarily of a single phase. The photomicrographs suggest that nenadkevite may have originally crystallized as a thorite-like tetragonal mineral, which subsequently became metamict and in some cases recrystallized as a new phase or phases after hydration and alteration. Further work, including synthesis, is necessary.

The new minerals uramphite (uranyl ammonium phosphate) and ursilite (a uranium silicate) are described in two short papers, which have been fully summarized by Fleischer.[1] Another paper discusses the paragenesis and mode of formation of natro-autunite. Sidorov and Rafalsky describe the hydrothermal synthesis of uraninite in a carbonaceous shale. A slice of the rock was heated in an autoclave with a uranyl sulphate solution for 2 or 3 days. Cubes of uraninite formed on and in the specimen, thus demonstrating the efficacy of organic material in precipitating hexavalent uranium from hydrothermal solutions.

Ambartsumian contributes the longest and perhaps the most interesting paper in the book, in which he gives the results of detailed thermal investigations on a number of hydrated uranyl minerals. It is noteworthy that meta-uranocircite, in contrast to meta-autunite and other minerals tested, is still strongly fluorescent after heating at 1000° C. Powder photographs and optical data confirm that the structure is essentially unchanged. It appears that the large size of the barium ion prevents the structure collapsing in spite of complete dehydration.

The radiometric papers contain little that is new. One of them reviews airborne prospecting as practised in Western countries but makes no reference to Russian methods.

In summary, the book contains much of interest to the specialist in uranium minerals. The translation is clear, but the half-tone illustrations, though numerous, are of poor quality.

J. E. T. Horne

[1] M. Fleischer, Amer. Min., 1959, vol. 44, p. 464.

BERRY (L. G.) and MASON (Brian). *Mineralogy: Concepts, Descriptions, Determinations*. San Francisco and London (W. H. Freeman and Company), 1959, xi+612 pp., 34 tables (excluding 26 pp. of determinative tables), 262 text-figs. Price 56*s*. 0*d*.

This well-produced book, 'designed to satisfy the requirements of an undergraduate course in mineralogy', is divided into three sections as indicated by the title. The section on concepts (278 pp.) contains the following chapters: Introduction; Crystallography; The chemistry of minerals; The physics of minerals; The genesis of minerals; Determinative mineralogy; The systematics of mineralogy. The chemical approach to the subject is lucid and concise, and the emphasis placed on geochemical principles throughout the book fills a long-felt need. It is thus to be regretted that the chapter on crystallography (138 pp.) is not uniformly clear, and although admirably conceived as a whole it is rendered heavy by too detailed a discussion (for the purpose of the book) of individual forms in the various crystal classes; International Symmetry Symbols are used freely, but the student is expected to grasp their meaning with little help from the authors. The great disappointment of the book is the decision of the authors to confine discussion of the optical properties of crystals to three pages in the physics chapter, and a quarter-sentence in that on determinative mineralogy (p. 268); thin-section methods are discussed in many textbooks, crushed-fragment methods in so few that the student is in danger of not realising their usefulness. Two hundred well-chosen species are described in the second section of the book (287 pp.), and the text is supplemented by clear diagrams and half-tone figures (157 in all). The eight chapters are arranged according to a condensed version of the Berzelius classification, and each begins with a periodic table of the elements concerned in that chapter; the relationships between analogous species are discussed, frequently with the aid of comparative tables, and the status of the silica group as silicates is perpetuated. The determinative tables are based on lustre and hardness, and minerals in each class are listed in order of increasing density; they appear to be convenient to use. The index is good, and the few misprints or mistakes seen by the reviewer are connected with the text-figures—e.g. hexoctohedral (fig. 2–66); the position of ϕ (fig. 2–33*a*). The diagrams and line drawings are clear throughout, although the latter would be far better without the perspective cube surrounding every crystal illustration regardless of symmetry. Aside from these comments, this textbook is excellent and deserves a place in all teaching libraries; it is a pity that the price is rather high for the average British student.

P. G. EMBREY